Tidal Power Plant

in Saemangeum

Hugo Swane

Hydraulic Engineering

Utrecht

May 2007

MSc Thesis

TIDAL POWER PLANT

IN SAEMANGEUM

Student:	Hugo Swane
Address	Admiraal de Ruijterweg 273-B
	1055 LV Amsterdam
Telephone	06-50501318
E-mail:	hswane@gmail.com
Institution:	Bouwdienst Rijkswaterstaat
University:	TU Delft
Faculty:	Civil Engineering
Master:	Hydraulic Engineering
Student number:	9818242

Examination committee:	prof.dr.ir. M.J.F Stive	TU Delft
	ing. G.A. Beaufort	Bouwdienst Rijkswaterstaat
	ir. J. van Duivendijk	TU Delft
	ir. H.J. Verhagen	TU Delft
	dr.ir. P.J. van Overloop	TU Delft

Preface

This is the MSc-thesis of Hugo Swane: Feasibility and design of a Tidal Power Plant at the Saemangeum project in South Korea. This report is the result of a study performed at the Bouwdienst Rijkswaterstaat in Utrecht, the Netherlands. The MSc-thesis is the last part of the curriculum of the Master of Science in Civil Engineering at the Delft University of Technology.

In 2005 I attended the course 'Water power engineering'. This course arose my enthousiasm for water power. One year later I was looking for an interesting subject for my graduation work. I decided to contact mr Hans van Duivendijk (lecturer of 'Water power engineering'). He advised me to contact the Bouwdienst Rijkswaterstaat, because they were at that moment studying the closure of the Saemangeum Estuary in South Korea. Wouldn't it be interesting to investigate the possibility to build and operate a Tidal Power Plant for the Saemangeum area?
Now, ten months later, I have not regretted following mr Van Duivendijk's advise.

I would like to thank the Bouwdienst Rijkswaterstaat for giving me the opportunity to write my thesis at their institution and for their hospitality. Special thanks goes out to mr Gé Beaufort, whose experience, knowledge and enthousiasm have been of great value for achieving this result.

Furthermore I would like to thank all members of my examination committee for their support.

Hugo Swane

Utrecht, May 2007

Abstract

Objective

This study investigates the possibility to build and operate a Tidal Power Plant (TPP) in Saemangeum in South Korea. The objective of the study is to investigate if a TPP would be technically possible and economically feasible for Saemangeum. This should result in a design for a Tidal Power Plant.
The subobjectives of the study are:

- To determine the best concept of a tidal power plant for the Saemangeum case

- To determine the best suitable location

- To determine the optimal generation scheme and dimensions and specifications of the plant

- To determine the energy output characteristics (installed power and energy output)

- To describe the building method

These decisions must all be made taking into account possible future shifts in facts in economy, energy prices and spacial planning ideas; there are several possible other future functions for the Saemangeum area which will affect the performance of the plant: The most important future functions will be polders for agricultural, industrial or residential purposes and a fresh water basin. A design without one of these functions is most likely to be rejected during the decision process. Remaining future functions will be a newly to be built Gunsan/ Saemangeum port.

Literature study

Tidal power has been used to grind grane since as early as the 8th century AD, while the first tidal electric power plants were built in the sixties of the 20th century in France and Russia. These existing plants and their performances have been studied as well as several feasibility studies made throughout the years, including the Sihwa project, a single, low basin plant which is at present under construction in South-Korea.
A large number of generation schemes have been developed in order to find effective ways of extracting energy from tidal basins. Practical engineering considerations and environmental concerns have reduced the number of feasible options to four: a single basin, double effect plant (generating twice per tidal cycle, both on the incoming and the outgoing tide), a single, high basin plant (generating on the outgoing tide), a single, low basin plant (generating on the incoming tide), a linked, double basin plant (existing of a high basin and a low basin, continuously generating). Of these schemes the linked, double basin plant

produces at a continuous rate, but the smallest amount of energy. The single basin, double effect plant requires a large tidal range to be the most productive scheme, usually about 9 m. This leaves the single, high basin and the single, low basin schemes as the most interesting schemes for the Saemangeum case.

A bulb turbine is the most suitable type of turbine for tidal power, because of the high efficiency at relatively low heads. The turbine parameters (runner diameter and efficiency) can be calculated for a given head and discharge.

Model of the Saemangeum basin

A Storage Area Approach Model is made (in Microsoft Office Excel) to predict the energy output. The possibility to vary the basin area (including the depth-storage relationship) is built in, as well as the possibility to vary the number, efficiency and rated head of turbines (related to the head and flow velocities), additional sluicing capacity and the possibility whether or not to use the turbines as pumps. Also the construction costs, a Net Present Value calculation and the annual energy output are some of the output parameters of the model (with varying discount rate, future energy price). The model predicts the energy output for three schemes: a single, high basin plant, a single, low basin plant and a single basin, double effect plant.

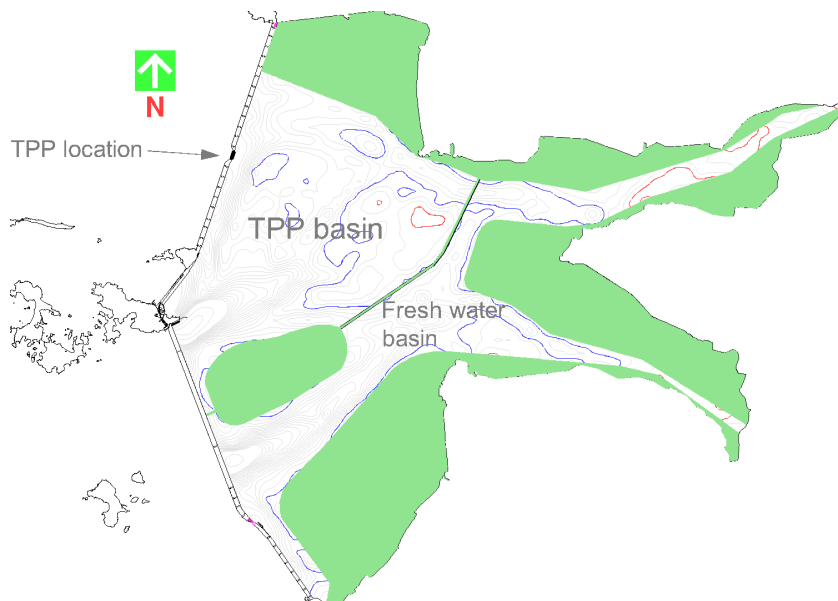### Development options for the Saemangeum area of 394 km^2

Figure 1: *Future Layoout of Saemangeum Area*

Three different layout possibilities are sketched. All three layouts have different basin areas (77 km^2, 114 km^2 and 302 km^2 at MSL). These three layouts have been compared with each other on different issues: The presence of possible future functions (like the

presence of polders, fresh water and an inter tidal zone), the annual energy output and the economic feasibility (Net Present Value). For various reasons it was decided that the layout with the basin area of 114 km^2 at MSL must be selected and equipped with a low basin plant: This layout contains a large inter tidal zone, both a fresh water basin and polders, and it turns out to be the economically most feasible option (neglecting the layout containing no changes to the area at all, as this layout would have no chance to be selected in reality due to the absence of other future functions). The selected layout contains a fresh water basin of 90 km^2.

TPP dimensions and characteristics

Generation will only take place in one direction, from sea to basin (flood generation). No extra sluicing capacity is needed, as the Sinsi sluices are already there and their 300 meters of sluice length are sufficient. Constructing extra sluicing capacity would only make the energy more expensive. The power house will consist of a structure measuring 338 m parallel tot the barrage, 59 m in flow direction and 34,8 m from the toe of the construction (bed protection) up to the road level. The powerhouse will be equipped with 18 bulb turbines (runner diameter 7.5 m) and generators, having a total installed capacity of 142 MW. The plant will generate approximately 454 GWh per year and the construction costs will amount to about 286 Million US$.
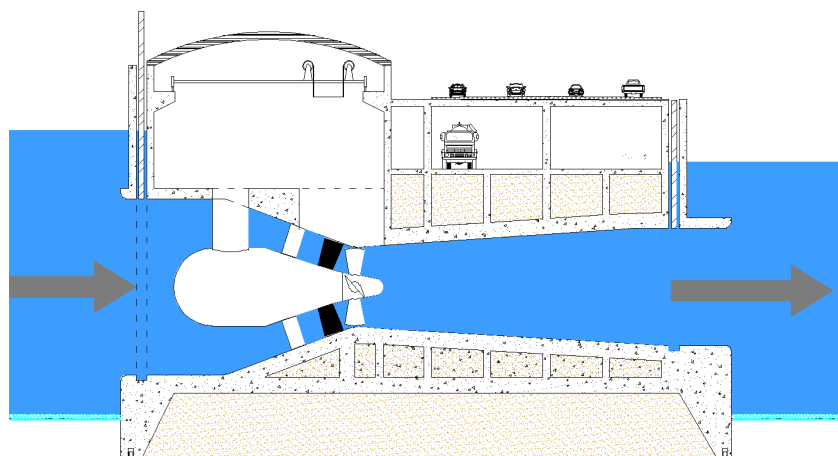

Figure 2: *Section of power house unit; water flows from sea to basin*

Construction method

There are two possible ways to build the TPP: The float-in method (construction in the wet) and the cofferdam-method (construction in the dry). The cofferdam method is chosen here, because of two reasons: First the required depth for the float-in method is much too small; A floating caisson (power house unit) has a draught of about 20 m, while the average depth in the basin is just about 8 m. This means that a channel would have to be dredged all the way from the dock or slipway where the caissons would be prefabricated

up to the TPP location. This channel would have to be several kilometers long, depending on where the dock or slipway would be located. The second reason for not selecting the float-in method is the risk of piping underneath the power house construction. It would be very hard to prevent piping from happening if the float-in method is used.

A cofferdam consisting of circular cells and connecting cells is built around the future TPP power house location. At the barrage side the circular cells have a diameter of 31.8 m and at the basin side the circular cells have a diameter of 25.2 m. These dimensions follow from failure calculations (sliding and turning around center of foundation level).

Economic feasibility

The given parameters have been determined by an economic optimisation. The numbers given above are based on assumptions: the plant's design has a maximal Net Present Value after 40 years, with a discount rate of 4 %, an annual rise of energy price of 4 % and an actual energy price of US$ 0,03 per kWh. This production price has been set at US$ 0,03 per kWh, because the plant is expected to be able to compete with other energy sources. Under these assumptions tidal power in Saemangeum turns out to be attractive and feasible. An important design parameter is the expected lifetime. In this study the lifetime is assumed to be 40 years. This is quite a pessimistic estimation, because the La Rance plant in France has already been in operation for 41 years, but the financial risks are minimised this way.

The Net Present Value after 40 years of operation is US$ 187.6 Million for a discount rate of 4 % and an expected annual rise of energy price of 4 %.

The break even point will be reached after 25 years of operation and the Internal Rate of Return is 6.5 %.

Table of Contents

List of Figures

List of Tables

List of Symbols and Abbreviations

Table 1: *List of abbreviations; All water levels refer to MSL*

Abbreviation	Definition of element
EL	Elevation Level
HHW	Highest High Water level
HWOST	High Water of Ordinary Spring Tides
IRR	Internal Rate of Return
LWOST	Low Water of Ordinary Spring Tides
MHW	Mean High Water
MLW	Mean Low Water
MSL	Mean Sea Level
MWL	Mean Water Level
NPV	Net Present Value
TPP	Tidal Power Plant
US$	United States Dollar; 1,34 US$ = 1 €

Symbol	Definition of element	Unit
A	Surface area tidal basin	m^2
A_b	Cross-sectional area of barrage/ estuary dam	m^2
A_c	Area of cofferdam circular cell + connecting cell	m^2
A_h	Surface area high basin	m^2
A_l	Surface area low basin	m^2
B_b	Unit cost of barrage material	$US\$/m^3$
B_{bed}	Unit cost of bed material	$US\$/m^3$
B_c	Unit cost of cofferdam material	$US\$/m^3$
B_p	Unit cost of power house material	$US\$/m^3$
B_{sl}	Unit cost of sluice gate material	$US\$/m^3$
C	Chézy's coefficient	$m^{1/2}/s$
C_b	Cost of barrage	US$
C_{bed}	Cost of bed protection	US$
C_c	Cost of cofferdam	US$
C_p	Cost of power house	US$
C_{sl}	Cost of sluice gates	US$
C_{t+g}	Cost of turbines and generators	US$
C_{tot}	Total construction costs	US$
C_D	Discharge coefficient	-
D	Step height (bed protection)	m
d_{50}	Nominal grain diameter	m

Symbol	Definition of element	Unit
d_o	Arm (line of action F_o - foundation plane)	m
d_i	Arm (line of action F_i - foundation plane)	m
D_b	Depth of barrage structure	m
D_c	Diameter circular cell cofferdam	m
$D_{part,req}$	Required diameter of particles for bed protection	m
D_t	Runner diameter of turbine	m
d*	Dimensionless grain diameter	-
E_{cycle}	Energy generated in one tidal cycle	GWh
E_{nat}	Natural energy potential	GWh
E_{pot}	Potential energy	GWh
E_y	Energy generated in one year	GWh
f	Frequency of electricity grid	Hz
F_{1t}	Throat area one turbine	m^2
f_c	Coefficient by Hoffmans (1993)	-
f_{gr}	Friction coefficient, gravel on rock	-
F_o	Resultant force from outside on cofferdam	kN
F_i	Resultant force from inside on cofferdam	kN
f_{sl}	Binary factor indicating if sluices are open or closed	-
F_{sl}	Flow area of sluices	m^2
f_t	Binary factor indicating if turbine's gates are open or closed	-
F_t	Throat area all turbines	m^2
g	Gravitational acceleration	m/s^2
h	Water level	m
H	Head	m
h_0	Original water depth	m
h_b	Basin water level	m
H_c	Height between ground level inside and outside cofferdam	m
H_p	Height of cofferdam's sheet piles	m
H_r	Turbine's rated head	m
h_s	Sea water level	m
H_s	Suction head	m
h_{sc}	Maximum scour depth	m
h_{sl}	Depth of sluice (water level till sill level)	m
k_r	(bottom) roughness coefficient	-
K_a	Active earth pressure coefficient	-
K_p	Passive earth pressure coefficient	-
K_0	Neutral earth pressure coefficient	-
L	Length of bed protection	m
L_b	Length of barrage	m
L_c	Length of closure	m
L_p	Length of power house (parallel to flow direction)	m

Symbol	Definition of element	Unit
L_{sl}	Length of sluices (parallel to flow direction)	m
$M_{0,d}$	Moment around centre of foundation plane cofferdam	kNm
m	Slope of barrage walls	
n	Rotational speed	rpm
N_p	Number of poles on generator	-
n_q	Specific rotational speed	rpm
N_t	Number of turbines	-
NPSE	Net Positive Suction Energy	J
P	Power	MW
P_{1t}	Power of one turbine	MW
p_{atm}	Atmospheric pressure	Pa
P_i	Installed power	MW
P_r	Rated power	MW
p_v	Vapour pressure	Pa
$P_{c,ave}$	Average vertical soil pressure in cofferdam	kPa
Q	Discharge	m^3/s
Q_{1o}	Discharge through one turbine in orifice mode	m^3/s
Q_{1p}	Discharge through one turbine when pumping	m^3/s
Q_{1t}	Discharge through one turbine when generating	m^3/s
Q_{bs}	Discharge from basin to sea	m^3/s
Q_d	Design discharge	m^3/s
Q_{in}	Discharge into tidal basin	m^3/s
Q_o	Discharge through all turbines in orifice mode	m^3/s
Q_p	Discharge through all turbines when pumping	m^3/s
Q_r	Turbine's rated discharge	m^3/s
Qr,d	Maximum absorbable shear force	kN
Q_{sb}	Discharge from sea to basin	m^3/s
q_{sl}	Specific discharge in sluices	m^2/s
Q_{sl}	Discharge through sluices	m^3/s
Q_t	Discharge through all turbines when generating	m^3/s
R	Tidal range	m
r	Radius of cells	m
R	Hydraulic radius	m
r_0	Coefficient by Hoffmans and Hinze	-
R_{max}	Maximum tidal range	m
R_{mean}	Mean tidal range	m
R_{rms}	Root-mean-square of tidal range	m
t	Time	s, min, hrs, y
u	Flow velocity	m/s
u	Water pressure	kN/m^3
$\overline{u}$	Vertically averaged velocity at end of protection	m/s

Symbol	Definition of element	Unit
$\overline{u}_c$	Critical flow velocity	m/s
V	Tidal prism	m^3
V$_b$	Volume of barrage material	US\$/m^3
V$_{bed}$	Volume of bed material	US\$/m^3
V$_c$	Volume of cofferdam material	US\$/m^3
V$_p$	Volume of power house material	US\$/m^3
V$_{sl}$	Volume of sluice material	US\$/m^3
W$_{c,e}$	Equivalent cell width of cofferdam	m
W$_p$	Width of power house (perpendicular to flow direction)	m
W$_{sl}$	Width of sluices (perpendicular to flow direction)	m
Y$_{basin}$	Length of bed (perpendicular to dam on basin side)	m
Y$_{sea}$	Length of bed (perpendicular to dam on sea side)	m

***Table 2:** Definition of symbols; Roman symbols*

Symbol	Definition of element	Unit
α	Dust bin parameter (scour calculation)	-
δ	Angle of wall friction	°
Δ	Relative density	-
η_g	Efficiency of generator	-
$\eta_{t,peak}$	Peak efficiency of turbine	-
η_t	Efficiency of turbine	-
η_{t+g}	Turbine and generator efficiency	-
γ_w	Specific weight of water	kN/m^3
$\gamma_{sat.soil}$	Specific weight of saturated soil	kN/m^3
κ_B	Capacity factor Bershtein	-
κ_T	Capacity factor Tester	-
ν	Kinematic viscosity	-
ϕ	Angle of internal friction	°
Ψ	Shield's parameter	
ρ_w	Density of seawater	kg/m^3
σ	Thoma's cavitation coefficient	-
σ	Grain pressure	kN/m^3
σ'	Effective grain pressure	kN/m^3
θ	Characteristic angle cofferdam and spandrel wall	°

***Table 3:** Definition of symbols; Greek symbols*

1 Introduction

1.1 Saemangeum

Saemangeum is located at the west coast of South Korea. It is an estuarine tidal flat on the coast of the Yellow Sea. After the Wadden Sea in the north of the Netherlands, Germany and Denmark, the west coast area of North and South Korea is the second largest shallow mud flats sea in the world.

After a food crisis in the 1970's the Korean government decided there was a need for agricultural land and fresh water (as a source for clean drinking water and irrigation), so it was decided that many locations, including Saemangeum, would be closed off from the sea by large dams. Other functions of the dams would be to alleviate flooding; at that time annual floodings inundated some 12000 hectares of crops in the basin of Dongjin and Mangyeung rivers. Construction of the dam at Saemangeum started in 1991.

The closure of the Saemangeum project took place in April 2006, after a long struggle between the government and environmental activists. The area is scheduled to be converted into either agricultural or industrial land in combination with a fresh water reservoir.

Figure 1.1: Satellite image of Saemangeum

Figure 1.2: Possible future land reclamation

The Saemangeum project lays just south of the estuary of the Geum River. Neighboring districts include Gunsan City, Buan County, and Gimje City. The estuary includes the mouths of the Dongjin and Mangyeong Rivers, on the coast of the Jeollabuk-do province. These rivers together have a mean discharge of 70 m^3/s, with a yearly maximum of 4000 m^3/s (once in 10 years).

The project of closing of the estuary began in 1991, but was slowed down by a series of court decisions. The completed seawall is some 33 km long, and replaces a coastline that was once more than 100 km long.

Though the gaps in the dam have been closed, the future of Saemangeum is still not

Figure 1.3: left: location of sluices; right: Garyeok sluices during construction

clear. There are plans to reclaim land for agricultural, industrial and residential purposes and to make a fresh water basin, as there is a shortage of fresh water in South-Korea. Because of the large tidal amplitude in combination with the basin already being there, it could also be extremely suitable for making a tidal power plant. Until a decision is made, the two discharge sluices in the seawall stay open so the tides can still enter the basin. Later the government will review the situation and it will then decide what destination Saemangeum will get. At the time of writing one probability seems to be that only the polder in the southern part (see Figure 1.2) will be reclaimed.

Also plans exist to extend the Gunsan port and industrial area to the northern half of the Saemangeum project.

1.2 Energy from seawater

Today's world is strongly dependent on electricity. At the moment fossil fuels are the main source of energy. The scarcity of fossil fuels (and thus the price) has forced the people to look at alternative sources of energy. The percentage of nuclear power and renewable energy sources is growing. As technology improves renewable energy becomes cheaper. Hydro power dams have been in use for a long time already. Now the technologies for solar power, wind energy, geothermal heat and different sorts of hydro power are developing fast. The biggest advantages of extracting energy from the sea are that no fuel is needed and that the sea is an inexhaustible and renewable source of energy.

In theory there are 5 ways to extract energy from seawater:

1. The tide

2. Waves

3. Marine current

4. Temperature difference between layers

5. Osmosis

Of the five methods mentioned above, at this moment tidal power seems to be the best option for energy production on a large scale. Since Saemangeum has a mean tidal range of 4.49 m and a large basin is already present (301 km^2 at mean sea level), Saemangeum seems to be the perfect place to build a Tidal Power Plant.

The tides store a tremendous amount of energy. 1.5 TW (TeraWatt) of tidal power is dissipated by friction and eddies alone. Tidal power plants can produce more energy than is dissipated in friction. From the point of view of the total energy balance, this can be explained by the removal of energy from the stationary tidal wave generated in the ocean and dissipated in cosmic processes.

1.3 Energy in South-Korea

For its energy production, South-Korea largely depends on other countries. Korea is a net energy importer, with its total energy consumption exceeding its production by a very large margin. Korea currently ranks as the 10th largest energy-consuming nation. The energy policy of the Republic of Korea is based on The Second National Energy Plan for 2002-2011. This document defines the Korean energy sector's strategy for the near term. As a result of a policy aimed at diversification, South Korea's dependence on Middle East oil has decreased by one-third since the early 1980s.

Recently climate change problems have also been an important factor forcing South Korea to change its traditional energy policy. Since the Kyoto Protocol has come into effect, the Korean government has announced a goal of increasing the supply of renewable energy from 2.3% in 2003 to 3% in 2006 and 5% in 2011[1].

- Oil - Korea has no oil production and no domestic oil reserves. All of its petroleum is imported.

- Gas - Korea does not produce natural gas in any significant quantity. Natural gas consumption in Korea has increased dramatically over the past decade and is now more than 400% greater than it was ten years ago. Korea's energy diversification policy has planned for extended use of natural gas, as well as other alternative fuels, in order to reduce its dependence on petroleum as a primary energy source.

- Coal - Korea is only a minor producer of coal and its production has decreased over the past decade. Korea's energy diversification policy has planned for extended use of coal, as well as other alternative fuels, to reduce its dependence on petroleum as a primary energy supply.

- Electricity - Electricity generation in Korea has dramatically increased, by nearly 250%, over the past decade. About one-third of Korea's electricity is now generated

---

[1]Source: www.cia.gov

by nuclear power, and this is expected to increase to more than 40% by the year 2010 There are 20 nuclear plants in operation in South Korea, 6 more are under construction. The Korean government estimates that electricity consumption will increase by about 4% per year through the year 2015. At present the annual electricity use per capita is about 7000 kWh[2]. This includes industrial use.

1.4 Problem description

1.4.1 Definition of the problem

The main goal is to investigate if a Tidal Power Plant (TPP) would be technically possible and economically feasible for Saemangeum. This should result in a design for a Tidal Power Plant.

1.4.2 Questions to be answered and choices to be made

What choices should be made?

- What concept of TTP should be chosen (1 or 2 basins, 1 or 2 directions, etc)? See Section 2.4.

- What would be the best location to build the TPP?
  Where along the dam (former opening in dam)?
  At the sea side or the basin side of the dam, or in the middle of the dam?

- What would be the TPP's optimal dimensions and specifications?
  Types and numbers of turbines and generators
  Sluices: number, locations, dimensions

- What would be the main characteristics?
  Capacity (MW)
  Energy output (GWh)
  Water levels and water volumes
  Differences between production at neap tide and spring tide

- How should it be built (construction method)?

- How can possible additional future functions of Saemangeum be taken into account and which effect would those other functions have on the TPP?
  Polders for agricultural, industrial or residential purposes
  Newly to be built Gunsan/ Saemangeum port
  Fresh water basins

---

[2]Source: www.eia.doe.gov

1.4.3 Design studies

The design is to be examined by use of a computer model (storage basin approach). It must be possible to vary the boundary conditions in order to incorporate possible additional future functions mentioned in Section 1.4.2. Furthermore an economic feasibility study is to be carried out.

1.4.4 Study approach

The next chapter contains a literature study; The theory of tidal power is described (history, advantages and disadvantages of tidal power, the different concepts of TPP's) as well as a study of precedents (existing plants and feasibility studies) and some theory of turbines.

In Chapter 3 it is thoroughly described how a Storage Area Approach Model of Saemangeum basin has been made.

Chapter 4 tells how to come to the design parameters by using approximation formulas and different development plans for the Saemangeum area are presented.

In Chapter 5 the dimensions of the power house structure and bed protection are calculated and the construction method is discussed.

The economic feasibility is discussed in Chapter 6; First the values of the economic parameters are determined and the construction costs are calculated. Then the Net Present Value is calculated and the sensitivity for changes in the economic parameters is checked.

In the last Chapter (Conclusion) the resulting design and main characteristics are listed, as well as recommendations for further studies.

2 Literature study

2.1 A brief history of tidal power

During the Roman occupation of England, tide mills were built to grind grain. These tide mills operated by storing water behind a dam during high tide. As the tide receded the water was let out from behind the dam, passing the water mill wheel in order to power the grinding stones of the mill.

In 1999 in Nendrum (UK) during archeological excavations a stone built tidal mill was unveiled, dating back to 787 A.D. The first tidemill in the Netherlands was located in Zierikzee (round 1220). As early as in the 12th century AD the first tidal mills in France were developed at the Atlantic coast. In the middle ages tidal power was mainly used for grinding grain. An example of this is the Eling Tide Mill, see figure 2.1[1].
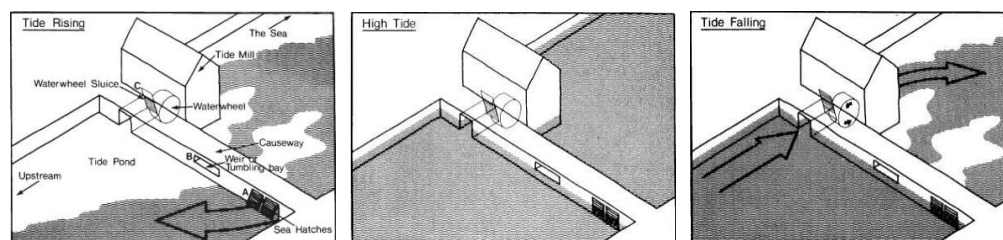
Figure 2.1: *The functioning of the first tidal mills. Diagrams from Eling Tide Mill Trust Ltd.*

In 1737 the treaty of hydraulic architecture of Belidor discusses tidemills of Dunkirk and seeks to ensure the continuity of operation of it, the first testimony in writing of the technique on the energy of the tides [Gibrat, 1966].

At the end of the 19th century the first ideas were born on how to gain electrical energy from the tides. But it took some more decades before the first attempt was taken to actually build a tidal power plant.

In 1913 Johannes Ringers designed a tidal power plant for Hansweert (Zeeland, the Netherlands). Minister Lely of Public Works gave his approval, but the TPP was never built. AEG, a German company, was supposed to supply the turbine, but since the first world war broke out in 1914 they never delivered the turbine.

In 1928 the French parliament approved the building and equipment of a pilot plant at L'Aber-Wrac'k. This plant was also never built.

In 1935 construction of a large TPP at Quoddy started (USA).

Several studies were done for other locations, for example: The Severn estuary and the Bay of Fundy. At that time at different occasions tidal power was considered too expensive for

---

[1]source: www.elingtidemill.wanadoo.co.uk

different reasons:

- In Russia (at Kislogubskaya (a 1940 project) the tidal power would cost twice as much as power supplied by a river power plant.

- Power supplied by L'Aber-Wrac'k would have cost 10 % more than thermal power.

- For the Severn a 1930 study showed that tidal power would have been 20 % more expensive than thermal power.

- Power supplied by the Quoddy TPP was twice as expensive as thermal power and four times as expensive as river hydropower plants.

At the end of the fifties there was a renewed interest in tidal power, because an energy deficit was threatening the western countries.

The "Moulin du Prat" is a 19th century mill, which has recently been renovated, located in the south of the Rance estuary. For a scheme of the functioning of this mill, see Figure 2.1 on page 7.

Figure 2.2: 19th century Moulin du Prat (left) and scale model of Moulin du Prat (right)

In 1890 Decoeur was the first to propose utilising the Rance estuary for electrical power production. During the First World War the price of coal was booming. This increased the interest in alternative energy sources, including gaining energy from the tides.

In 1918 The "Commission de la Houille Bleue" (Blue Oil Commission) was established. In the twenties they analyzed several project locations and designs.

In 1921 Boisnier published a study in which he recommends particularly to use the La Rance estuary for a tidal power plant, because there both the economic and the natural conditions were most suitable.

In july 1960 the French government decided to build the Rance TPP instead of an nuclear power plant. It has now been in operation since 1966 and its yearly true output is about 544 GWh. The installed capacity is 240 MW. The Rance estuary is 2 km wide in some places and penetrates into the mainland as far as 21 km. The river runoff varies between 0.5 and 120 m^3/s. The tide has a regular semidiurnal pattern (index 0.05), see Section 2.2.

The range varies between 13.5 m (highest tide, with a coefficient of 1.2, recurrence once in 28 years) to 3 m at neap tide, the average tidal range at equinox is 11.36 m, the average tidal range 8.45 m, the average neap tide range is 5.4 m (coefficient 0.45). The tidal flow varies as a function of the range between 4.000 and 20.000 m^3/s. In the river estuary there are large areas uncovered at ebb; as the surface area varies between 4.75 km^2 at lowest and 22.6 km^2 at highest spring tide, 130 million m^3 sea water flow into and out of the basin. A single basin, double effect plant was built.

In 1968 the pilot TPP at Kislaya Guba (0.4 MW) in Russia was taken into operation.

In 1984 the pilot TPP at Annapolis (18 MW) in Canada was taken into operation.

In 2005 the construction of Sihwa TPP has started in South Korea. It is expected to be operational in 2009.

2.2 The tides

The tides are caused by the gravitational attraction of the Sun and the Moon on the Earth and the rotation of the Earth. Since the Earth rotates relative to the Moon in one lunar day (24 hours, 50 minutes), each of the two tidal bulges travel around the earth at that speed, leading to one high tide every 12 hours and 25 minutes. The height of the high and low tides (relative to mean sea level) varies. Around new and full Moon when the Sun, Moon and Earth form a line (a condition known as syzygy), the tidal forces due to the Sun reinforce those of the Moon. The tides' range is then at its maximum: this is called the spring tide. This word is derived from the Dutch verb 'springen', meaning to jump or to leap up. When the Moon is at her first quarter or third quarter, the Sun and Moon are in an angle of 90° to each other seen from the Earth and the forces due to the Sun partially cancel out those of the Moon. At these points in the lunar cycle, the tide's range is at its minimum: this is called the neap tide.
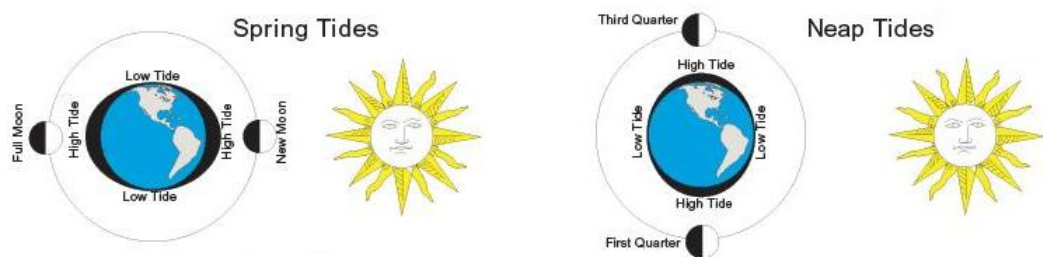
Figure 2.3: Spring tide and neap tide caused by the Moon and the Sun

There are many tidal components. The main two are:

- The principal lunar component: M_2

  The tide-element caused by the Moon is by far the largest component. The lunar tide-generation force at any point on the globe is equal to the difference between the force of attraction by the Moon and the centrifugal force caused by the rotation of the

Earth-Moon-system. The time between two full moons is called the synodic month and is equal to 29 days, 12 hours, 44 min and 3.3 s on average.

- The principal solar component: S_2

  The tide caused by the Sun is, according to Newton's theory, governed by the same principles as the lunar tide, but due to the distance between the Sun and the Earth its value is 2.17 times smaller. The gravitation strength between two masses decreases with the distance.

Table 2.1: *Tidal components with their abbreviations, periods and relative sizes (if the sea would cover 100 % of the Earth's surface)*

Main components	Name	Period (hours)	Relative size
Principal lunar	M_2	12.42	100
Principal solar	S_2	12.00	47
Large lunar elliptic	N_2	12.66	19
Lunar-solar declinational	K_2	11.97	13
Lunar-solar declinational	K_1	23.93	58
Principal lunar declinational	O_1	25.82	42
Principal solar declinational	P_1	24.07	19

Around the world different tide patterns are observed:

- Diurnal tide: One high and one low tide per day.
- Semidiurnal tide: Twice occurring high and low tide sequences, high and low tides are both at the same level.
- Semidiurnal mixed tide: Combination of diurnal and semidiurnal tides patterns. Each high tide reaches different heights and each low tide falls to different levels.

If one wants to know if a certain site has a diurnal, semidiurnal or a semidiurnal mixed tide, the ratio $(H_{K1} + H_{O1})/H_{M2}$ should be calculated;

0 - 0.5: semidiurnal

0.5 - 4: mixed tide

> 4: diurnal tide

In the case of Saemangeum: Ratio ≈ 0.2 so Saemangeum has a semidiurnal tide.

The period of inequality is 14.2 days on average. A period of about 18 years should be considered for a complete analysis of all tidal inequalities (223 lunar months, the so-called Chaldean period or Saros cycle) [Bernshtein, 1965]. The Saros cycle is an eclipse cycle with a period of 18 years, 11 days, and 8 hours that can be used to predict eclipses of the Sun and Moon. One Saros after an eclipse, the Sun, Earth, and Moon return to approximately the same relative geometry, and a nearly identical eclipse will occur.

The local amplitude strongly depends on the shape of the coast. In bays and inlets the funnel-effect can be huge: At the entrance of the Bay of Fundy the tidal difference is only
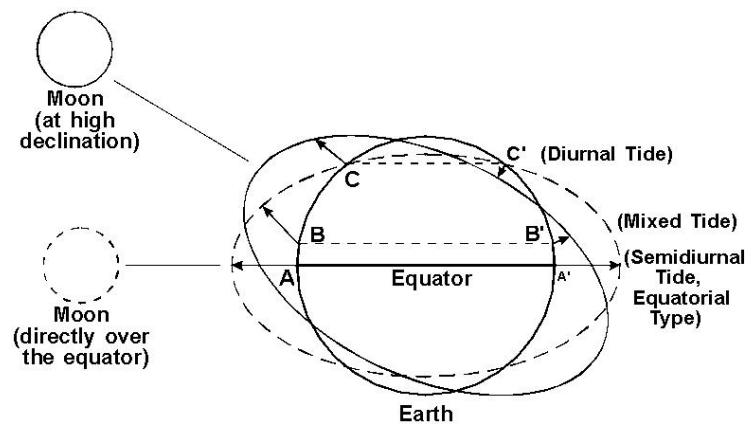
Figure 2.4: *Lunar declination tide component*

2 meters, while at the end the difference is 16.8 m. Tidal power offers an enormous global potential: $7 \cdot 10^{16}$ kWh per year energy potential [Bernshtein, 1965].

The tidal amplitude can increase due to:

• Resonance: proportion between wave length and length of estuary has to be 2 to 4.

• The funnel effect in an estuary

• The force of Coriolis

2.3 Why tidal power?

2.3.1 Advantages

There are many reasons to choose for tidal power:

• The most logical reason: There must be a relatively nearby need for electricity.

• Tidal power does not produce CO_2.

• Constant and predictable monthly average output

• Constancy and predictability over the years

• Countries like France and South-Korea now strongly depend on one sort of energy: nuclear energy. A diversity of power-supply is attractive to be independent of other countries.

• No sharp seasonal variations (change of seasons, drought, rainy years)

• No long term changes

• The technological accident-risk is much smaller in comparison to for example nuclear plants and hydropower-dams.

• People won't have to move (like in China: 3 million people moved for the building of the Three Gorges Dam).

• An additional advantage is that the barrage can serve as a protection against flooding.

2.3.2   Disadvantages

Disadvantages of tidal power plants:

• Most concepts of TPP's (see Section 2.4) produce blocks of energy; this means that during parts of the day the plant produces energy, but the other parts of the day there is no energy-output. The power grid must be able to compensate these blocks without energy production by means of other energy plants.

• For generating energy, a large discharge is necessary, because the head is relatively low. This requires huge structures and thus makes it expensive.

• In order to maximize the power generation, turbines should be able to change direction of rotation periodically. This makes the technology more complicated (and expensive) than river hydropower.

• The tidal range is not constant. A variable head means a variable output. There are diurnal, fortnightly and seasonal variations (vary by a factor 3). This means that the power delivered varies by a factor 8! (because P $= \frac{1}{2}$ AH^2, [Van Duivendijk, 2004])

• Due to storm surges sometimes the low water level outside the basin will not be low enough, which reduces the energy output.

• Turbines cannot operate under a head less than half a meter (in case of bulb turbines this is usually even 1.5 meter or more).

• Salt water makes operation and maintenance expensive (corrosion).

• The change of the tide in the basin and the presence of a barrage has effects on the flora and fauna, see Section 2.5.

Finally, in spite of the potential negative effects of such an installation on local societies, on fauna and on the local flora, the tidal energy remains a source of completely clean, renewable energy and without any risk. This makes tidal energy an excellent choice for the future.

2.4   Different concepts of tidal power plants

Throughout the years a large nuber of imaginative schemes have been produced in order to find effective ways of extracting energy from tidal basins. Practical engineering considerations and environmental concerns have reduced the number of feasible options to four. Three of them comprise one basin, one comprises two linked basins.

• (a) Single-basin, double effect plant
  The simplest tidal power plant consists of a basin, separated from the sea by a barrage, part of which is a powerhouse equipped with hydraulic turbines. Water enters and leaves the basin through the turbines, generating energy on both the incoming and outgoing tides. Such turbines are referred to as double effect turbines. In addition, sluices could be provided in the barrage to raise or lower the water level in the basin to maximise the energy production.

- (b) Single, high-basin plant

  A single basin plant, equipped with sluices and single-effect hydraulic turbines, will be referred to as a single, high-basin plant if the sluices, together with the turbines in the sluicing mode, are used to fill the basin to its highest possible level at high tide and the water is released through the turbines during the ebb, generating power under the maximum possible head.

- (c) Single, low-basin plant

  By the same token, sluices and single-effect turbines can be used to lower the water level in the basin at low tide to its lowest possible level and generate energy at high tide by turbining from sea to basin. Such a plant will be referred to as a single, low-basin plant.

- (d) Linked-basins plant

  Such a plant consists of two basins, one high and one low with a single-effect power plant in between generating energy from the high to the low basin. The dikes separating the basins from the sea would have sluices for filling the high and emptying the low basin. The energy production pattern for such a plant is shown in Figure 2.6.

The output of the single basin plants can be augmented by pumping water near slack tide against a low head in one direction and releasing the same amount of water under a higher head in the opposite direction. Such pumping operations would be performed by the turbine-generators working in reverse as pump-motors.

Figure 2.5 shows three different operating modes for single basin TPP's, showing water elevations of sea and basin vs. time:
(a) single basin, double effect plant, generating energy on both incoming and outgoing tides.
(b) single high-basin plant, generating energy on outgoing tide only.
(c) single, low-basin plant, generating energy on incoming tide only.
Legend: L_s - water level on sea-side of barrage; L_b - water level in tidal basin; T - turbining; Sl - sluicing; H_1 - start-up head for direct turbining; H_2 - stopping head for direct turbining; H_3 - start-up head for reverse turbining; H_4 - stopping head for reverse turbining (direct turbining means from basin to sea, reverse means from sea to basin);
(1): Start of either idle or pumping period (In case of idle period, basin level stays constant until power generation or sluicing starts. In case of pumping into basin, basin level rises until pumping stops. In case of pumping out of basin, basin level goes down until pumping stops);
(2): Start of sluicing.
Vertical-hatching indicates the tidal energy that can be converted to electrical power without pumping, cross-hatching means extra energy thanks to pumping. Note that turbining periods start sooner when pumping is employed, because the starting head is reached
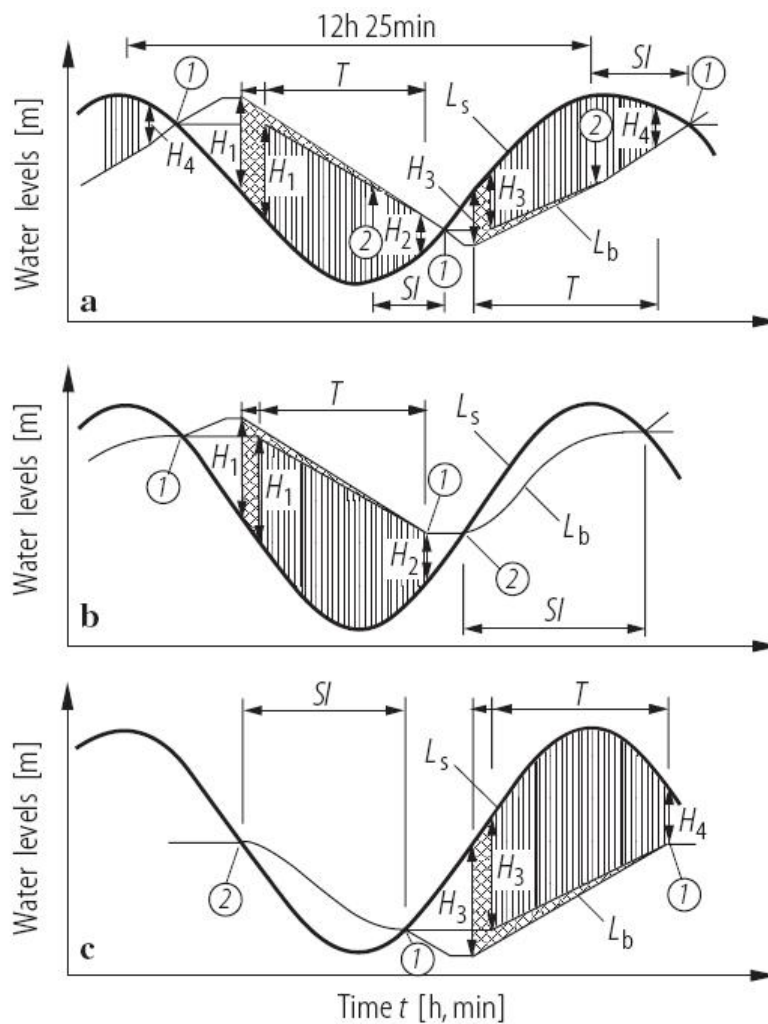
Figure 2.5: *Three operating modes for single basin TPP's*

sooner. Energy required for pumping is not accounted for in the figure.

The energy production patterns for each of the above three types of single-basin plants are shown in Figure 2.5 (a), (b) and (c). Note that, in Figure 2.5 (a), the plant is equipped with sluices. Sluices are not an essential part of a single basin, double effect tidal power plant.

In comparing the above three types of tidal power plants, it is clear that a plant of type (a) produces four blocks of energy per Moon day while plants of types (b) and (c) produce only two such blocks in the same time frame. This indicates that the energy produced by a plant of type (a) would in general be easier to absorb in an electric utility system than the energy produced by either one of plants (b) or (c), because such a system requires a constant input.

When comparing the plant types (a), (b) and (c) on the basis of the amount of expected

energy production, it appears that a plant of type (c) produces the least. A plant of type (b) is superior to one of type (a) in a tidal regime in which the mean tidal range R_{mean} is less than 9 to 10 m while a plant of type (a) is superior in larger tidal ranges [Song & Van Walsum, 2006].

When would one ever choose a plant of type (c)? Such a plant should be considered in case a single high-basin plant is in operation and the construction of an additional plant is being considered. Having a plant producing energy on the outgoing tide, it would make sense from an energy absorption point of view to build the next plant to produce energy on the incoming tide. Such a combination of two independently operating but yet complementary single-basin schemes will be referred to as a paired-basins scheme. There are also site-specific reasons to choose for a plant of type (c): In the case of Sihwa (South-Korea) the reason was mainly because the dikes would not have to be raised, which saves a lot of money if the basin is surrounded by dikes. Also the authorities wanted to change the landscape as little as possible.

Technically it may be quite feasible to operate one and the same plant, if fitted with double-effect machines, in all three of the above listed modes of operation, switching from one mode to another in response to the electric power market's demands. The La Rance plant for instance has the flexibility that such a varying operation requires. However, experience with operating the La Rance plant has shown that, from an environmental point of view (see Section 2.5), regularity in operating a tidal power plant is very important. Since environmental considerations do carry much weight, it has been assumed in this section that single-basin tidal power plants of the future will be designed for and operated in only one of these three modes.

Over the years, the problem of getting energy on demand out of a tidal power plant has been intensely studied. Many of the hundreds of patented inventions deal with the challenge of making the tides provide power on demand. All such efforts have so far resulted in reduced output at an inflated cost per kWh of energy produced.

Various tidal power schemes studied worldwide have all pointed out that a single basin scheme is most suitable for extracting the maximum amount of energy out of a given site at the lowest unit cost. Double or multiple basin schemes appear to produce energy at a unit energy cost which is much too high.

However, none of the double basin schemes considered was to be designed and operated to yield energy at the lowest possible unit cost, but with a purpose to provide a constant output of power.

Figure 2.6 shows the operating mode for a linked-basins TPP with large sluicing capacities, showing water elevations at sea, in the high- and in the low-basin vs. time, giving continuous power. Legend: L_s - water level on sea side of barrages; L_h - water level in high-basin, L_l - water level in low-basin, (1) - sea does no longer replenish water in the high-basin, sluicing stops; (2) - low-basin can start shedding water into the sea, turbining

and sluicing start; (3) - low basin can no longer shed water into the sea, turbining & sluicing stop; (4) - sea can start to replenish water in the high-basin, sluicing & turbining start; H_1 - turbining head at end of "incoming tide" cycle and at start of "outgoing tide" cycle. (All the turbining from high- to low-basin.) At the bottom on the right the power output curve is plotted.
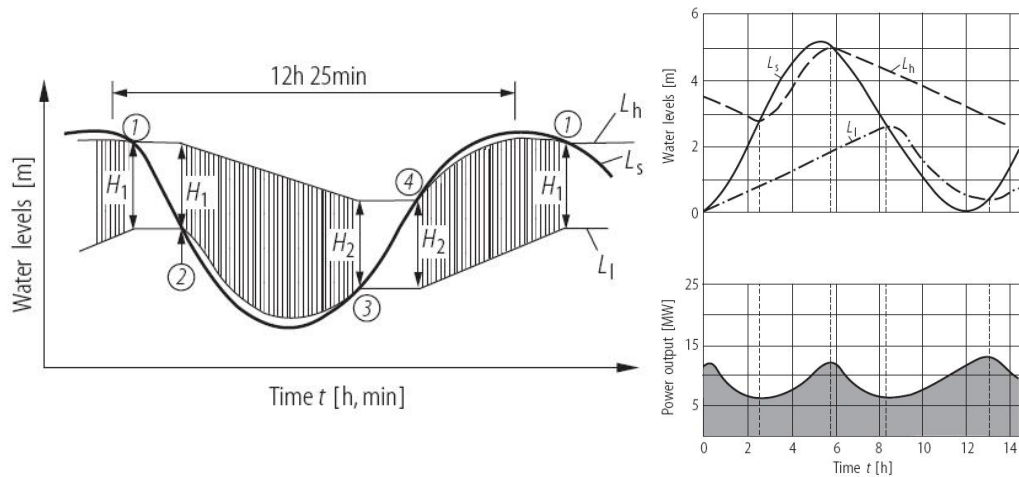
Figure 2.6: *Operating mode for a linked-basins TPP*

With a linked-basins plant, water will pass from sea through sluices to the high-basin, from the high-basin through the turbines to the low-basin and from the low-basin through sluices to the sea. With two passages through sluices, it is important to have a large and efficient sluice capacity to keep head losses across the sluices to a minimum.

In conclusion, tidal power by its very nature is a reliable and predictable energy producer. Forcing it to produce power on demand has proven to be economically counter productive. Moreover, it has been shown that a fixed pattern of plant operation is desirable for environmental reasons. Therefore, a TPP should consistently be operated to maximise energy output. It will depend on site conditions which of the four types of TPP's is most suitable.

Paired basins scheme

A configuration of two combined single basin plants (one of which is a low basin plant, one of which is a high basin plant) is called a paired basin scheme. This is a combination of two different concepts and so is the power output; In Figure 2.7 it can be seen that the main advantage of paired basins is that there is a relatively constant power output, which is favourable for the electricity grid. At high tide the low basin plant generates, while at low tide the high basin plant contributes energy to the electricity grid.
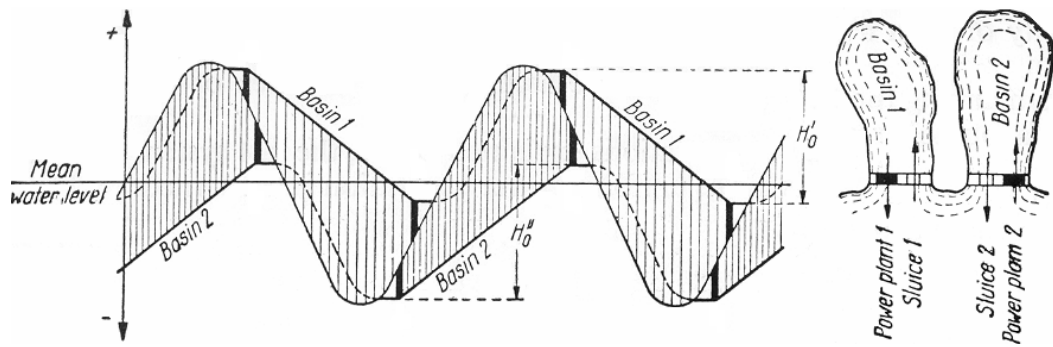
Figure 2.7: *Paired basin scheme; left: operation scheme, right: layout of basins*

2.5 Tidal power and the environment

Traditionally, engineering feasibility studies concentrated on finding the economically most attractive scheme. That scheme was then subjected to environmental analysis. This approach was considered acceptable in the past. Such a conventional study sequence in analysing a project's feasibility is no longer suitable when it comes to tidal power. Along our world's shorelines, the environmental concerns are so numerous and serious that, if they are not faced head on from the start, a great deal of engineering time and effort will be wasted on a project that was doomed to being discarded on environmental grounds.

Large amounts of tidal energy can be generated in extremely isolated locations such as Ungava Bay in northern Québec, Canada, and Siberia, Russia. If and when the hydrogen economy (as energy storage system) materialises, these remote resources would become ready to be harnessed to provide the energy for hydrogen production by means of hydrolysis.

Main environmental problems caused by large-scale tidal barrages

• Barrages block naval traffic. Locks can be installed, as they have been in France, or not, as in Canada. The lock allows some traffic, but it is a slow and costly alternative to free access to the ocean.

• Barrages impede fish migration. Anadromous fish spawn in fresh water and migrate to salt water, then return after three or four years to spawn and die, drawn to the exact location of their birth. Fish are, therefore, instinctively obliged to pass through the turbines of an intervening barrage at least twice. Some fish actually pass through the turbines multiple times. The mortality rate for fish passing through the low-head turbine is about 6 %. Fish ladders are sometimes provided, but the mortality rate of fish using fish ladders is slightly higher than that of passing through the turbines and most fish avoid them.

• Barrages change the size and location of the intertidal zone. The intertidal zone is the area that is alternately wet and dry during the tidal cycles. The alternately wet and dry habitat is unique and only certain types of plants and creatures thrive there. A barrage rearranges the tidal cycle and changes the water levels, thereby moving the wet/dry inter-

tidal zone, obliging plant and animal life to adapt or move to a new location.

• Barrages change the tidal regime downstream. Canada's Bay of Fundy has the largest tidal range in the world and has been the subject of numerous studies of proposed tidal power plant installations. Huge barrages have been proposed and one of the major concerns was the fact that coastal process modelling conjectured that the highest tides downstream of the barrage might be raised as much as 25 cm as far as Boston, more than 1250 km away. This finding was controversial, but, even the possibility of such an impact was seen as sufficient to draw lawsuits from every property owner with a flooded basement from Nova Scotia to Cape Cod.

• Morphological problems. The balance of sediment transport can be disrupted.

During construction there can be temporary environmental problems. During the construction of La Rance TPP the estuary was cut off from the sea for 3 years. In these three years almost all marine animal and plant life had disappeared. After the estuary reopened, marine worms (110 species), shellfish (47 species including lobster, common crabs, spider crabs velvet swimming crabs) and fish (70 species including bass, spout, pollack) have returned to settle in the inlet: thanks to their passage through valves and turbines, a wide variety of marine animal life has reappeared.

Economic Problems of Barrages

The environmental problems of tidal barrages have created opposition from environmental groups and local inhabitants, requiring either costly efforts to overcome the objections through further studies or abandonment of the proposals. The barrage also suffers from high capital costs and a relatively low load factor of about 28% (environmental considerations limit generation to single-effect ebb tide-only generation).

2.6   Study of precedents

Although the first plans to build tidal electric power plants were made in the 19th century, there are only a few operational plants in the world; most of them are pilot plants. For a long time tidal power has been considered to be too expensive. The only large scale TPP in the world was built in the sixties in Brittany, France, in the Rance estuary near Saint Malo. Nowadays, due to booming oil prices and the demand for renewable energy, tidal power has become interesting again. There are plans to build TPP's in the Severn estuary (Wales), the Bay of Fundy (Nova Scotia, Canada) and the Gulf of Cambay (Gujarat, India). At this moment the largest TPP in the world is under construction at Sihwa, South Korea, see subsection 2.6.2. Numerous feasibility studies have been done throughout the years, see subsection 2.6.4. This section discusses the performances of La Rance, Sihwa (expected performances) and Annapolis (pilot plant in Canada).

2.6.1 La Rance

To get a visual idea of how a TTP works, the La Rance Tidal Power Plant in France has been visited. This TPP is a most important reference, because it is the only one in the world that was built to produce energy for commercial purposes. All other TPP's in the world are either study-projects, or built on such a small scale that they are not useful as references. The La Rance estuary is situated in the northwest of France in the province of Brittany. Because of the shape of The Channel the tides are very high. The Rance estuary was superbly suitable for building a TPP, because with a relatively short dam (750 meters) a large volume of water could be used for operational purposes.
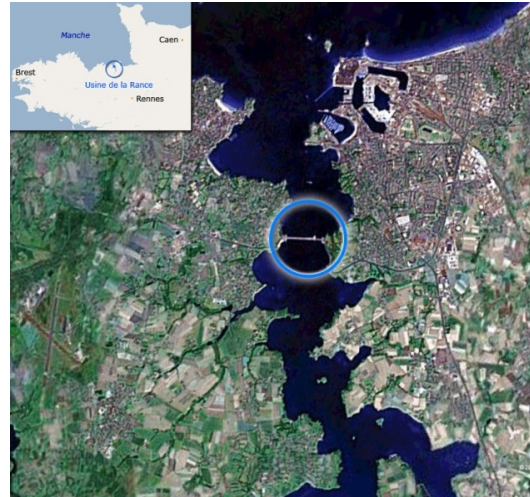
Figure 2.8: *Sattelite image of La Rance estuary with barrage*

In January 1961 the works started and in July 1963 La Rance was cleaved in two. In 1966 the TPP was inaugurated by president Charles de Gaulle and the last bulb-group was brought into service in December 1967.
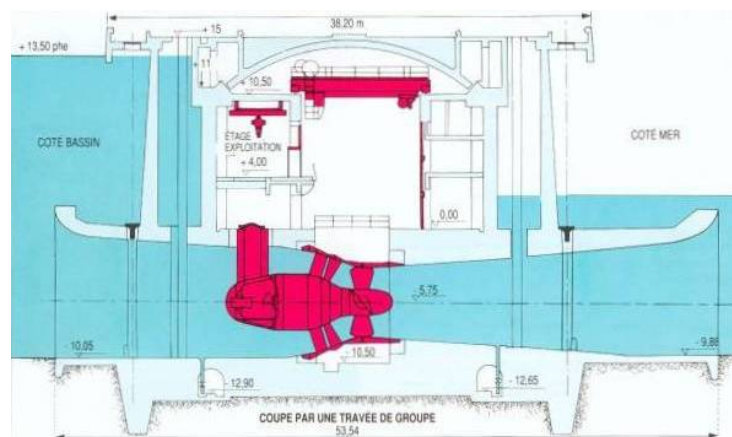
Figure 2.9: *Cross-sectional view of La Rance Turbine*

La Rance Turbines

The type of turbines use for the La Rance plabt are horizontal axis Bulb turbines. The blades of the turbines can change directions depending on the flow direction and speed. The plant is also equipped with pumps that allow water to be pumped into the basin when
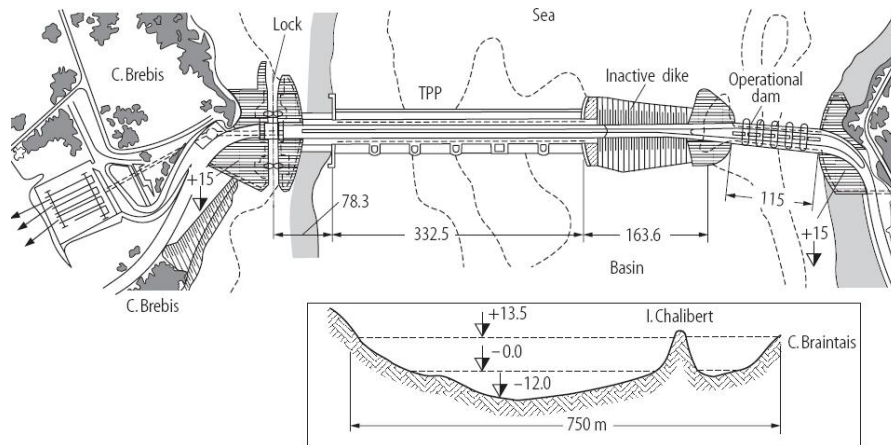
Figure 2.10: *Map of dam and sluices and depth profile at La Rance TPP*

Table 2.2: *Figures and facts about La Rance TPP*

Area at MSL	17	km^2
H$_r$	5.6	m
R$_{max}$	13.5	m
R$_{mean}$	8.45	m
R$_{spring,ave}$	10.9	m
P$_i$	240	MW
E$_{y,net}$	600	GWh
Length of barrage	750	m
Length of power house	332.5	m
Length of sluices	115	m
N$_t$	24	
P$_{i,t}$	10	MW
Construction costs then	620	MFF
Construction costs now	534	M€

Table 2.3: *Overview of 7 consecutive years of operation of La Rance TPP. Legend: DT-Direct turbine, RT-Reverse turbine, DP-Direct pumping, RP-Reverse pumping, OT-Off turbine.*

Year	Production (GWh)			Period (total for the 24 units)						
	Gross	Net	True	DT	RT	DP	RP	OT	Total	Hours
1980	503	495	485	64	5	3	0.1	28	100	116800
1981	570	562	500	61	2	16	0	21	100	134700
1982	607	599	511	59	2	18	0	21	100	151000
1983	610	601	503	57	6	17	0.1	20	100	255900
1984	609	601	494	58	3	18	0	21	100	257500
1985	612	603	485	58	5	19	0	18	100	158000
1986	595	586	487	58	3	20	0	19	100	156400

the sea level is close to basin level at high tide. This allows for more electricity to be generated if there is an anticipated increase in demand.

The data from Tables 2.2 and 2.3 are taken from a booklet provided by EDF (Electricite De France) [EDF, 1996].

2.6.2 Sihwa

South-Korea is not unfamiliar with TPP's, because at this very moment a TPP is being built in Sihwa. Like Saemangeum, Sihwa was an estuarine tidal flat that has been dammed. The installed capacity is going to be 254 MW, what makes this plant slightly larger than the Rance TPP and therefore this will, for the time beeing, be the largest TPP in the world. The project is expected to be completed by 2009.

Figure 2.11: *Satellite image of Sihwa*

The project will cost approximately US$ 250 Million. The project will consist of a power house for 10 bulb turbines with direct driven generators including gates and other equipment. The power plant is designed to be operated in one direction: from the sea to the Sihwa Lake (low basin plant). The reasons to choose for flood generation (as opposed to ebb generation, which would be more profitable) are: The authorities want to change as less as possible. Also the ebb generation would require higher dams and dikes. In doing so, the plant will generate electric power by using the head between the high tide and the reservoir level.

The Korea Water Resources Corporation (KOWACO) is the governmental water authority of South Korea and acts as the project developer/ owner. Daewoo, as leader of

Figure 2.12: *Impression of TPP Sihwa; Legend: 1-Turbines and generators; 2-Sluice gates; 3-Connecting structure; 4-Wing wall; 5-Road; 6-Tourist site; 7-Administration facilities; 8-Construction bay/ central control room.*
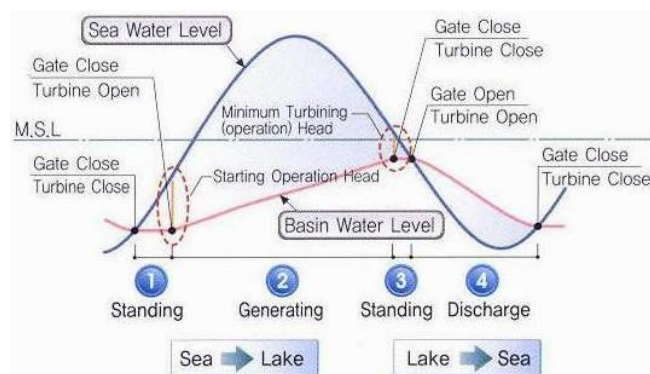
Figure 2.13: *Operation cycle of TPP Sihwa*

the Korean joint venture with other civil companies, is the project's main contractor. VA Tech Hydro, an international supplier of equipment and services for hydropower plants, was awarded a contract from Daewoo Engineering & Construction for engineering and delivery of the main electromechanical components. The project sum VA Tech receives for supplying all electromechanical equipment is US$ 94 Million.
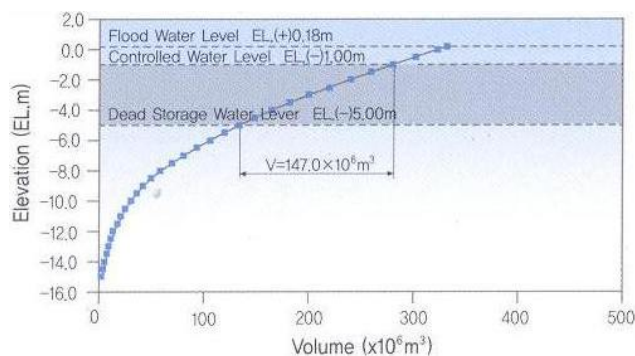
Figure 2.14: *The relationship between water level and volume of lake Sihwa*

In Figure 2.14 an elevation-volume curve is displayed. Between the water levels EL -1.00 m (controlled water level) and EL - 5.00 m (dead storage level) the volume is V = $147 \cdot 10^6$ m^3.

Not only will the project generate power, also the existing water quality of the Sihwa Lake will be significantly improved. Due to industrial facilities taking process water out of the lake and releasing waste water into it, the lake is heavily polluted. Regularly flushing the Sihwa Lake with seawater was seen as an acceptable method of remediation. Such an investment would only be cost-effective, if the operator simultaneously gained profit out of the energy production of a tidal power plant.

2.6.3 Annapolis

In 1984 the first (and only) TPP of North America became operational in Nova Scotia (Canada), near the village Annapolis. Construction began in 1980. The plant's generating cycle starts with the incoming tide, when the sea level reaches the level of the reservoir; the sluice gates are opened to fill the head pond. When the pond reaches its maximum level (less than high tide in the case of Annapolis), the sluice gates close to trap the seawater upstream from the turbine. As the tide recedes, a head develops between the head pond and the seaside. When a head of 1.6 meters or more is produced, the gates of the distributor assembly are opened. These gates control the flow of water through the turbine. The power generating phase of the cycle continues until the level of the head pond has dropped to within 1.6 meters of the incoming tide, which it does in just over five hours. Then, the wicket gates close, awaiting a repeat of this twice daily tidal cycle. The Annapolis system uses a single-effect turbine that generates electricity only in one direction - when the flow of water is towards the sea. During one tidal cycle (about 12 hours), the Annapolis station comes on for five hours, then it's off for seven hours, generating about 40 GWh annually, enough energy to power over 4000 homes. Nova Scotia Power's Annapolis Tidal Power Generating Station attracts over 40,000 tourists annually [anonymous, 2002].
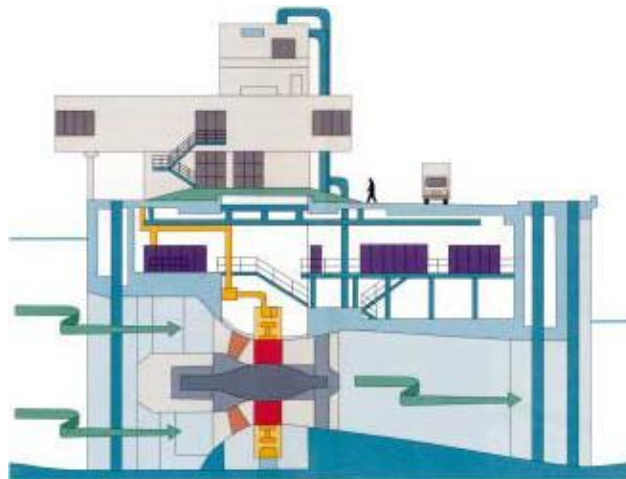
Figure 2.15: Cross section of Annapolis TPP with one straflo rim-type turbine

Table 2.4: *Main parameters of Annapolis turbine & generator [DeLory & Eng, 1986]*

Diamater of turbine runner	7.6	m
Number of blades	4	
Number of wicket gates	18	
Normal operating head range	1.4 to 6.8	m
Maximum operating head	7.1	m
Rated operating head	5.5	m
Turbine output at rated head	17.8	MW
Turbine maximum output	19.9	MW
Discharge at rated head	378	m^3/s
Turbine efficiency (at rated head)	89.1	%
Rated speed	50	rpm
Generator efficiency	96.5	%

2.6.4   Overview of worldwide feasibility studies

Table 2.5: *Existing TPP's and Feasibility studies (Sihwa: under construction)*

Parameter	Existing plants			Feasibility studies	
	La Rance	Annapolis	Kislaya Guba	Sihwa	Mersey
A$_{MSL}$	17	15	1.1	42.4	60
R$_{mean}$	8.45	6.4	2.4	5.57	6.45
H	5.6	5.5	1.35	5.82	
E$_y$ nett (GWh)	540	45	0.6	552.7	1500
P$_i$	240	17.8	0.4	254	700

Data of Mersey barrage from the lecture notes of 'Water power engineering' [Van Duivendijk, 2004] and data of Sihwa from booklet provided by plant contractor and government [KOWACO & DAEWOO, 2006].

As can be seen from Table 2.6, a large number of places are suitable for tidal power plants, compared to the number of existing plants. Thus far it has simply been too expensive to build a TPP, compared to traditional fossil fuel plants. Now that the prices of fossil fuels are rising, tidal power becomes an interesting feasible alternative.

Table 2.6: Overview of worldwide feasibility studies

Country	Location	Mean tidal range (m)	Basin area (km^2)	Capacity to be installed (MW)	Calculated annual output (TWh/year)	Annual plant load factor (%)
Argentina	San Jose	5.8	778	5040	9.4	21
	Golfo Nuevo	3.7	2376	6570	16.8	29
	Rio Deseado	3.6	73	180	0.45	28
	Santa Cruz	7.5	222	2420	6.1	29
	Rio Gallegos	7.5	177	1900	4.8	29
Australia	Secure Bay	7.0	140	1480	2.9	22
	Walcott Inlet	7.0	260	2800	5.4	22
Canada	Cobequid	12.4	240	5338	14.0	30
	Cumberland	10.9	90	1400	3.4	28
	Shepody	10.0	115	1800	4.8	30
India	Gulf of Kutch	5.0	170	900	1.6	22
	Gulf of Khambat	7.0	1970	7000	15.0	24
Korea (Rep)	Garolim	4.7	100	400	0.836	24
	Cheonsu	4.5			1.2	
Mexico	Rio Colorado	6-7			5.4	
UK	Severn	7.0	520	8640	17.0	23
	Mersey	6.5	61	700	1.4	23
	Duddon	5.6	20	100	0.212	22
	Wyre	6.0	5.8	64	0.131	24
	Conwy	5.2	5.5	33	0.060	21
USA	Pasamaquoddy	5.5				
	Knik Arm	7.5		2900	7.4	29
	Turnagain Arm	7.5		6500	16.6	29
Russia	Mezen	6.7	2640	15000	45	34
	Tugur	6.8	1080	7800	16.2	24
	Penzhinsk	11.4	20530	87400	190	25

2.7 Turbines

2.7.1 Types of turbines

The first truely high-efficient water turbine was constructed by Benoit Fourneyron in 1827. Its first installation was in a saw-mill in Pont sur l'Ognon (France). Fourneyron's turbine was of the radial-outflow type (see Figure 2.16) and reached a maximum efficiency of 85%.

The behaviour of a turbine is predominantly determined by the parameters listed in Table 2.7.

Categorising turbines

There are a wide variaty of hydroturbines. A first distinction can be made between impulse and reaction turbines.

An impulse (equal pressure) turbine is a turbine that is driven by high velocity jets of
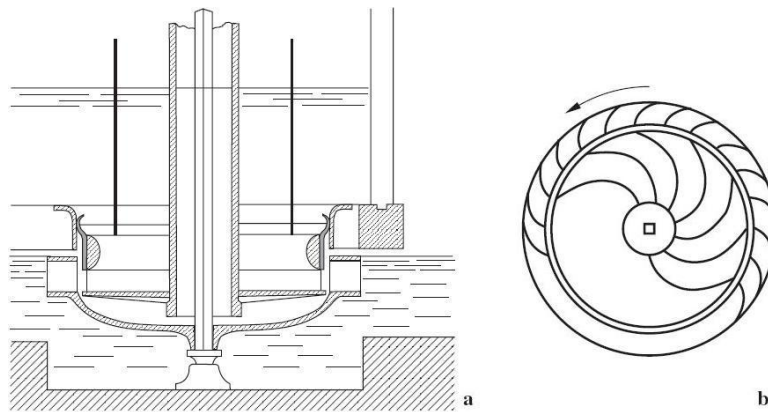
Figure 2.16: *Fourneyron turbine; (a) Meridional section. (b) Cross section.*

Table 2.7: *Turbine parameters*

Parameter	Symbol	Unit	Notes
Head	H	m	Difference in water levels across turbine
Flow of water	Q	m^3/s	
Throat area of turbine	F	m^2	
Rated power output	P_r	kW	
Turbine efficiency	η_t	%	
Runner diameter	D	m	
Rotational speed	n	rpm	revolutions per minute

water from a nozzle directed on to vanes or buckets attached to a wheel. The resulting impulse spins the turbine and extracts kinetic energy from the fluid flow. Before reaching the turbine the fluid's pressure head is changed to velocity head by accelerating the fluid through a nozzle. This preparation of the fluid jet means that no pressure casement is needed around an impulse turbine.

A reaction (overpressure) turbine is a type of turbine that develops torque by reacting to the pressure or weight of a fluid; the operation of reaction turbines is described by Newton's third law of motion (action and reaction are equal and opposite). In a reaction turbine, unlike in an impulse turbine, the nozzles that discharge the working fluid are attached to the rotor. The acceleration of the fluid leaving the nozzles produces a reaction force on the pipes, causing the rotor to move in the opposite direction to that of the fluid. The pressure of the fluid changes as it passes through the rotor blades. In most cases, a pressure casement is needed to contain the working fluid as it acts on the turbine; in the case of water turbines, the casing also maintains the suction imparted by the draft tube.

Most types of turbines exploit the principles of both impulse turbines and reaction turbines. However, a few, such as the Pelton turbine, use the impulse concept exclusively. In general one can say that impulse turbines are designed for high head plants and reaction turbines are better suited for low head plants like tidal power plants. In Table 2.8 the different types of turbines are listed in relation to the head they are used for.

Another way to categorise turbines is the manner in which the flowing water hits the blades of the rotating runner or wheel:

Axial turbines:	Propeller and Kaplan turbine;
Half-axial turbines:	Deriaz type;
Radial turbines:	Francis type;
Tangential turbines:	Pelton wheel.

Single and double regulated turbines:

Single regulation by means of the guide vanes only: Francis, propeller, Straflo

Double regulation by means of guide vanes and adjustable runner blades: Kaplan, Bulb, Deriaz

Table 2.8: *Head-flow ranges of hydro turbines*

Turbine Type	Head Classification		
	High (≥50m)	Medium (10-50m)	Low (≤10m)
Impulse	Pelton Turgo Multi-jet Pelton	Crossflow Turgo Multi-jet Pelton	Crossflow
Reaction		Francis (spiral case)	Francis (open-flume) Propeller Kaplan
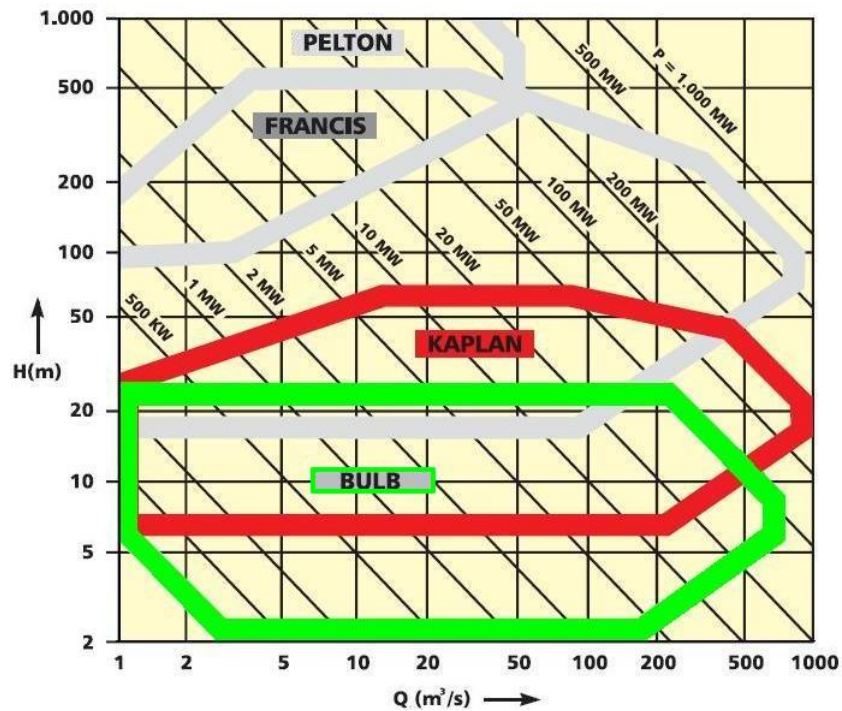
Figure 2.17: *Turbine application chart*

From Table 2.8 it is clear that for tidal power plants reaction turbines must be chosen,

because of the applicability at relatively low heads. In Figure 2.17 more turbine application data are plotted in a graphical chart. The applicability of a turbine in this figure not only depends on the available (effective) head, but also on the magnitude of the flow through the turbine. The black diagonal lines indicate the power that corresponds with that specific combination of head and flow. In the chart wide ranges of heads (2 to 1000 m) and flow (1 to 1000 m^3/s) are shown. The maximum head for Saemangeum will never be (much) higher than the average spring tidal range (most probably lower), which is 6.49 meters. According to the chart the best (and only) option is a Bulb turbine. Most (pilot) tidal power plants in the world are equipped with bulb turbines. Bulb turbines are submerged horizontal axis Kaplan turbines.
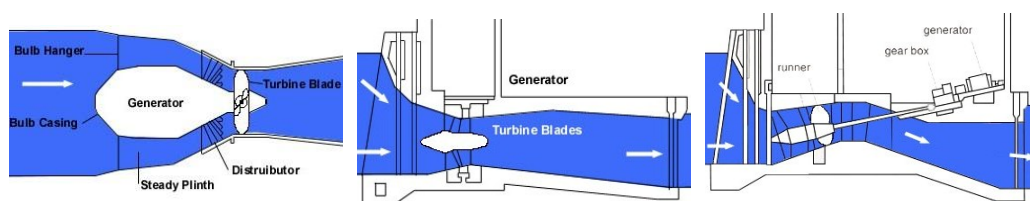
Figure 2.18: Sketches of a bulb-, rim (straflo)- and tubular-turbine (by Boyle, 1996)

Kaplan turbines

The Kaplan turbine was invented by Viktor Kaplan in 1912. It is applied to low heads. There are roughly three types of Kaplan turbines. The main difference between these types is the location of the generator with respect to the turbine. In a conventional Kaplan turbine (vertical axis) the fluid has to pass several bends which causes additional flow losses. In 1919 the idea of a tubular arrangement existed, avoiding unnecessary bends and leading to more favorable flow conditions. The tubular Kaplan turbine is preferably applied to smaller capacities.

Bulb turbines

For low heads horizontal axis Bulb turbines will be an alternative to the vertical Kaplan turbines. The Bulb turbine offers more favourable inlet flow conditions to the runner than a vertical Kaplan turbine. These favourable flow conditions have the effect that the runner diameter of a Bulb turbine may be made 15 % smaller than for a vertical Kaplan turbine under otherwise equal conditions. The flow conditions will also reduce the cavitation risk for the Bulb turbine, which means less submergence is needed than for the vertical Kaplan turbine.
The Bulb turbine is still more favourable if only one unit shall be built because the scroll casing of a vertical Kaplan turbine makes the power station much wider. The pressure will be limited to 15 - 20 m head for Bulb turbines [Kjølle, 2001].

Bulb turbines incorporated the generator-motor unit in the flow passage of the water. These turbines are used at the La Rance power station in France. The main drawback is that water flows around the generator, making maintenance difficult.

A bulb turbine is founded below on concrete, it is supported from the side and is accessible from above via shafts that also accomodate electricity cables and hydraulic pipelines. The guide vanes for the discharge regulation are situated on the outside. Some characteristics are:

- The streamlines are straight; therefore the yield is slightly higher than that of a Kalplan turbine with a vertical axis.

- Simple design of the cicil engineering structures.

- Centre to centre distance betweeen the units can be smaller than in a design including spiral casing.

- The bulb turbine support is quite stiff, which makes the turbine more sensitive to vibrations than the vertical Kaplan.

- Generator diameter is limited by the bulb dimensions, which limits the flywheel effect and with that the stability of the grid.

- Cooling of the generator is more difficult than for the vertical Kaplan turbine.

The maximum dimensions of the bulb turbine are therefore much smaller (up to about 7 to 8 m) than in the classical vertical concept.

2.7.2   Efficiency of turbines

Two characteristics of tidal power based on filling and emptying of a basin are the variable head and the variable discharge. This means that a turbine should be compatible to a variable head and discharge. At the same time it should be as efficient as possible. Turbines cannot convert all the potential energy of the water into elecric energy. There are three types of energy losses:

1. Leakage losses: loss of water bypassing the blades of the turbines.

2. Hydrodynamic losses: fluid friction along blade and wall surfaces and vortices.

3. Mechanical losses in bearings and sealings.

Turbine manufacturers try to minimise these losses. Each turbine is designed with specific optimum values for the head (H) and flow (Q). The turbine efficiency has its maximum for a specific design head (H_{design}) and design flow (Q_{design}). The turbine efficiency can be plotted in a diagram as a function of the head or the ratio between head and design head, or as a function of the flow or the ratio flow/ design flow.In the graph of Figure 2.19 the

efficiency is shown as a function of relative discharge. It is clear that Kaplan turbines have the highest efficiency if the discharge is less than about 80 % of the maximum discharge. This is beneficial for tidal power plants. In Figure 2.20 the turbine efficiency is plotted as a function of the head.
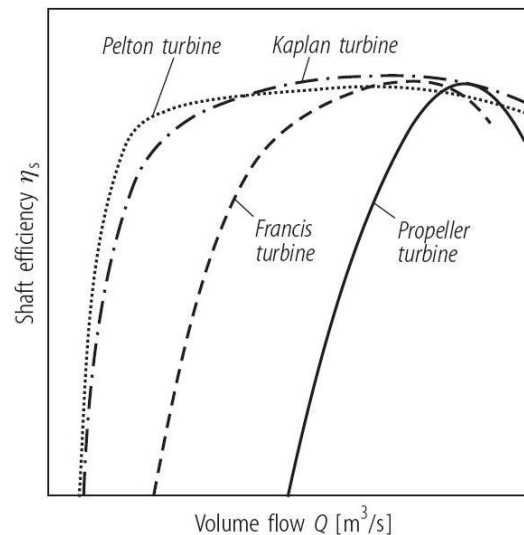
Figure 2.19: *Shaft efficiency vs. volume flow rate for different types of turbines (at constant head and constant speed)*
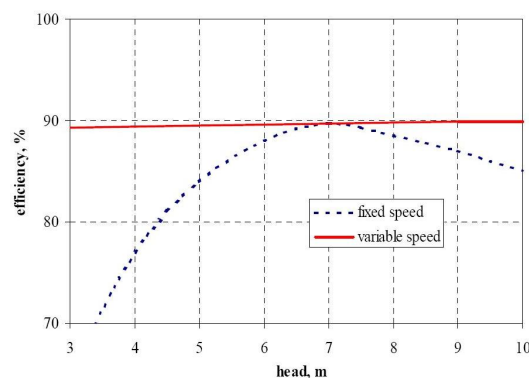
Figure 2.20: *Effect of head and variation on turbine efficiency*

If the efficiency is plotted as a function of both the head and the flow rate, this is called an "efficieny hill chart". An example of a hill chart is given in Figure 2.21. This is a hill chart [Remery, 1982] for a bulb turbine that works in two directions and also includes information about pumping.

In the Tables 2.9 and 2.10 information for La Rance is listed and in Figure 2.22 a hill chart is plotted that is very similar (not 100% the same) for La Rance's turbines.

Generating from basin to sea

In Figure 2.22 a hill chart of turbines designed for La Rance is shown. These are not the turbines that are actually installed, but the chart is based on real turbine testing. Some
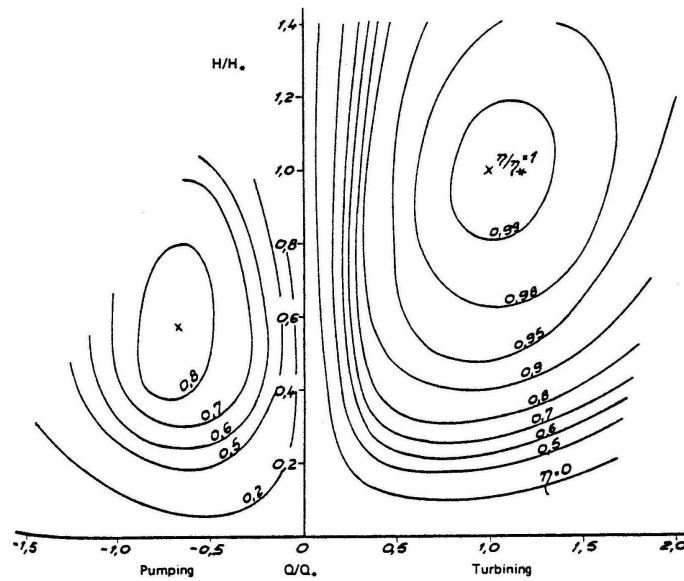
Figure 2.21: *Efficiency Hill Chart of a double regulated bulb turbine (by Remery)*

Table 2.9: *Performance of turbines La Rance, generating*

Head (m)	11	9	7	5	3
Generating from basin to sea:					
Power per turbine (MW)	10	10	10	8	3.2
discharge (m^3/s)	110	130	175	260	200
Generating from sea to basin:					
Power per turbine (MW)	10	10	9.5	5.5	2
discharge (m^3/s)	130	155	230	195	135

Table 2.10: *Performance of turbines La Rance, pumping from sea to basin*

Head (m)	1	2	3	6
Power per turbine (MW)	10	10	10	10
discharge (m^3/s)	225	195	170	105
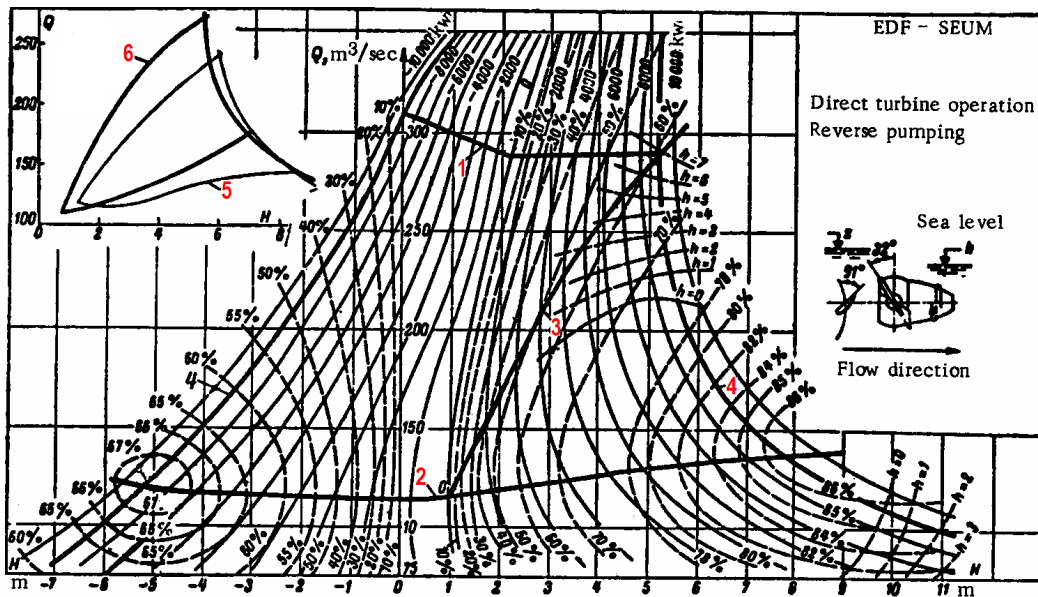
Figure 2.22: *Hill Chart of La Rance Turbines for ebb generation (from basin to sea) and reverse pumping. For flood generation the efficiency is about 14 % lower than in this figure, for pumping in the other direction it is about 7 % higher.*

characteristic points in the chart are numbered:

1. Guaranteed operational line;

2. Maximum efficiency line;

3. Maximum output line;

4. Line of restriction by turbine capacity;

5. Boundary lines of the characteristics of the model: D = 500 mm (scale model testing before actual construction);

6. Boundary lines of the full-scale unit: P = 9 MW; z = water level in the estuary; h = sea level.

3 Modelling Saemangeum basin

To determine the optimum equipment scale of a certain tidal power location, many variables should be considered. It is not possible to solve the problem by an analytical method, because these variables become complicated. Therefore, repeated calculations are needed for determining the optimum exploitation scale. During the preliminary designs, the following steps are usually carried out for deciding the draft size of TPP's. Since one of the main purposes of Saemangeum project is to reclaim land, the available area of basin reservoir capacity should be easy to change to a smaller area in the model. The mean tidal range is 4,49 m and the active volume for the generation of the actual basin between the mean high water level and mean low water level is $1.34 \cdot 10^9$ m^3. This is the volume of water between h = - 2.25 m and h = 2.25 m (this is referred to as the tidal prism). A significant part of this volume of water cannot be used for energy generation, because bulb turbines normally stop generating when the head drops below a certain point. On the other hand, the volume will largely increase in case the turbines would pump extra water into the lake. In this case look at Figure 3.1 how the minimum possible head influences the active volume. Pumping is not accounted for in this figure.
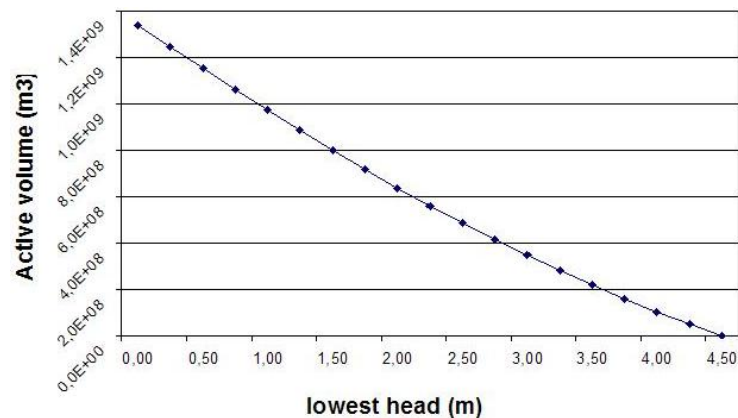
Figure 3.1: *Active Volume at mean tide vs lowest head*

The discharged volume of water for generation per second of tidal power plants can be obtained when the generating time is available. In the case of flood type, after emptying the basin during the ebb tide, the generation begins when the head is sufficiently high (usually 1.5 till 2 m, depending on the turbine) for start of generation during the flood tide. The TPP stops its operation if the level difference is less than about 1 m (depending on the turbine) resulting from the raising of basin level and the lowering of sea level. The available generating time for one tide is generally 4 hours and 30 minutes for one directional generation and about 5 hours and 45 minutes for two directions (At La Rance these 5 hours and 45 minutes consist of 3 hours 35 minutes ebb generation and 2 hours 15 minutes flood

generation on average).

Numerical models are commonly utilized to estimate energy output and productivity per year for a TPP under given oceanic conditions. First, the optimum conditions for generation ought to be obtained according to generation capacity, sluice capacity, and specifications of turbine-generators. After that, the maximum output of electricity generation can be procured for each tide. The total annual energy output of the annual 705.5 different tides is obtained using these procedures. These kinds of calculations are carried out according to varying sluice capacities with fixed generation capacity. The approximate construction costs for each case could be estimated from the costs during TPP's designs. The energy cost per year, which includes operation and maintenance costs, is estimated. Compared with civil and power plant construction costs forming the greater part of the total costs, operation and maintenance costs are relatively small. This means that the optimum scale of TPP's showing the least construction cost per kWh can be selected after consideration of construction cost for annual output.

A storage area approach model is made in order to determine the design variables. This model is made in Microsoft Excel and will from now on be referred to as the Storage Area Approach Model.

3.1   Storage Area Approach

Nomenclature:

A	Surface area tidal basin	m^2
C_D	Discharge coefficient	-
D_t	Runner diameter of turbine	m
F_{sl}	Flow area of sluices	m^2
F_{1t}	Throat area one turbine	m^2
F_t	Throat area all turbines	m^2
f_{sl}	Binary factor indicating if sluice gates are open or closed	-
f_t	Binary factor indicating if turbine's gates are open or closed	-
h_b	Basin water level	m
h_s	Sea water level	m
h_{sl}	Depth of sluice (water level till sill level)	m
N_t	Number of turbines	-
Q_{1o}	Discharge through one turbine in orifice mode	m^3/s
Q_{1p}	Discharge through one turbine when pumping	m^3/s
Q_{1t}	Discharge through one turbine when generating	m^3/s
Q_{in}	Discharge into tidal basin	m^3/s
Q_o	Discharge through all turbines in orifice mode	m^3/s
Q_p	Discharge through all turbines when pumping	m^3/s
Q_{sl}	Discharge through sluices	m^3/s
Q_t	Discharge through all turbines when generating	m^3/s
q_{sl}	Specific discharge through sluices	m^2/s
W_{sl}	Width of sluices	m

3.1.1   modelling the tides

The first aspect that has to be taken into account to analyze the functioning of a tidal power plant is the tide itself. Recorded data in tabular form can be used to model the evolution of water level.

In the past measurements of the tide have been performed by NEDECO [NEDECO & Delft Hydraulics, 1992]. The extreme and mean values were measured at 5 different places near the dam, see Table 3.1.

Table 3.1: *Tidal ranges for 5 locations along the dam [NEDECO & Delft Hydraulics, 1992]*

Location Non-Harmonic Constants	1: Bieung Island	2: Yami Island	3: Daejang Island	4: Duri Island	5: Daehangri Island
Approximate LLW (m)	-3.571	-3.614	-3.434	-3.545	-4.335
Spring tide range (m)	6.026	5.892	5.524	5.936	7.257
Mean tide range (m)	4.523	4.244	4.136	4.412	5.327
Neap tide range (m)	3.020	2.596	2.748	2.888	3.397
Time ranges of tide (h,min)	+0h03m	-0h14m	-0h20m	-0h12m	-0h31m
Ratio of the tidal ranges	1.00	0.99	0.92	0.99	1.22

On the basis of the tide ranges in the table above, it would be logical to locate the TPP near Daehangri Island, because there the tidal difference is the largest.

A disadvantage would be that according to the most recent plans, the polder in the south part of Saemangeum will be built first. Unfortunately, no recent information about the tides is known(anders formuleren). For that reason, modelling is performed by means of the tide table of Gunsan Outer Port (located just north of Saemangeum). The mean tidal range for Gunsan Outer Port is 4.49 m.

Although for a reliable mean value of the tidal range, a period of 18 years of astronomical tide data should be considered (See Section 2.2), for this study only 8 months of tidal data have been taken into account: January until August 2006, see appendix A (tide table). The tide at Saemangeum has the following characteristics:

- $R_{mean} = 4.49$ m;
- $R_{rms} = 4.68$ m;
- $R_{max} = 7.60$ m;

The tidal power potential of a site being proportional to the square of the tidal range, it has been argued that in calculating the annual tidal energy output of a given site, the root-mean-square tidal range for that site should be used. This however will result in too optimistic an estimate since, due to the generators' limiting capacity, the peak of spring-tide generation is shaved off. A more cautious approach is therefore to base the annual energy output on a calculation, based on the mean tidal range of the given site. Assume a semi-diurnal tide of sinusoidal shape. With a duration of one tidal cycle of 12 h 25 min,

i.e. 44700 s:

$$h_s = sin[2\pi \cdot (t + 11175)/44700] \cdot R_{mean}/2 \qquad (t \; in \; seconds)$$

$$h_s = sin[2\pi \cdot (t + 186.25)/745] \cdot R_{mean}/2 \qquad (t \; in \; minutes) \qquad (3.1)$$

3.1.2   modelling the basin level

From the hydrographic chart (see appendix B) and table (see Figure 3.2) it is calculated that

$$Q_{in} = A\frac{dh_b}{dt} \qquad (3.2)$$

$$h_b(t+1) = h_b(t) + V_{in}(t)/A(t) \qquad (3.3)$$

It is assumed that the water level of the basin will be horizontal under all operating conditions (no head differences within the basin).

$$H(t) = h_s(t) - h_b(t) \qquad (3.4)$$

$$\Delta V(t) = (Q_t(t) + Q_p(t) + Q_o(t) + Q_{sl}(t)) \, \Delta t \qquad (3.5)$$

Where Δ t = 1 minute. $Q_t(t)$ is the discharge through the turbines when turbining/ generating, $Q_p(t)$ is the discharge through the turbines when pumping, $Q_o(t)$ is the discharge through the turbines when they are in orifice mode, $Q_{sl}(t)$ is the discharge through the sluices. If the direction of flow in from sea to basin, the flow is defined positive (because h_b rises). Flow from the basin to the sea is negative (because h_b falls). At one time only one of the parameters $Q_t(t)$, $Q_p(t)$ and $Q_o(t)$ can be nonzero, so when one is positive, the others must be zero (because a the turbine cannot pump, generate or be in orifice mode at the same time). The discharge of the Dongjin and Mangyeong Rivers is neglected.

Water Level	Storage Area (km^2)
-4	121.3
-3	160.5
-2	208.6
-1	254.9
0	301.7
1	347.0
2	374.7
3	390.9
4	394.0
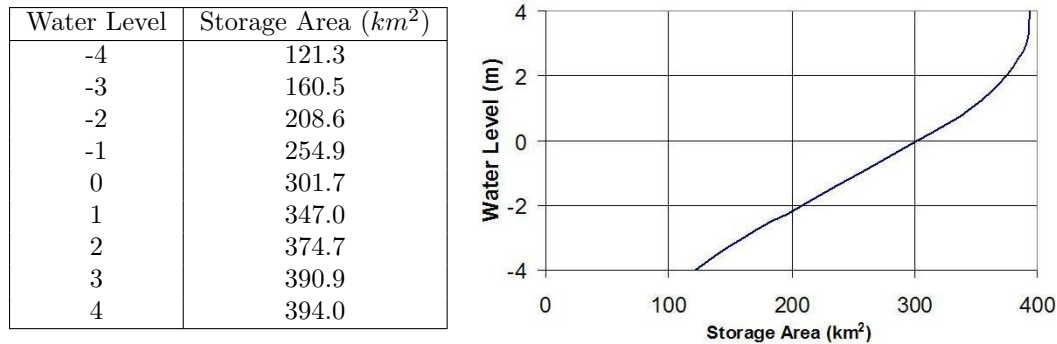
Figure 3.2: *Relation between area and water level*

3.1.3   modelling the sluices

At the moment there are two dewatering/ drainage sluices. For their specifications, see Table 3.2.

Table 3.2: Existing dewatering/ drainage sluices

	Sinsi	Garyeok
Location	East of Sinsi Island	Bukgaryeok Island
Gate Sill elevation Gate type Dimension max. discharge	EL.(-)6.50 m radial gate 30m x 14.5m x 10ea 8812 m^3/s	EL.(-)6.50 m radial gate 30m x 14.5m x 8ea 7050 m^3/s
Navigation lock sill elevation Dimension	EL.(-)6.50 m 16m x 12.5m x 62m	EL.(-)6.50 m 16m x 12.5m x 30m
Fish way	ladder type	ladder type

$$Q_{sl} = q_{sl} \cdot W_{sl} \tag{3.6}$$

If $(\mathrm{h}_b + \mathrm{h}_{sl}) \geq \frac{2}{3}(\mathrm{h}_s + \mathrm{h}_{sl})$, the flow is non-critical and is described by:

$$q_{sl} = C_{Ds} \cdot (H + h_{sl}) \cdot \sqrt{2g\,(H + h_{sl})} \cdot f_{sl} \tag{3.7}$$

If $(\mathrm{h}_s + \mathrm{h}_{sl}) \geq \frac{2}{3}(\mathrm{h}_b + \mathrm{h}_{sl})$, the flow is critical and then is described by:

$$q_{sl} = C_{Ds} \cdot \frac{2}{3}(H + h_{sl}) \cdot \sqrt{\frac{2}{3}g\,(H + h_{sl})} \cdot f_{sl} \tag{3.8}$$

where h_{sl} is the depth of the sluice (from sill level to mean sea level); f_{sl} is a binary factor equal to 1 when the sluices are open, and equal to 0 when closed.

3.1.4   modelling the turbine's discharges

As long as a turbine operates at less than its generator limiting output, the flow through one turbine Q_{1t} is defined as

$$Q_{1t} = C_{Dt} \cdot F_{1t} \cdot \sqrt{2g\,|H|} \cdot f_t \cdot \frac{|H|}{H} \tag{3.9}$$

Where f_t is a binary factor equal to 1 when the turbine's gates are open (turbines either generating energy, pumping or in orifice mode), and equal to 0 when the gates are closed. This discharge has a positive value for H > 0 (which means flow from sea to basin). When the turbine is in orifice mode (not generating, neither pumping, but letting water pass through in order to increase the sluicing capacity), the formula does not change (except from the value of the discharge coefficient, which might change because of the different

angle of the turbine's blades):

$$Q_{1o} = C_{Do} \cdot F_{1t} \cdot \sqrt{2g\,|H|} \cdot f_t \cdot \frac{|H|}{H} \tag{3.10}$$

The discharge through one turbine when it is pumping is defined as:

$$Q_{1p} = \frac{P_{1r}}{\eta \rho g H} \cdot f_t \tag{3.11}$$

The above formulas account for only one turbine. For the total number of turbines, a factor N_t must be added:

$$Q_t = N_t \cdot C_{Dt} \cdot F_{1t} \cdot \sqrt{2g\,|H|} \cdot f_t \cdot \frac{|H|}{H} \tag{3.12}$$

$$Q_o = N_t \cdot C_{Do} \cdot F_{1t} \cdot \sqrt{2g\,|H|} \cdot f_t \cdot \frac{|H|}{H} \tag{3.13}$$

$$Q_p = \frac{P_{rated}}{\eta \rho g H} \cdot f_t \tag{3.14}$$

3.1.5 Power generation modelling

The power of the turbine is determined by:

$$P = \eta \rho g Q_t H \tag{3.15}$$

When the point on the hill chart is reached where P = P_{rated}, P will remain constant. From that moment on, the Q_t in this formula must be replaced by:

$$Q_{t,r} = \frac{P_r}{\eta \rho g H} \tag{3.16}$$

Now an Excel spread-sheet is made. The formulas above are integrated in a model. The model assumes a constant water level for the duration of time intervals of 60 seconds. At the end of each time interval the water levels are re-calculated and kept constant for the next time interval. Every 60 seconds there is also an opportunity to change the operating parameters to indicate that from that point onwards, sluices are to be open or closed, the turbine are to be generating, pumping, in orifice mode or closed . The assumed value for η should also be adjusted every 60 seconds with help from a hill chart (for example see Figure 3.3) or turbine parameter determining formulas, see chapter 2. At the end of the computer run at t = 745, the water level in the basin should be identical to that at the beginning t = 0. If this is not the case, then by trial and error another basin water level at t = 0 is used until $h_b(0)$ equals $h_b(745)$.

Power output and generated energy are computed for each 60 second interval and the total amount of energy produced is the sum of a generating cycle of 745 minutes. For the tidal range either R_{mean} or R_{rms} must be chosen (still to be decided).
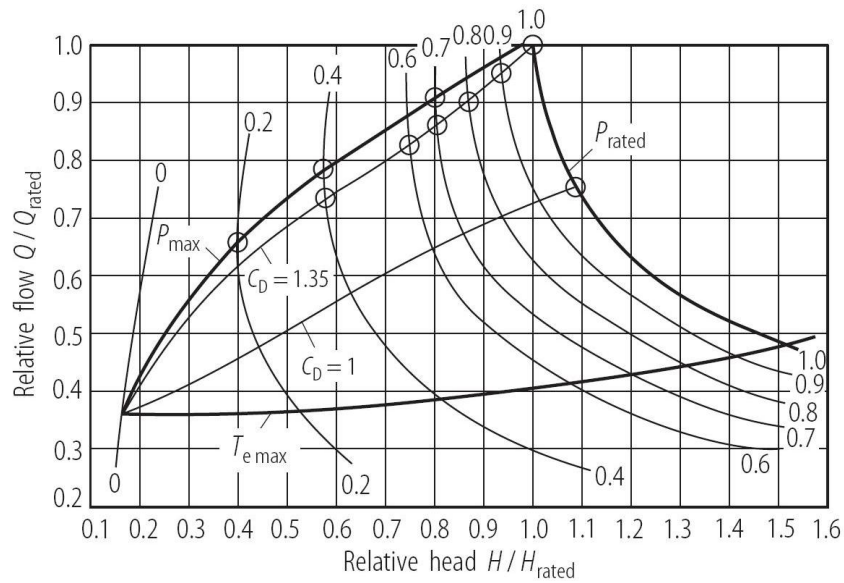
Figure 3.3: *Performance chart for double-regulated turbine-generator*

3.2 Optimisation of schemes

Figure 3.4 shows the operation of a single basin single tide working TPP with regulation for maximum output of the average spring tide and the average neap tide for the La Rance TPP (generating only from basin to sea). At the top the operation is shown, at the bottom the traject through the hill chart is plotted:

1-beginning of idle discharge (level equalization);

2-curve of generator capacity restriction;

3-optimum-high-water-cycle (basin filled to high-water level at beginning of cycle);

4-line of maximum efficiencies.

There is a difference in operation between spring tide and neap tide. Note that at spring tide the turbines are in operation for almost seven consecutive hours, while at neap tide this is only about four hours. The reason for this big difference is that at spring tide the required operation head for the turbines is reached much sooner than at slack tide, while the period of the tidal cycle remains constant.
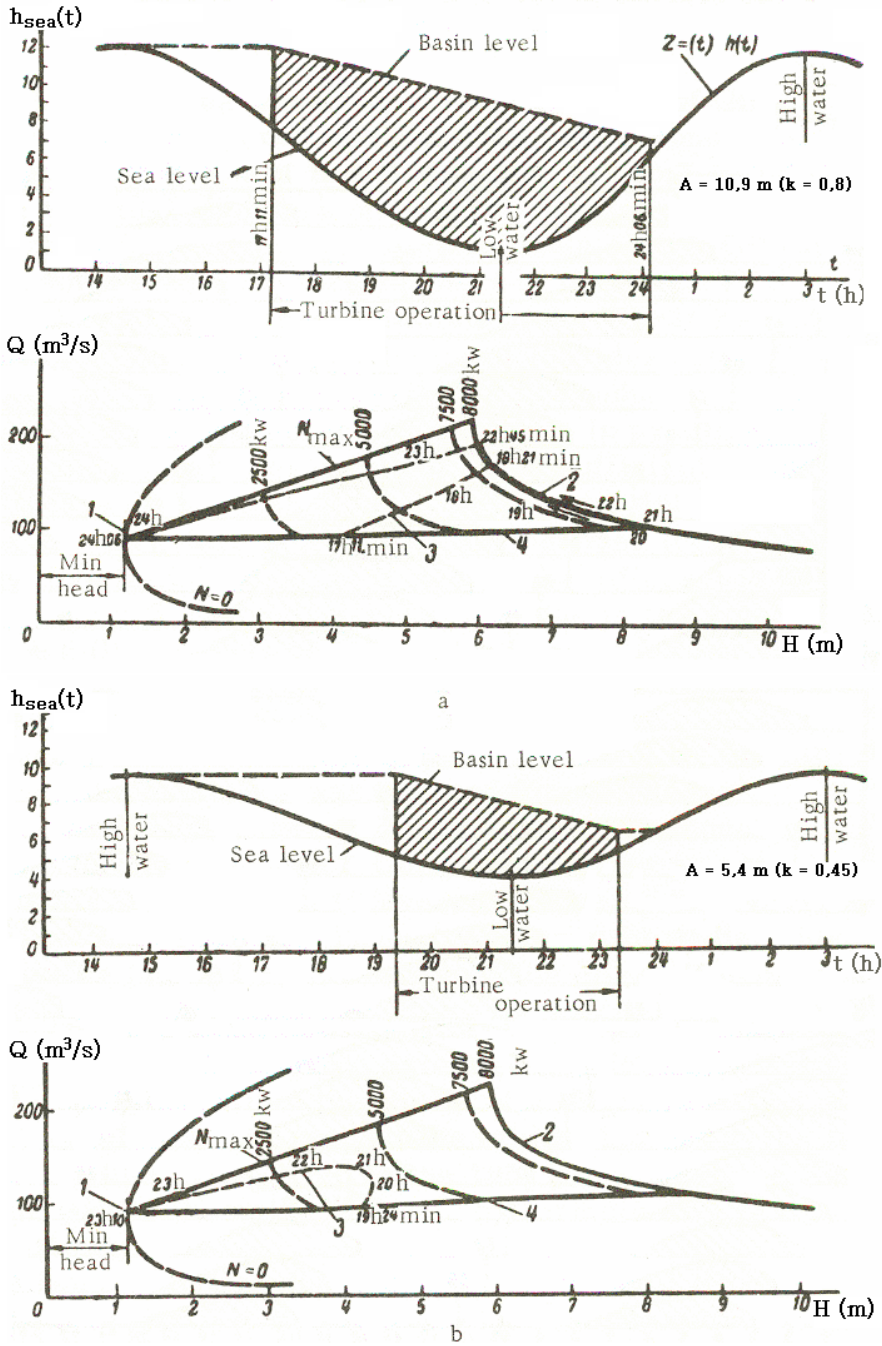
Figure 3.4: *Operation and hill chart-traject for La Rance; Upper two diagrams: spring tide, Lower two diagrams: neap tide*

3.3   Theory of turbine dimensions and efficiency

RETScreen [RETScreen International, 2004] has published a manual to predict turbine parameters.

$$D_t = k_1 \cdot Q_d^{0.473} \tag{3.17}$$

$$n_q = k_2 \cdot h^{-0.5} \tag{3.18}$$

$$\hat{e}_{nq} = \{(n_q - 170)/700\}^2 \tag{3.19}$$

$$\hat{e}_d = (0.095 + \hat{e}_{nq})\left(1 - 0.789 \cdot D_t^{-0.2}\right) \tag{3.20}$$

$$e_p = (0.905 - \hat{e}_{nq} + \hat{e}_d) - 0.0305 + 0.005 \cdot R_m \tag{3.21}$$

$$Q_p = 0.75 \cdot Q_d \tag{3.22}$$

$$e_q = [(n_q - 170)/700]^2 \tag{3.23}$$

$$P = 8.22\frac{Q_u H}{1000} \tag{3.24}$$

D_t	Turbine runner diameter
n_q	Specific speed
$\hat{e}_{nq}$	Specific speed adjustment to peak efficiency
$\hat{e}_d$	Runner size adjustment to peak efficiency
e_p	Turbine peak efficiency
Q_p	Peak efficiency flow
Q_d	Design flow
e_q	Efficiencies at flows above and below peak efficiency flow
k_1	Constant; $k_1 = 0.41$ for $D_t \geq 1.8$ m
k_2	Constant; $k_2 = 800$ for Kaplan turbines
R_m	Turbine manufacturer or design coefficient; 2.8 to 6.1 (default 4.5)

Using the equations in the tables above, the dimensions of the turbines can be determined and the efficiency can be predicted. It is clear that the efficiency of the turbines cannot be considered as a constant! This is also proven by the hill charts. To determine the rotational speed, the following formula can be used [Schweiger & Gregori, 1992]:

$$n_q = n\frac{Q^{0.5}}{H^{-0.75}}$$

Another formula to calculate the capacity of a turbine than the one provided by RETScreen is the formula provided by Remery [Remery, 1982]:

$$P = \frac{QH}{102}\eta_t \tag{3.25}$$

With P in MW. This formula looks quite similar to equation 3.24. For $\eta_t = 0.84$ these formulas give exactly the same value for P.

The formulas stated above and the calculated specifications can in the end be compared to existing large low-head turbine installations, all equipped with bulb turbines. See Table 3.3 [Heung-Nyun Kim, Doo-Hyun Paik, Deuk-Kyu Park, 2004].

Table 3.3: *Large low-head turbine installations and their specifications*

Country	Site	Turbine Diameter (m)	Capacity (MW)	Rated Head (m)	Units #
Austria	Altenworth	6	38.9	14	9
Canada	Jenpeg, Manitoba	7.5	31.1	10.7	6
	Annapolis	7.6	20	5.5	1
USA	Racine	7.7	24.6	6.2	2
France	Avignon	6.25	30	10	4
	La Rance	6.35	10	5.75	24
Germany	Iffezheim	5.8	28.3	11.7	4
Korea	Sihwa[1]	7.5	25.4	5.82	10

3.4   Turbine parameters for Saemangeum

3.4.1   Dimensions and rotational speed of turbines

To determine the ideal, most efficient dimensions of an axial turbine, Schweiger and Gregori developed a method to calculate the optimal turbine runner diameter [Schweiger & Gregori, 1992]. The turbine diameter, specific speed, speed and power are all determined by the rated head and discharge per turbine. According to Schweiger and Gregori it should be possible to determine the dimensions of a turbine as well as the relationship between head and discharge without having available hill charts (normally provided by the suppliers).

In the rest of this study it is assumed that the turbines cannot start operating at a lower head than 1.5 meter. Although this is not in accordance with the calculation methods and models used in the following sections, in reality one must accept this as a fact. Many years of experience with existing plants (including La Rance, Kislaya Guba and Annapolis) teach us this. But once in operation, turbines can continue turbining when the head drops below 1.5 meter until the head is 1.0 meter.

An accurate estimate for the rated head is given by Song and Van Walsum [Song & Van Walsum, 2006] (see Section 4.3 and Appendix C):

$$H_r = 0.66 \cdot R_{mean} \approx 3.00 \ m \tag{3.26}$$

Bearing in mind that all turbine parameters are only dependent on the head, they can now be calculated accorrding to the method of Schweiger and Gregori. The formulas given

by are:

$$H = 920650 \cdot n_q^{-2.058} \qquad (3.27)$$

$$K_u = 0.8434 + 0.00456 \cdot n_q \qquad (3.28)$$

Where K_u is the so called peripheral velocity coefficient.

First the specific rotational speed n_q must be derived from equation 3.27 and then the value for K_u can be calculated:

$$n_q = \left(\frac{920650}{H} \right)^{\frac{1}{2.058}} = 463.63 \ rpm. \ (at \ H = 3 \ m)$$

$$K_u = 0.8434 + 0.00456 \cdot n_q = 2.958$$

The discharge per turbine and turbine diameter are calculated by the following formulas:

$$Q_{1t} = F_{1t} \sqrt{2gH_r} \qquad (3.29)$$

$$D_t = \frac{K_u \cdot 60 \cdot \sqrt{2gH_r}}{\pi n} \qquad (3.30)$$

These parameters can only be calculated by iteration, because the turbine area F_{1t} is directly related to the diameter D_t. The computer simulation (see chapter 3) shows that for $H_r = 3.0$ m the best values are $Q_{1t} = 336$ m^3/s and $D_t = 7.5$ m.

The actual rotational speed n can be calculated from the following equation:

$$n_q = n Q_{1t}^{0.5} H^{-0.75} \qquad (3.31)$$

From this equation it follows that (for $n_q = 463.63$ rpm, $Q_{1t} = 336$ m^3/s and $D_t = 7.5$ m) n = 57.66 rpm.

According to Krueger from the United States Department of the Interior [Krueger, 1976], generators can only operate at predefined, fixed rotational speeds.
The rotational speed nearest the design speed is selected subject to the following considerations: A multiple of four poles is preferred, but standard generators are available in some multiples of two poles. If the head is expected to vary less than 10 % of the design head, the next greater speed may be chosen. A head varying in excess of 10 % from design head suggests the next lower speed. In the case of Saemangeum the head varies more than 50 %, so the next lower speed should be used.

$$n = \frac{120 \cdot f}{N_p} \qquad (3.32)$$

Where N_p is the number of poles and f is the frequency of the local electricity grid. In

South-Korea the electricity grid operates at a frequency of 60 Hz, so the number of poles can be calculated:

$$N_p = \frac{7200}{57.66} = 124.87$$

Keeping in mind the considerations mentioned above, the number of poles is now fixed at 126 rpm, from which it follows that the rotational speed n must be 57.14 rpm (which is the next lower speed below 57.66 rpm if a multiple of two poles is chosen for the number of poles). This rotational speed must be kept constant during the operation. Knowing that H will vary during a tidal cycle and thus n_q as well (according to formula 3.27), it can be seen from Equation 3.31 that n can be kept constant by varying Q. This means that the discharge should be regulated by blade angle adjustments according to the diagram in Figure 3.5 in order to keep n constant.
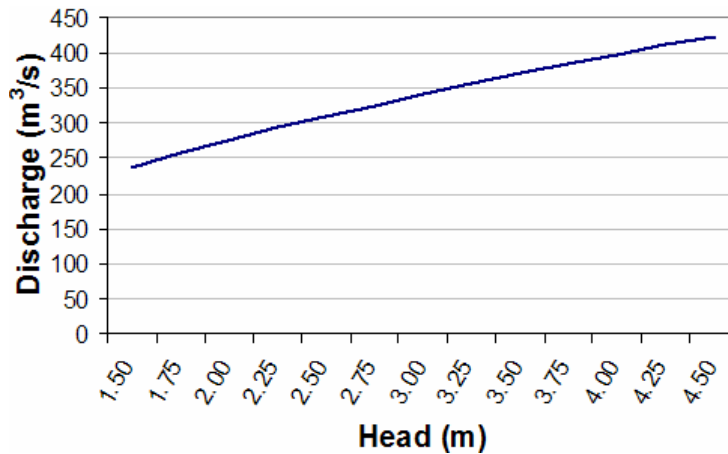
Figure 3.5: *Relationship between discharge and head*

3.4.2   Efficiency

Using the formulas provided by RETScreen [RETScreen International, 2004] (see Section 3.3), the relationship between the discharge and the turbine efficiency can be calculated. The result is plotted in Figure 3.6. As can be seen from the calculations and the figure, the maximum efficiency will be 0.850. At the lowest head at which the turbine operates (H = 1.0 m), the discharge is Q_{1t} = 191 m^3/s. According to the RETScreen method the efficiency is 0.828 at that discharge level. The efficiencies at low discharges can be magnified by chosing a lower H_r, but this would lower the peak efficiency. The Storage Area Approach Computer Model shows that the optimal head is 3.0 m.

3.4.3   Power

The power per turbine is accurately approximated by:

$$P_{1t} = \frac{8.22 \cdot Q_{1t}H}{1000} \tag{3.33}$$
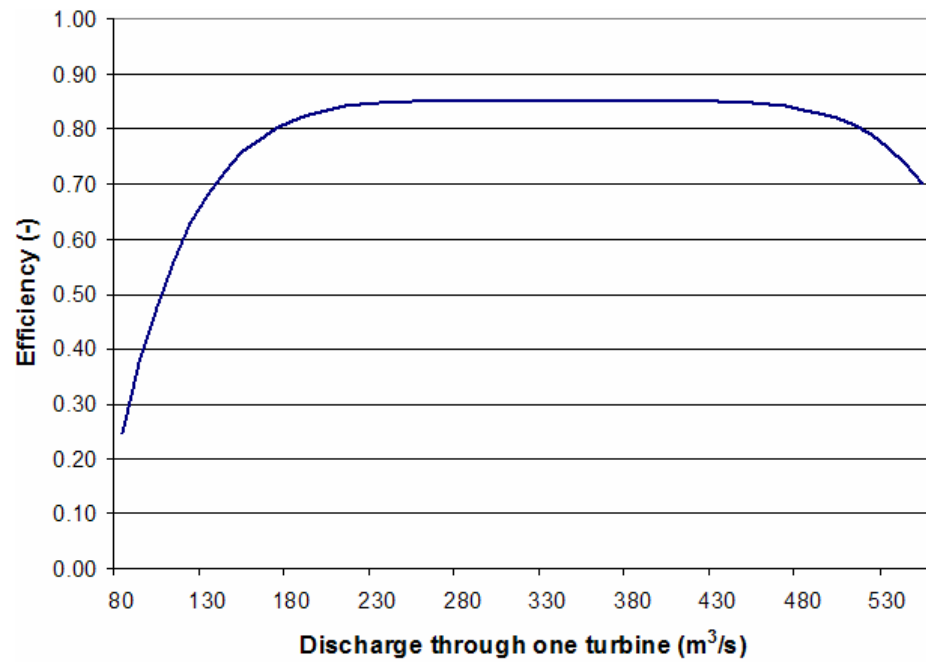
Figure 3.6: *Efficiency vs discharge;* $\eta_{t,peak} = 0.850$
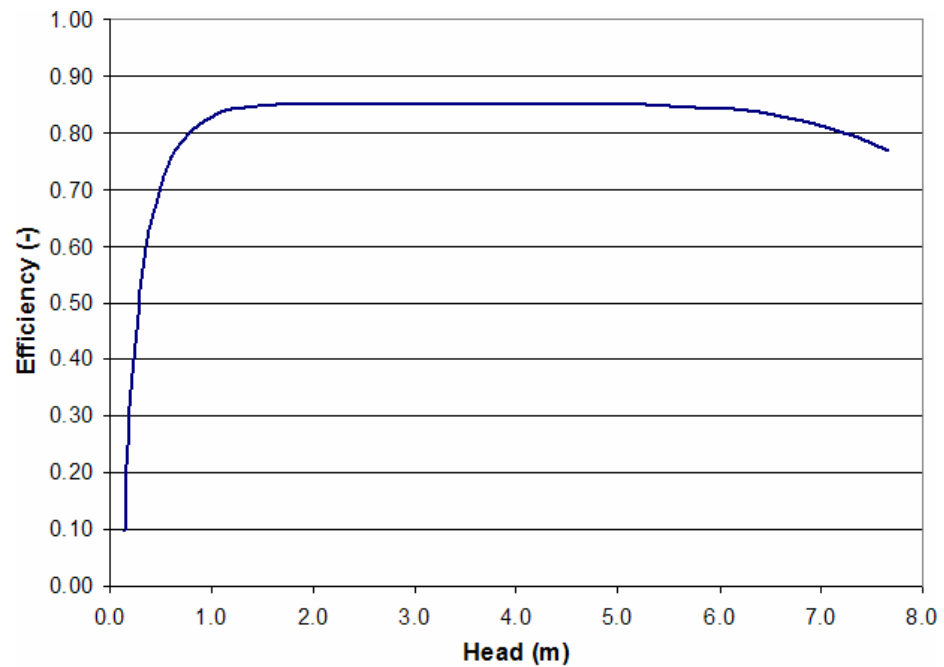
Figure 3.7: *Efficiency vs Head;* $\eta_{t,peak} = 0.850$

Filling in $Q_{1t} = 342$ m^3/s and $D_t = 7.5$ m gives $P_{1t} = 8.44$ MW. The resulting turbine dimensions and parameters for the Saemangeum TPP are listed in Table 3.4.

Table 3.4: *Turbine parameters*

Rated head	H_r	3.0	m
Design discharge	Q_d	342.06	m^3/s
Design flow	u_d	7.57	m/s
Diameter	D	7.50	m
Design speed	n	57.14	rpm
Design specific speed	n_q	463.63	rpm
Throat area	F	44.18	m^2
Power of one turbine	P_{1t}	8.44	MW
Peak Efficiency	$\eta_{t,peak}$	0.850	-
Peripheral velocity coefficient	K_u	2.96	-

3.5   Economic Feasibility in Model

The Storage Area Approach Model also contains an economic feasibility calculation. This will be discussed later on in Chapter 6. The construction costs are estimated by a method developed by Fay and Smachlo [Fay & Smachlo, 1983a]. This method is also discussed in Chapter 6 and in Appendix D.

4 Designing the TPP

4.1 Design specifications

What has to be determined?

- Number of flow directions in which power is generated (1 or 2)

- Number of basins

- Size of basin(s)

- In case of one direction: which direction?

- Need for extra sluicing capacity (and size)

- In- and outflow at different locations?

- Location in the dam (in the direction of the dam)

- Location perpendicular to the dam

- Depth of turbines/ powerhouse

- Number and type of turbines/ generators

- Building method

- External factors: Fresh water basin, land reclamation, LNG-terminal, new Sae-mangeum port

On what criteria are these decisions made?

- Availability of head and quantity of water

- Power generation capacity

- Costs and benefits

- Environmental considerations (presence of inter tidal zone)

- Local terrain-situation (geotechnical profile, shape)

- Fluid mechanical characteristics: Flow velocities

- Possibility to adapt to future changes in the development plan of Saemangeum.

- Optimal combination of H and Q (because P is proportional to both of them)

4.2   Natural energy potential of a site

Robert Gibrat introduced the expression 'natural energy' [Gibrat, 1966] which is a useful concept in estimating the tidal energy potential of a tidal basin. It is a measure for the maximum amount of energy a site could provide if all conditions would be optimal. To understand this, consider a tidal basin. The basin is separated from the sea by a barrage equipped with an infinite number of 100% efficient, double effect turbine-generators, meaning that the machines can generate electrical energy on both the incoming and the outgoing tide. The maximum amount of energy that could theoretically be extracted during one tidal cycle from this basin would be obtained by letting the basin instantaneously fill up through its 100% efficient turbines, from its lowest possible level to its highest level at the moment the ocean tide is at its highest. The water in the basin would then be kept at this highest level and again instantaneously released through the turbines from basin to sea at the moment the sea level is at its lowest. This theoretical maximum amount of energy which can be extracted during one tidal cycle is referred to as the one tidal cycle natural energy of that basin. For a 100% efficient hydro plant, the energy E in [J] supplied by a water volume V (tidal prism) falling over a height of h meters is

$$E = \rho g V h \tag{4.1}$$

The power output P in [W] of such a plant is then

$$P = \rho g Q h \tag{4.2}$$

The energy $E_{nat,cycle}$ in [Wh] generated by filling and emptying a tidal basin in this manner through one tidal cycle thus becomes

$$E_{nat,cycle} = \rho g V R / 3600 \tag{4.3}$$

Since the energy potential of a basin is proportional to the square of its tidal range, one can use the root-mean-square value of the tidal ranges over a year's duration, R_{rms}, to calculate $E_{nat/year}$ in [Wh]. The total number of tidal cycles per year is 705.5. For the tidal prism the volume corresponding to R_{rms} must be used. This is referred to as V_{rms} (but this is not the root mean square of the tidal prism!). Thus the amount of natural energy, dissipated per year in one tidal basin is

$$E_{nat/year} = 705.5 \cdot \rho g V_{rms} R_{rms} / 3600 \tag{4.4}$$

Substituting the known values for ρ and g simplifies the formula:

$$E_{nat/year} \approx 2000 \cdot V_{rms} R_{rms} \tag{4.5}$$

With $E_{nat/year}$ in Wh. Further simplification of estimating $E_{nat/year}$:

$$E_{nat/year} \approx 0.7 \cdot AR^2 \tag{4.6}$$

where $A = A_{HHW}$ [km^2] and $R = R_{max}$ [m]. This provides indeed a simplification since R_{max} is often directly available from the tide tables, and A_{HHW} can be simply measured from hydrographic charts. What percentage of a basin's natural tidal energy potential can be realized depends on a number of factors.

The natural energy potential of Saemangeum can now be calculated:

$$E_{nat/year} \approx 2000 \cdot V_{rms} R_{rms} = 2000 \cdot 1.39 \cdot 10^9 \cdot 4.68 = 13.000 \ GWh = 13.0 \ TWh$$

4.3   Rules of thumb for preliminary design

Since 1966 several TPP's have been operated and numerous feasibility studies have been prepared. Many lessons were learned during that period and are likely to remain valid for the next few years. Song and Van Walsum gathered those lessons into a few rules of thumb which might assist to evaluate the tidal energy potential of a site [Song & Van Walsum, 2006]. This method is described in Appendix C.

For Saemangeum these rules of thumb lead to the following assumptions:

Step 1:

Since $R_{mean} = 4.49$ m < 9 m and Saemangeum is now one large basin, a single, high-basin plant should be chosen for maximum energy output. If absorption in the energy utility system would cause problems, consider single basin, double-effect plant. But since the Sihwa plant is located not to far away and this is a single, low-basin plant, there might also be the possibility to make these plants paired-basins: Saemangeum should then be a single, high-basin plant. If there will be land reclamation in Saemangeum, there might also be the possibility to make a linked-basins scheme, since then the construction costs of an extra dam to create a second basin would not be as high as they would be now.

Step 2:

In the following calculations $E_{nat/year}$ is used. $E_{nat/year}$ is calculated in Section 4.2.

An accurate estimate for the rated head is given by Song and Van Walsum [Song & Van Walsum, 2006] (see Section 4.3 and Appendix C). If Saemangeum were to be a single, high-basin plant, the following values result from the equations given above:

$$H_{rated} \approx 0.66 \cdot R_{mean} = 2.96 \ m$$

$$P_{installed} \approx 0.09 \cdot E_{nat/year} = 0.09 \cdot 13000 = 1170 \ MW$$

If Saemangeum were to be a single basin, double-effect plant, the following values result from the equations given above:

$$H_{rated} \approx 0.5 \cdot R_{mean} = 2.25 \ m$$

$$P_{installed} \approx 0.1 \cdot E_{nat/year} = 0.1 \cdot 13000 = 1300 \ MW$$

Step 3 and 4: In the modeling and design pumping will be performed by the turbines and the existing sluices are integrated in the model. Also the necessity of extra sluicing capacity is investigated.

4.4   Predictions with approximation formulas

Apart from Gibrat's method (Section 4.2) in the literature several different approximation formulas can be found to predict the annual energy output if the basin area and tidal range are given. These approximation formulas are listed here and are tested on existing TPP's, to test their applicability. The relevant parameters for these approximations are listed in Table 4.1. An overview of the results these formulas would give for Saemangeum are listed in Table 4.2.

Table 4.1: Main Power output Design parameters

Parameter	Symbol	Unit (+ value)
Power	P	MW
Energy	E	GWh
Head	H	m
Mean tidal range	R_{mean}	4.49 m
Discharge	Q	m^3/s
Tidal prism	V	m^3
Area of basin	A	km^2
Throat area of turbine	F	m^2
Turbine efficiency	η_t	%
Discharge coefficient	C_d	[-]
Gravity	g	9.81 m/s^2
Density	ρ	1025 kg/m^3

4.4.1   Approximation formulas for installed power

The following approximation formulas for installed power are found. For the meanings of the symbols and their units, see Table 4.1.

- Bernshtein [Bernshtein, 1965]:

$$P = 0.170 \cdot AH^2 \qquad [MW] \qquad\qquad (4.7)$$

The annual plant load factor for TPP's is between 21 and 34 %. Annual plant load

factor = product of ex-post measured electricity generation in the "verification period" and the factor 100 divided by the product of the net capacity and the hours in the verification period.

- University book "Water power Engineering" [Van Duivendijk, 2004]:

$$P = \frac{1}{2}AH^2 \tag{4.8}$$

H = average head [m], with H $\approx 0.7 \cdot$ R$_{mean}$

- Weicheng Wu [Weicheng Wu, 1999]:

$$P = 0.226 \cdot AR^2_{mean} \tag{4.9}$$

4.4.2 Approximation formulas for annual energy output

The potential natural energy of a site can be calculated by:

$$E_{pot} = 1.97AR^2_{mean} \qquad [GWh] \tag{4.10}$$

R$_{mean}$ is the average tidal range (m)
A is the basin area (km^2).
According to Bernshtein, the yearly amount of energy that can be obtained in a single basin TPP with maximum-output regulation is:

$$E_y = 1.97\kappa_B AR^2_{mean} \qquad [GWh] \tag{4.11}$$

K$_B$ can be called 'installation efficiency': this constant has the value 0.34 for a single basin, two directions plant or 0.224 for a single basin, one direction plant.

Jefferson Tester [Tester, 2005]:

$$E_{cycle} = \frac{\kappa_T mgR}{2} = \frac{\kappa_T \left(\rho AR\right) gR_{mean}}{2} = 1397\kappa_T AR^2_{mean} \qquad [kWh] \tag{4.12}$$

Here κ_T is a capacity factor, between 0.20 and 0.35. Tester advises to use 0.33. Since there are 705.5 tides per year, the annual energy is predicted by:

$$E_y = 0.997 \cdot \kappa_T AR^2_{mean} \qquad [GWh] \tag{4.13}$$

4.5 Conclusions: preliminary design parameters

In Table 4.2 the approximation formulas of the preceding sections have been tested on existing plants, Sihwa and the Mersey feasibility study, performed by the Mersey Barrage

Table 4.2: *Approximation formulas tested on existing, future and possible TPP's*

	La Rance	Annapolis	Sihwa	Mersey	Saemangeum
A (km^2) at MSL	17	15	42.4	60	301.7
R$_{mean}$ (m)	8.45	6.4	5.57	6.45	4.49
V (10^6 m^3)	102	67.2	147	270	950
H (m)	7.4	5.5	5.82	4.5	3
P$_i$ (MW)	240	18	254	700	[-]
E$_y$ (GWh) net	540	45	552.7	1500	[-]
γ (%)	63%	69%	60%	60%	59%
t$_{cycle}$ (hrs)	6	5.7	5.5	5.7	5.3
Power predictions [MW]:					
Gibrat:	236	120	256	486	1170
Bernshtein:	206	104	224	424	1034
Duivendijk:	297	151	322	612	1490
Weicheng Wu:	274	139	297	564	1375
Energy production predictions [GWh]:					
Bernshtein:	536	271	580	1102	2684
Tester:	399	202	433	821	2001

Company. In the last column the formulas are used to predict the power and yearly energy output for Saemangeum.

Some remarks must be added:

La Rance is assumed to be a single-effect plant. The reason for this assumption is that in reality 78% of the time it operates as a single-effect plant and only 22 % as a double-effect plant.

The values of the parameters concerning the Annapolis plant are not very useful, as this plant is highly under dimensioned.

The values of the feasibility study for the Mersey Barrage differ quite much from the other numbers, probably because of the not negligible amount of river runoff.

Conclusions

- Gibrat's prediction for power to be installed seems to be very accurate; In La Rance's case the error in comparison with the installed power is less than 2 %, while for Sihwa the error is less than 1 %! The fact that the Annapolis TPP is not designed for maximum energy generation amplifies this presumption. However there is an obstacle for using this formula: the assumed head for Saemangeum is estimated with Gibrat's method: H$_{rated} \approx 0.66 \cdot$ R$_{mean}$. The heads at La Rance and Sihwa are much higher than Gibrat suggests (La Rance: H$_{rated} = 0.88 \cdot$ R$_{mean}$ and Sihwa: H$_{rated} = 1.04 \cdot$ R$_{mean}$). A plausible reason could be that pumping is not accounted for in Gibrat's method.

- Bernshtein's method for estimating the annual energy output also looks very reliable. For La Rance the error is less than 1 %, for Sihwa less than 5 %.

- According to the most reliable approximation formulas the installed capacity for Saemangeum should be 1170 MW and the annual energy output would be 2684 GWh. These values have been used as the start values for a trial and error iterative optimisation in a Microsoft Excel spreadsheet.

4.6   Development of Saemangeum

Ever since the damming of Saemangeum was started in 1991 a wide variety of future destinations have been proposed. The main destinations are the following:

- Fresh water basin
- Polders for both agriculture and industries
- Nature reserve
- Recreation
- Alternative energy

Figure 4.1: *Layout proposed by KRC: fresh water reservoir of 117.6 km^2 and reclaimed tidal flats of 282.4 km^2*

The plans of KRC (Korea agriculture & Rural infrastructure Corporation) include the following characteristics: Desalinized reservoir of 117.6 km^2 and reclaimed tidal flats of 282.4 km^2. The inland development is scheduled till 2011.
Development direction:
- to secure large-scale agricultural lands: integrate research on new agriculture and biotechnology.
- to make an outpost of alternative energy development: attract research institutes and

foreign universities.

- to develop integrated tourism and leisure complex: link with Seonyoodo Marine Tourism Complex.

Saemangeum New Port:

- to develop North East Asia's logistics and production zone: develop Saemangeum as Asia's main port.

Logex proposed to build a new port at the South-West of Saemangeum, located between Sinsi Island and Garyeok Island (World Logistics Expo Organising Committee, 2007, Jeonbuk).

Thusfar no plans have been proposed to develop the area (or part of the area) as a tidal power basin. In the following section some layouts for future development are proposed, each with different basin size and other destinations, like polders and a fresh water basin.

4.7   Different layouts for the future

Since some of the destinations mentioned above are beyond discussion, it would not be realistic to claim the whole area for a TPP. At least a part of the area should be reserved for fresh water and farmland. From an environmental point of view the continuation of the tidal movement, including the presence of an inter tidal zone, would be favourable, as well as renewable energy utilisation.

Taking this into account and looking at the bathymetry, three different area layouts are proposed. The polders are mainly situated in the shallow areas and the relation between the area of fresh water and polders is kept at about the same proportions.
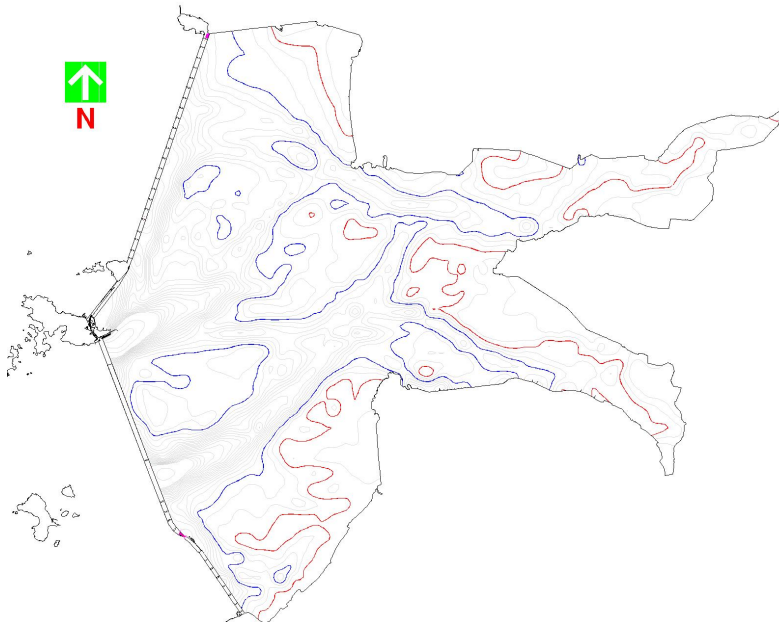
Figure 4.2: Layout 1: No polders, no fresh water reservoir

4.7.1   Layout 1: Basin area 394.0 km^2

The first Layout option exists of leaving the layout the same as it is now. It will contain no polders, nor fresh water. The whole area can be used for the TPP.

Advantages of this layout are that the TPP can be built at maximum capacity and there is a large inter tidal zone (thus environmental friendly). Furthermore all sea dikes already exist.

The main disadvantages are the absence of a fresh water basin and polders. The optimal
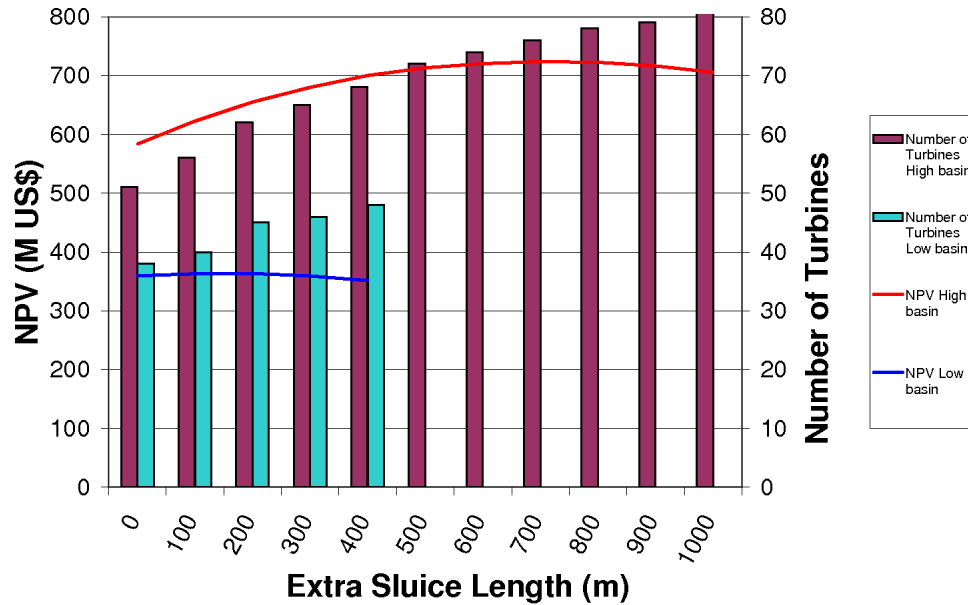
Figure 4.3: *Determination of TPP parameters by maximising the NPV*

dimensions of the TPP are determined with an economic feasibility study. This will be explained later in Chapter 6, but the results are given here. For different sluice lengths the Net Present Value (NPV) is calculated for a range of numbers of turbines. The result is given in Figure 4.3. The economically most feasible option would be a high basin plant (generating at ebb tide) with 76 turbines (powerhouse would stretch out over 1425 m) and an additional sluicing capacity of 750 meters. This adds up to the existing sluicing capacity of the Sinsi and Garyeok sluices. The NPV would then be 724 Million US\$ (after 40 years, 4% discount rate, 4% annual rise of energy price, see Chapter 6). If a low basin plant would be built, the figures would be different; the optimum then lies at 43 turbines, 140 meters of extra sluicing capacity, resulting in an NPV of 364 Million US\$. These numbers are the output of the Storage Area Approach Model.

4.7.2   Layout 2: Basin area 114.6 km^2

The second Layout option contains 89.6 km^2 of fresh water and 189.8 km^2 of polders. The advantages are that only a small part of total area (29 %) is occupied by the TPP, so

there's still much space left for a fresh water basin and farmland. In this layout there is an inter tidal zone, thus it is environmentally friendly. No extra sluicing capacity is required; Sinsi sluice (300 m) is sufficient, so there's no need to construct extra sluices.

The main disadvantage is that an extra dam must be built to separate the fresh water from the sea water.
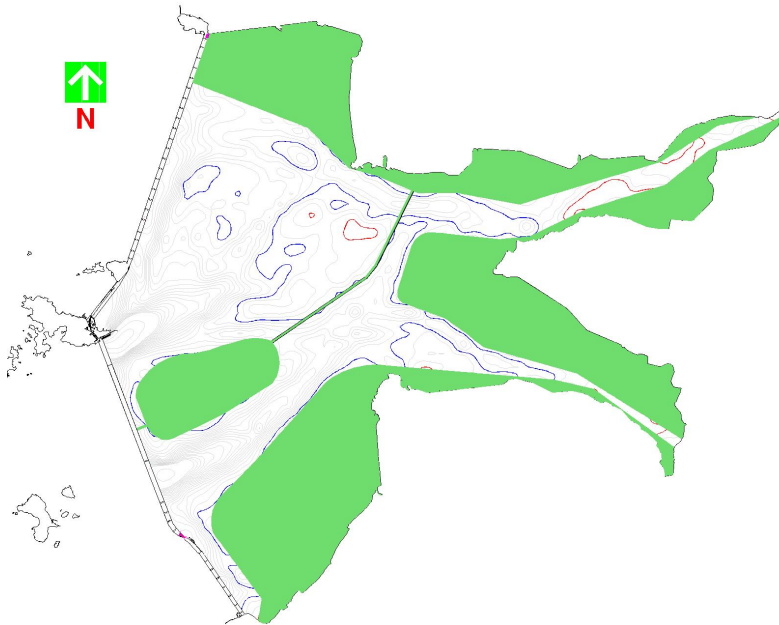
Figure 4.4: *Layout 2*
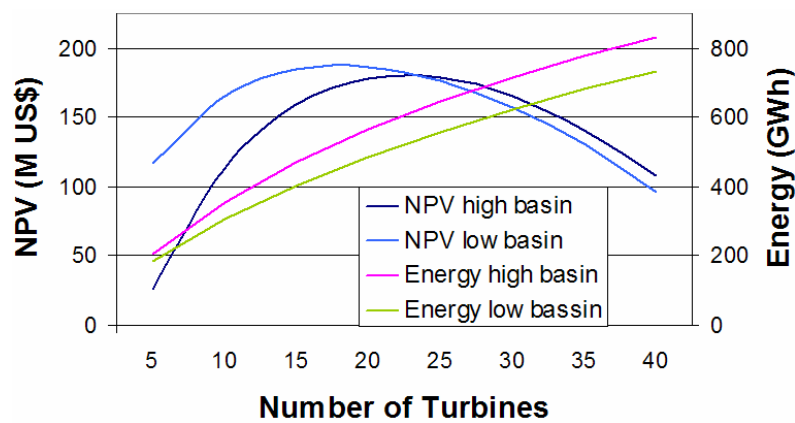
Figure 4.5: *NPV and energy output for both the high basin and low basin scheme for layout 2*

The Storage Area Approach Model's output for this layout is shown in Table 4.3.

Table 4.3: *Optimal parameters for Layout 2*

Generation mode	N_t	L_{sl} (m)	NPV (M US$)	E_y (GWh)	P_i (MW)
High basin plant	23	300	180.2	614.9	183
Low basin plant	18	300	187.6	453.8	142

4.7.3 Layout 3: Basin area 76.6 km^2

The third Layout option contains 89.6 km^2 of fresh water and 227.8 km^2 of polders. Advantages of this layout are that only a small part of total area (19 %) is occupied by the TPP, so there's still much space left for fresh water basin and farmland. This layout contains relatively much farmland compared to layout 2.

The disadvantages are the lack of an inter tidal zone and a small basin area, thus less energy output.

The Output of Storage Area Approach Model is shown in Table 4.4.
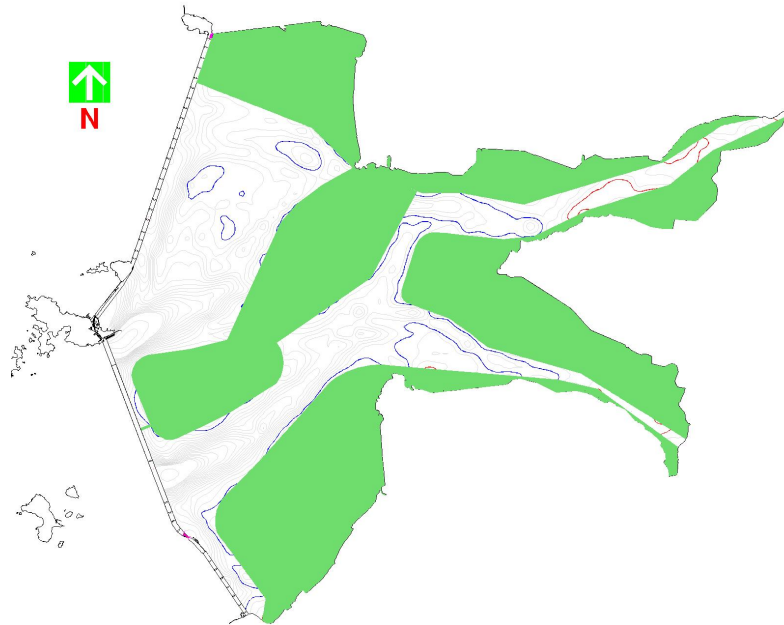
Figure 4.6: *Layout 3*

Table 4.4: *Optimal parameters for Layout 3*

Generation mode	N_t	L_{sl} (m)	NPV (M US$)	E_y (GWh)	P_i (MW)
High basin plant	18	300	138.8	499.5	145
Low basin plant	16	300	173.1	409.5	126

4.7.4 Selection of optimum layout

Layout 1 is not selected, because the absence of a fresh water basin and polders does not make this a realistic option for the future. Layout 2 is selected for the design of the TPP

Table 4.5: *Relationship Basin area - water level for three Layout options*

Water Level	Storage Area (km^2)		
(m MSL)	Layout 1	Layout 2	Layout 3
4	394.04	114.62	76.60
3	390.86	114.62	76.60
2	374.67	114.62	76.60
1	347.00	114.62	76.60
0	301.66	113.60	76.60
-1	254.92	106.02	76.40
-2	208.63	96.93	75.71
-3	160.47	83.84	72.76
-4	121.27	69.31	63.14

for two reasons: The first and most important reason is the presence of a large intertidal zone, provided a low basin scheme is selected. This makes it a very interesting and realistic option. The second reason is that of the 4 possible schemes (layout 2 low and high basin, layout 3 low and high basin) it is the economically most feasible option (see Tables 4.3 and 4.4). No additional sluicing capacity is required, because the sluicing capacity of the Sinsi sluices is sufficient. It is thereby assumed that the speed at which the sluices are opened and closed is not a restriction here. The Garyeok sluices are not connected to the TPP basin, but to the fresh water reservoir.

As was stated earlier in this section, it would be wise to select a design that would have a realistic chance to be built in reality. Taking this into account, an intertidal zone could have a positive effect on the decision process. If a high basin scheme would be chosen, there would be no intertidal zone. A low basin scheme would create an intertidal zone as sketched in Figure 4.7. In the end this low basin scheme also turns out to be cheaper than
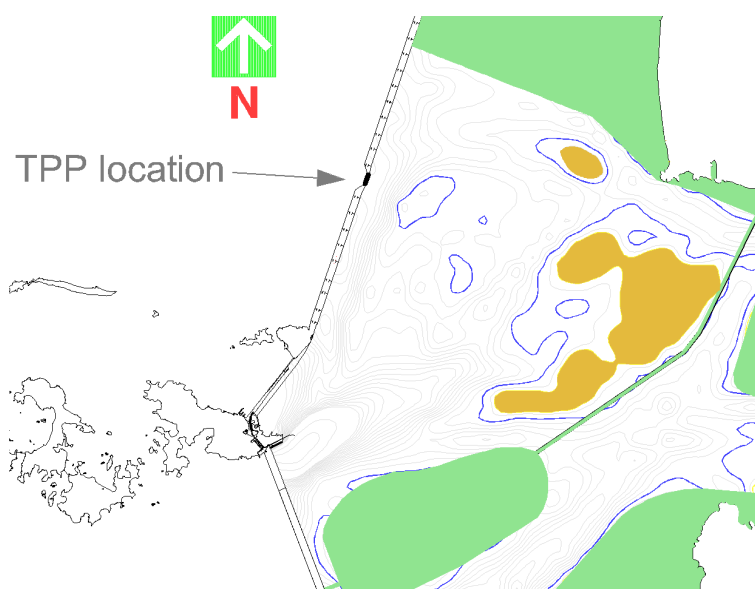
Figure 4.7: *Layout 2 with a low basin scheme (flood generation); the brown hatched part is dry at a basin level of -1.5 m (the dark line is at EL -3.0)*

the high basin scheme, because the water levels inside the basin are at all time about 2.35 m (output Storage Area Approach Model) lower than in case a high basin would be chosen. It should be realised that the crest level of the dikes protecting the adjacent polders from flooding are designed taking this basin level into account. This implies that for a high basin scheme the dikes should be about 2.35 meters higher than for a low basin scheme, which would cost a significant sum of money, as the dikes have a total length of 30.8 km (including the dam separating the basin from the fresh water basin, not including the present estuary dam structure). This is taken into account for all optimisations with the Storage Area Approach Model.
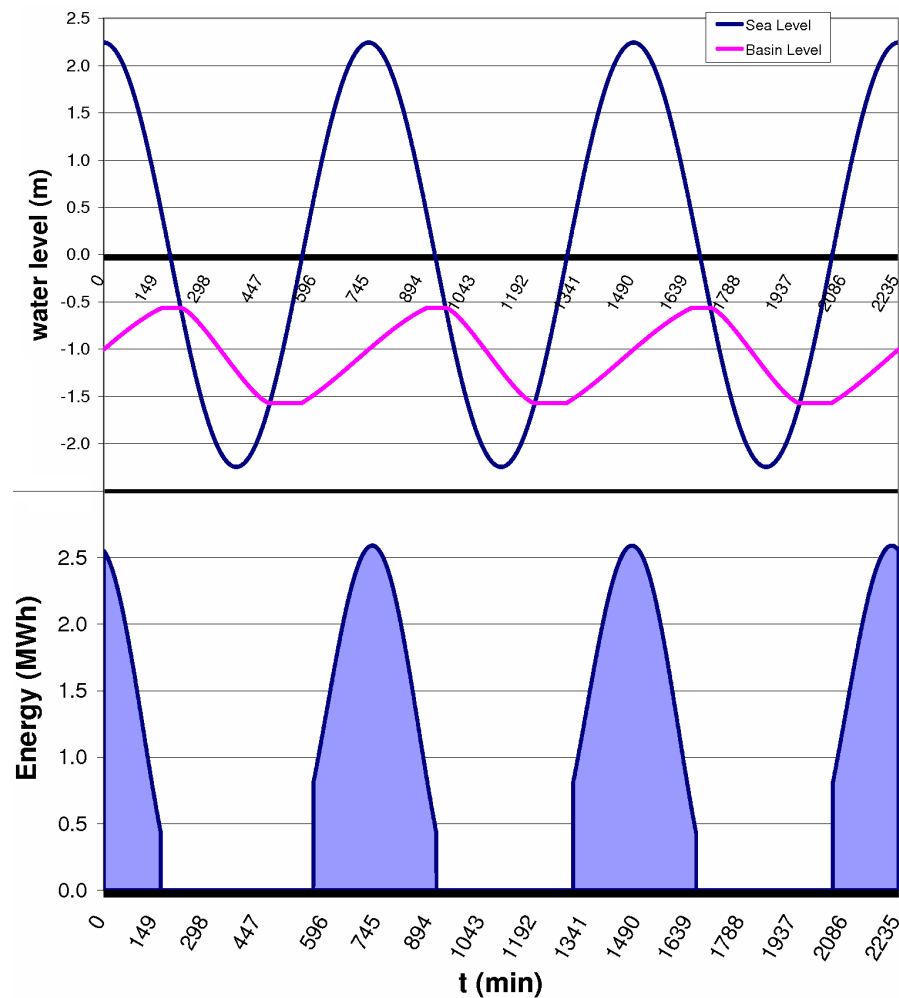
Figure 4.8: *Graph of water levels (sea = blue, basin = pink) and blocks of energy generation as a function of time at mean tide for three tidal cycles (output of Storage Area Approach Model)*
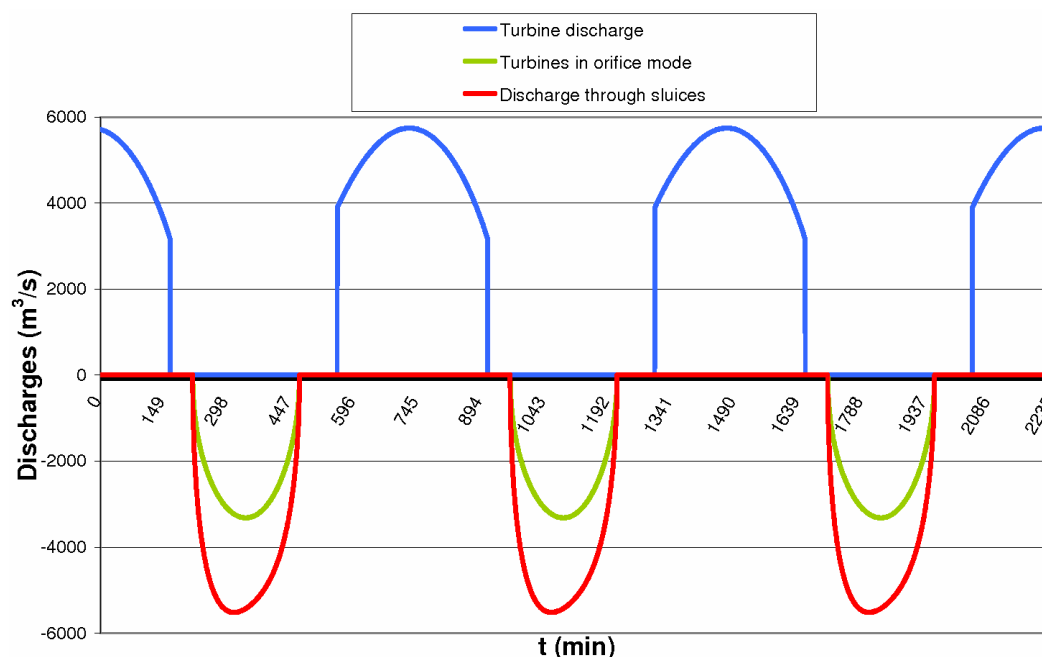
Figure 4.9: *Progression of discharges during one tidal cycle: total discharges through turbines (generating or in orifice mode) and through the Sinsi sluices (output of Storage Area Approach Model)*

4.8 Location of TPP

Given that a new port will be built west of the southern dam (between Sinsi Island and Garyeok Island), as well as the fact that quite some space is required, it stands to reason to locate the TPP in the northern estuary dam, at a location with suitable geotechnical conditions (see appendix B) and with a suitable initial depth, to minimise dredging costs. Therefore the TPP will be located near the former closure gap number 3, as there is still a tidal gulley.

The TPP could be built on the seaside, the basinside or in the middle of the existing estuary dam. The last option is not a good idea, because in that case the estuary dam's function as a sea defence structure would be at risk. This leaves two realistic options, of which constructing inside the basin is the best, because of the lower water levels inside; HHW at sea = + 4.75 m, while at the moment and in the future the tidal range inside the basin is much smaller; the maximum water level inside the basin is about EL +1.0 m. This requires a lower cofferdam height and the wave climate is friendlier. Another advantage of constructing the TPP inside the basin in comparison to constructing it outside the basin is that wave attacks will be much less powerfull. Thus the construction site will be inside the basin.

5 Dimensions and Construction

In this chapter the design of the tidal power plant at Saemangeum is developed. First the final dimensions (and electromechanical characteristics) of the turbines are calculated. Knowing the diameter of the turbines, the dimensions of the powerhouse can be calculated in conjunction with the specific site conditions (extreme tides and geotechnical data). In the last section the construction method is explained.

5.1   Dimensions of powerhouse

To determine the dimensions of the powerhouse, empirical formulas are used [Raabe, 1985] and [Miller, 1978]. For the dimensions of the draft tube, see Figure 5.1.

The height of the powerhouse is mainly governed by water levels and waves. Other aspects, such as a projected road on the barrage and spaces for maintenance and operation, may also influence the structural design. A road necessitates a structure height such that wave overtopping occurs with low frequency, say once per 50 years.
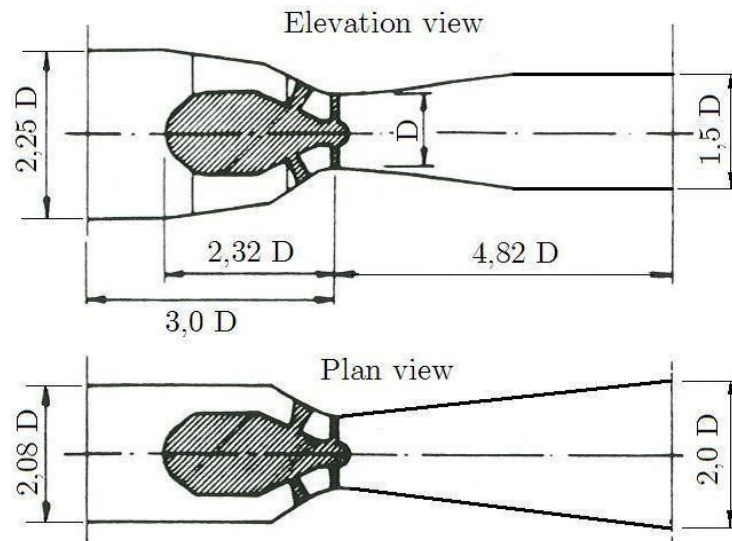
Figure 5.1: *Ideal bulb turbine dimensions (Miller and Raabe)*

According to [Miller, 1978] the centerline of the turbine should be at least $0.75 \cdot D$ below LWOST, so that the turbine is at all times guaranteed to be submerged. For Saemangeum ($D_t = 7.5$ m and LWOST = - 3.30 m, see table 5.1) this means that the centerline should be at least at a depth of EL - 8.93 (referred to MSL).

5.1.1 Water levels and geotechnical data

The sand layer at EL - 28.5 m (referred to MSL) is the first layer that is strong enough to support the structure. The bearing capacities of the weathered rock zone layer is at least as strong as the bearing capacity of the sand layer. From tests conducted on samples from boreholes (see appendix B) average lower bound values for sand have been assessed [NEDECO & Delft Hydraulics, 1992]:

- effective friction angle ϕ ' $= 33°$
- angle of wall friction $\delta = 22°$
- saturated density: 20 kN/m^3

Table 5.1: *Water levels Saemangeum*

Level	abbreviation	compared to MSL
Highest High Water level	HHW	4.75
High Water level of Ordinary Spring Tides	HWOST	3.19
Mean Sea level	MSL	0.0
Low Water level of Ordinary Spring Tides	LWOST	-3.30
Lowest Low Water level	LLW	-3.95

5.1.2 Cavitation

When the hydrodynamic pressure in a liquid falls below the vapour pressure of the liquid, there is a formation of the vapour phase. This phenomenon induces the formation of small individual bubbles that are carried out of the low-pressure region by the flow and collapse in regions of higher pressure. The formation of these bubbles and their subsequent collapse is called cavitation. These collapsing bubbles create very high impulse pressures on the construction parts nearby accompanied by substantial noise. The repetitive action of such collapses in a reaction turbine close to the runner blades or hub for instance result in pit-corrosion of the material. With time this pit-corrosion degenerates into cracks formed between the pits and the metal is snatched from the surface. In a relatively short time the turbine can be severely damaged and needs to be shut-off and repaired.

Cavitation can be avoided by limiting the operation range of the turbines and by placing the turbine units sufficiently deep.

Cavitation is characterised by the cavitation coefficient σ (Thoma's sigma coefficient) [ESHA, 2004] defined according to IEC 60193 standards as:

$$\sigma = \frac{NPSE}{gH} \tag{5.1}$$

Where NPSE is the net positive suction energy defined as:

$$NPSE = \frac{p_{atm} - p_v}{\rho} + \frac{u_{throat}^2}{2} - gH_s \tag{5.2}$$

Where:

p_{atm}	atmospheric pressure	[Pa]
p_v	water vapour pressure	[Pa]
u_{throat}	average flow velocity in turbine's throat	[m/s]
H	head over turbine	[m]
H_s	suction head	[m]

$$H_s = \frac{p_{atm} - p_v}{\rho g} + \frac{u^2}{2g} - \sigma H \qquad (5.3)$$

To avoid cavitation, the turbine should be installed at least at H_s. A positive value of H_s means that the turbine runner is over and above the downstream level, a negative value that it is under the downstream level. The value of p_{atm} is normally about 101.000 Pa at sea level and p_v is about 880 Pa for seawater of 10°C.

The Thoma's sigma is usually obtained by a model test. Statistical studies have made it possible to come to the following empirical formula to predict Thoma's sigma for Kaplan turbines [ESHA, 2004]:

$$\sigma = 3.164 \cdot 10^{-4} \cdot n_q^{1.46} + \frac{u^2}{2gH} \qquad (5.4)$$

The head over the turbines can never be more than the difference between HHW and LLW at sea. This is 8.70 m. So the σ should be calculated for H $= 0$ (orifice mode) up to H $=$ 8.70 m ($= 4.75 + 3.95$). The result is plotted in Figure 5.2.
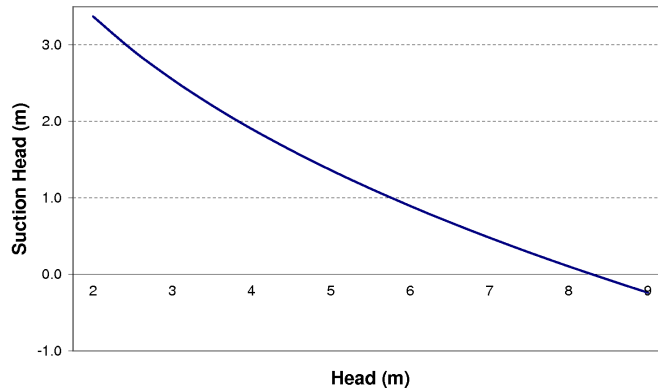
Figure 5.2: *Suction head vs Head*

Cavitation will not occur if the head is smaller than 8.29 m. In reality this head will never be reached, because if the water level on the outside is at its highest point (i.e. HHW $= 4.75$ m), the water level inside will not be lower than E.L. -2.25 m (This is the Storage Area Approach Model output for LLW in the basin if the tidal range is set at 8.70 m), resulting in a maximum possible head over the turbines of 7.00 m.

5.1.3 Stability

The dimensions of the draft-tube have been defined by the empirical equations by Miller and Raabe. The height of the powerhouse below and above sea level follow from the geotechnical data, tidal data and the characteristics of the barrage. In Section 5.1.2 it was concluded that cavitation does not influence the depth of the centerline of the turbines.

The leading failure mechanism for the powerhouse structure is uplift. This could happen if one turbine is dewatered for maintenance, while both at sea and in the basin the water level is at the highest possible point: EL + 4.75 m at the sea side and EL - 0.79 at the basin side.
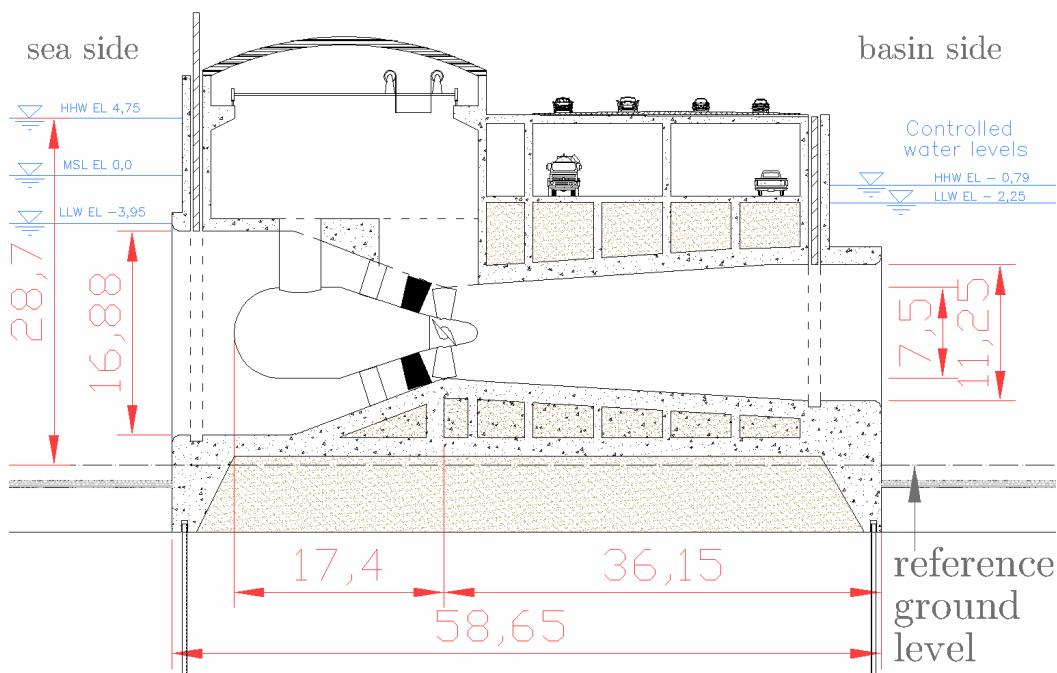
Figure 5.3: *Power house unit with reference ground level for uplift calculation (= median of area below horizontal concrete ground level)*

The power house is a gravity structure; Its own weight must be sufficient to meet safety factors against sliding, overturning and floatation. A unit in dewatered condition must not result in uplift of the structure. This will be avoided by constructing sections containing several chambers to be filled with ballast (sand, hydraulic fill). In Figure 5.3 these ballast chambers are shown (brown hatching). Some rough calculations show the need for sand ballasting:

One powerhouse unit contains about 9900 m^3 of concrete. The horizontal section of a unit is 1100 m^2, so this means that without filling the compartments with granular material, the water depth cannot be higher than about 22.5 m above the reference ground level (see the striped line and the text in the lower right corner of Figure 5.3) of the power house

unit. This reference ground level is at EL - 23.95 MSL. The specific weight of concrete is 25 kN/m^3.

When the empty compartments are filled with granular material (specific weight 18 kN/m^3), 7000 m^3 of sand is added, allowing the water level to rise another 12.6 m. This is sufficient, because the HHW is 28.7 m above the power house reference ground level.

Furthermore part of the structure will contain water (the parts just outside the gates: 1329 m^3), which will decrease the uplifting force, and the weight of the turbine is about 5 tons, which will increase the down force. As long as the water level at sea stays below 36.3 m above reference ground level, uplift will not occur (22.5 m due to the weight of the concrete, 12.6 m due to the weight of the sand and 1.2 m due to the weight of the water just outside the gates, but inside the box simplification of the power house). Since at HHW the height of the sea level above the reference ground level is 28.7 m, this condition is fulfilled with a safety factor 1.26 (= 36.3 / 28.7).

Connecting the powerhouse units increases the down force if only one of the connected units is dewatered at the time.

The dimensions of the power house structure are shown in Figure 5.3.
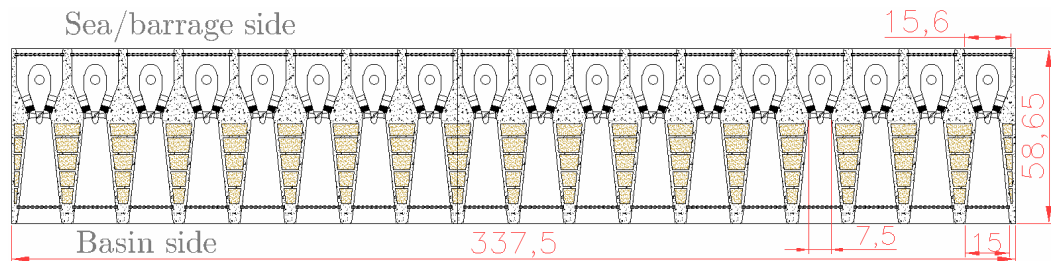
Figure 5.4: *Plan view of powerhouse, horizontal section at turbine-axis level*
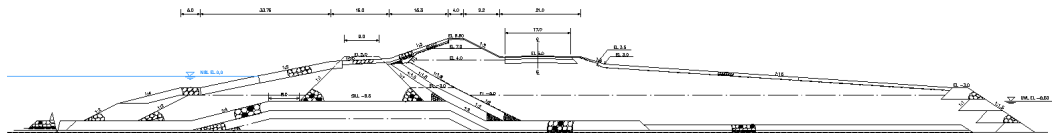
Figure 5.5: *Dam section at TPP location*
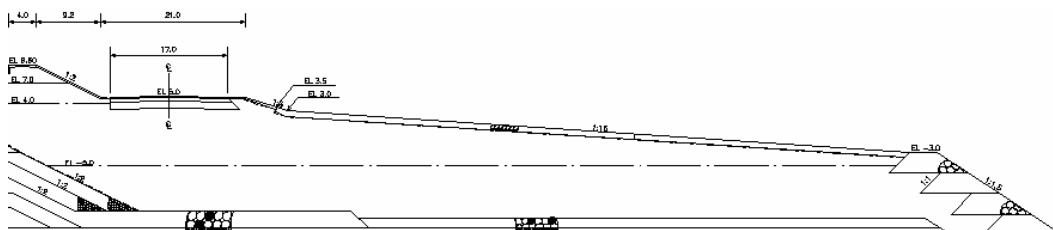
Figure 5.6: *Dam section at TPP location, basin side*

5.2   Construction method

A choice must be made between the construction of a cofferdam (construction in the dry) or the use of a float-in power house technique (construction in the wet).

5.2.1   Construction in the wet

Construction in the wet should be considered when major portions of the plant are to be built in an area exposed to ocean environment and a great number of repetitive construction operations are to be performed.

Although this is called "in the wet" most of the construction is performed on dry land under closely controlled conditions. Such construction would be carried out in a dry-dock or on a slipway. The prefabricated elements would then be floated out and placed in their permanent position when conditions of climate, tide and currents are favorable, thus reducing the "in the wet" activities to an absolute minimum.
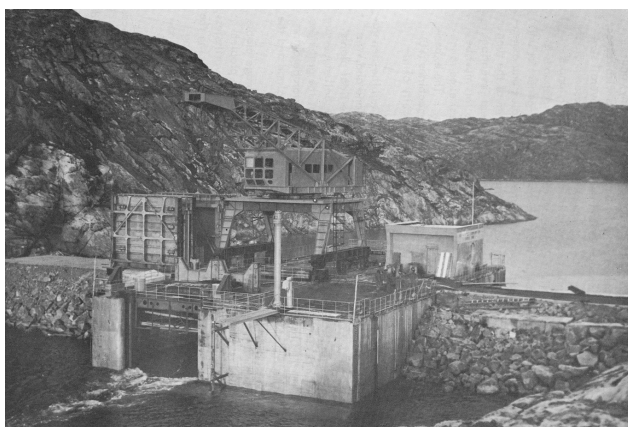
Figure 5.7: The plant in Kislaya Guba was constructed using the float-in method

With the exception of Kislaya Guba (Russia), no TPP's have been built in the wet, but numerous preliminary designs have been prepared.

Many uncertainties exist as to the applicability and cost of the float-in technique. The biggest obstacle for using this method for the Saemangeum TPP is the depth required for transportation. The height of the structure from the toe of the structure to the road level is 34.80 m. If the shafts openings would both be closed (watertight) and the construction were floated into place, it would have a draught of 20 m. This means that a channel would have to be dredged from the dock or slipway (where the caissons would be constructed) to the TPP location with a depth of at least 21 m, which is about 13 m deeper than the average depth of the basin. This channel could have a length of up to 5 km!

Another disadvantage of the caisson float-in method is that the subsoil below foundation level cannot easily be protected against piping. To protect against piping, a sheet piling

should be installed below the structure. It is very hard to construct this sheet pile wall in such a way that it is well connected with the caissons.

5.2.2   Construction in the dry

Each tidal power site will have its own characteristics which will determine the optimum choice of construction methods. When opting for construction in the dry, a cofferdam must be made. A cofferdam is a structure that permits dewatering of an area and constructing the structure in the dry. A dewatered area can be completely surrounded by a cofferdam structure or by a combination of natural earth slopes and a cofferdam structure. The type and dimensions of construction depends upon the depth, soil conditions, fluctuations in the water level, availability of materials, working conditions desired inside the cofferdam.

***Table 5.2:** Specifications soil characteristics*

H_c	Height between ground level inside and outside cofferdam	30.72	m
H_p	Height of cofferdam's sheet piles	40.22	m
ϕ	Angle of internal friction	33	°
δ	Angle of wall friction	22	°
$\gamma_{sat.soil}$	Specific weight of saturated soil	20	kN/m^3
γ_w	Specific weight of water	10.06	kN/m^3
θ	Characteristic angle cofferdam and spandrel wall	45	°
K_a	Active earth pressure coefficient	0.265	-
K_p	Passive earth pressure coefficient	3	-
K_0	Neutral earth pressure coefficient	0.6	-
f_{gr}	friction coefficient, gravel on rock	0.5	-
D_c	Diameter circular cell cofferdam	?	m
$W_{c,e}$	Equivalent width cofferdam	?	m
$P_{c,ave}$	Average vertical soil pressure in cofferdam	?	kPa
$M_{0,d}$	Moment around centre of foundation plane cofferdam	?	kNm
Qr,d	Maximum absorbable shear force	?	kN
F_o	Resultant force from outside on cofferdam	?	kN
F_i	Resultant force from inside on cofferdam	?	kN
d_o	Arm (line of action F_o - foundation plane)	?	m
d_i	Arm (line of action F_i - foundation plane)	?	m

Where the cofferdam structure can be built on a layer of impervious soil (which prevents the passage of water), the area within the cofferdam can be completely sealed off. This is most likely the case in Saemangeum. Where the soils are pervious, the flow of water into the cofferdam cannot be completely stopped economically, and the water must be pumped out periodically and sometimes continuously.

Because of the large dimensions, a cellular cofferdam is needed. The same kind of cofferdam structure has been used for constructing the La Rance TPP and is momentarily used for the Sihwa plant. The cofferdam can be installed as follows: Welded distribution piles assure the connection between primary cells and spandrel walls (arches connecting
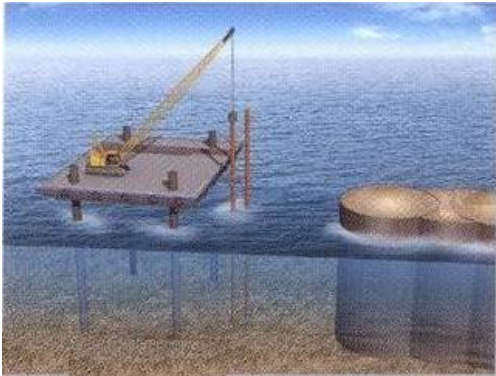
Figure 5.8: *Pin pile installation*

Figure 5.9: *Template installation*
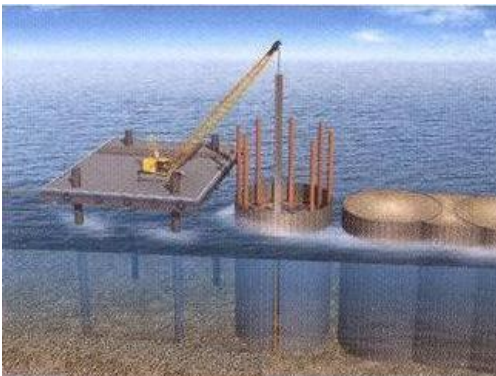
Figure 5.10: *Sheet pile driving*

Figure 5.11: *Filling circular cells with sand*

Figure 5.12: *Installing spandrel walls*
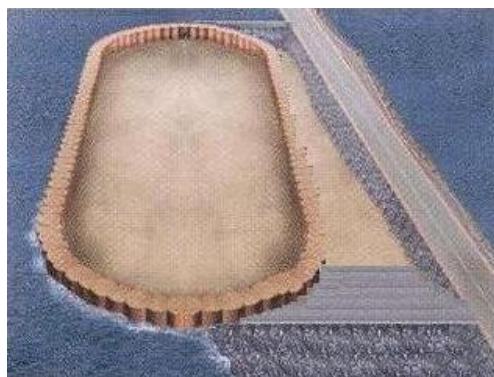
Figure 5.13: *Dewatered construction site*

the main, circular cells; see Figure 5.14). The construction of a circular cell is performed in-situ. The flat sections are lifted from a pontoon by crane and driven to the required depth at the site with the aid of pile driving devices. For the definition of circular cells and spendral walls, see Figure 5.14. The process of installation of the cofferdam is shown in Figures 5.8 to 5.13 (Sources: [KOWACO & DAEWOO, 2006] and [Lee, Kwang-soo, 2006]).
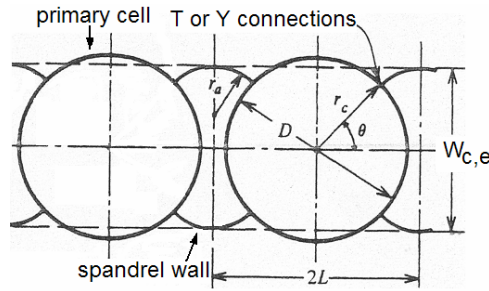
Figure 5.14: *Plan of circular cells with connecting cells (formed by arcs/ spendral walls)*
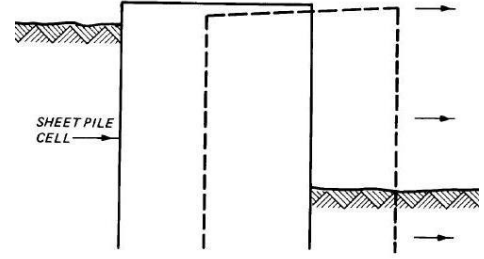
Figure 5.15: *Failure due to sliding*

The depth up to which the sheet piles are installed is EL - 38 m, assuming that the sheet piles will only enter the first meter of the rock layer at EL - 37 m.

To calculate the stability of the cofferdam one should use the equivalent cell width $W_{c,e}$, defined by

$$W_{c,e} = \frac{A_c}{2L} = 0.875 \cdot D_c \tag{5.5}$$

Where A_c is the area of the main circular cell plus one connecting cell and 2 L is the center-to-center distance between the circular main cells (again see Figure 5.14). The height between ground level inside and outside cofferdam is defined as H_c.

The depth of the sand layer is at E.L. -28.5 m and the top is at E.L. + 2.22 m. The cofferdam at the barrage side must resist the highest loads. The ground level of the barrage intersects the cofferdam at E.L. +2.22 m. The weight of saturated sand is 20 kN/m³. The active earth pressure coefficient is calculated by:

$$K_a = \frac{\cos^2 \phi}{\cos \delta \left(1 + \sqrt{\frac{sin(\phi+\delta)sin\phi}{cos\delta}}\right)^2} \tag{5.6}$$

For $\phi = 33°$ and $\delta = 22°$ this gives $K_a = 0.265$. The passive earth pressure coefficient K_p = 3.0 according to the following formula:

$$K_p = \frac{1 + \sin \phi}{1 - \sin \phi} \tag{5.7}$$

Two failure mechanisms must be investigated: Sliding (moving horizontally) and tipping over (rotating around center of foundation level of cofferdam).

Failure due to Sliding

Sliding (see Figure 5.15) occurs when the resisting force against sliding is smaller than the lateral pressure exerted on the cofferdam by the soil or the water. For safety a factor 1.25 is used, so the ratio resisting force against sliding to lateral forces must be at least 1.25. At the basin side of the construction pit this means

$$\frac{f_{gr} W_{c,e} H_c \gamma_{sat.soil}}{1/2 \cdot \gamma_w H_c^2} \geq 1.25 \tag{5.8}$$

Assuming totally saturated soil both in the barrage and in the cofferdam, this means that the Diameter of the cofferdam cells must be at least 22.06 m.

At the barrage side the width of the cofferdam is calculated as follows:

$$\frac{f_{gr} W_{c,e} H_c \gamma_{sat.soil}}{1/2 \cdot (\gamma_w + K_a(\gamma_{sat.soil} - \gamma_w)) H_c^2} \geq 1.25 \tag{5.9}$$

This leads to a minimum diameter of 27.84 m.

Failure due to Tipping over

The turning moment around the center of the foundation level in the rock layer is calculated with the Terzaghi-method. This method models the cellular cofferdam to vertical slices gliding with respect to each other, like a series of books falling over on a shelf. The Terzaghi method uses only the rigidity of the shape of the cofferdam structure. The method checks if there is no slide due to shear stresses along the vertical mid-plane. A linear distribution is assumed of the vertical pressure on the foundation due to the moment M_0, caused by the external forces with respect to the middle of the foundation plane. This will not occur as long as the weight of the sand fill of the cofferdam is enough and thus the equivalent width should be large enough.
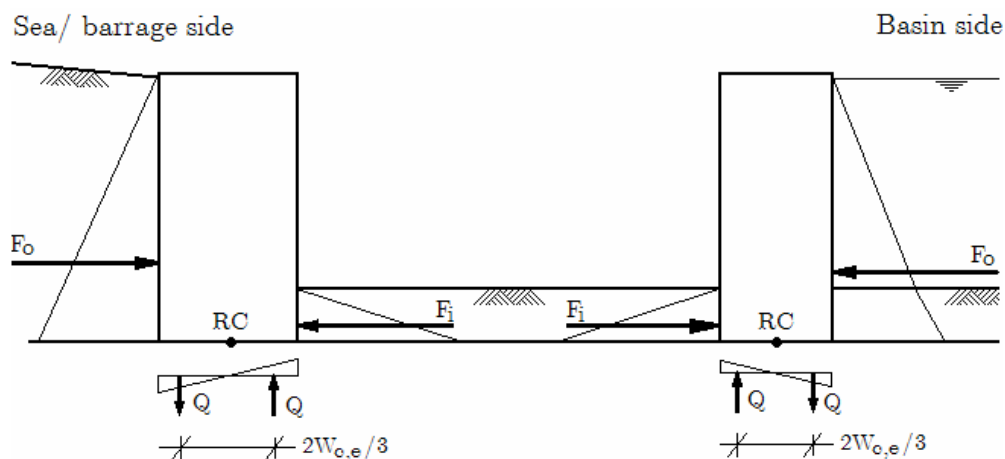
Figure 5.16: *Loads on cofferdam for determining moment about RC (RC = rotation centre)*

The maximum absorbable shear force in the vertical plane in the middle of the cofferdam ($Q_{r,d}$) is determined by multiplying the average vertical soil pressure $P_{c,ave}$ with the vertical length of the sheet piles and with $\tan \phi$. Here the neutral earth pressure coefficient must be used; $K_0 = 0.6$ [Van Tol & Everts, 2002]. The equivalent cofferdam width $W_{c,e}$ must be that large that Q_d in the formula below resists the turning moment $M_{0,d}$. The following equations show how to calculate the relevant parameters. F_o is the resultant force exerted by the soil (or water for the cofferdam at the basin side) on the cofferdam on the outside, while F_i is the resultant force exerted by the soil on the inside of the construction site on the cofferdam. See Figure 5.16.

$$Q_d = \frac{3M_{0,d}}{2W_{c,e}} \tag{5.10}$$

$$P_{c,ave} = \frac{1}{2}\left(\gamma_w + K_0(\gamma_{sat.soil} - \gamma_w)\right)H_s \tag{5.11}$$

$$M_{0,d} = F_o d_o - F_i d_i \tag{5.12}$$

$$F_o = \frac{1}{2}\left(\gamma_w + K_a(\gamma_{sat.soil} - \gamma_w)\right)\cdot H_p^2 \tag{5.13}$$

$$F_i = \frac{1}{2}\left(\gamma_w + K_p(\gamma_{sat.soil} - \gamma_w)\right)\cdot (H_p - H_c)^2 \tag{5.14}$$

$$Q_{r,d} = P_{c,ave}H_s \tan \phi \tag{5.15}$$

For both the basin side cofferdam and the barrage (sea) side cofferdam $P_{c,ave}$ and thus $Q_{r,d}$ can be calculated:

$$P_{c,ave} = \frac{1}{2}\cdot(10 + 0.6\cdot(20 - 10))\cdot 40.22 = 321.8\ kN$$

$$Q_{r,d} = 321.8\cdot 40.22\cdot \tan 30 = 7472\ kN$$

For the cofferdam on barrage side counts:

$$F_0 = \frac{1}{2}12.65\cdot 40.22^2 = 10232\ kN$$

$$F_i = \frac{1}{2}40\cdot 9.5^2 = 1805\ kN$$

$$M_{0,d} = 10232\frac{40.22}{3} - 1805\frac{9.5}{3} = 131461\ kNm$$

Now the required equivalent cofferdam width follows from:

$$W_{c,e} = \frac{3M_{0,d}}{2Q_d} = \frac{3 \cdot 131461}{2 \cdot 7472} = 26.39 \ m$$

This is less than the required equivalent width against sliding, which was 27.84 m. Conclusion: The equivalent cell width of the cofferdam at the barrage/ sea side should be 27.84 m, which means that the diameter of the circular cells should be 27.84 / 0.875 = 31.82 m. Bearing in mind that normally a berm at the inside of the cofferdam is constructed, the resisting force will be significantly larger.

For the cofferdam on basin side counts:

$$F_0 = \frac{1}{2}10 \cdot 40.22^2 + \frac{1}{2}2.65 \cdot 9.5^2 = 8088 + 120 = 8208 \ kN$$

$$F_i = \frac{1}{2}40 \cdot 9.5^2 = 1805 \ kN$$

$$M_{0,d} = 8088\frac{40.22}{3} + 120\frac{9.5}{3} - 1805\frac{9.5}{3} = 103097 \ kNm$$

Now the required equivalent cofferdam width follows from:

$$W_{c,e} = \frac{3M_{0,d}}{2Q_d} = \frac{3 \cdot 103097}{2 \cdot 7472} = 20.70 \ m$$

This is less than the required equivalent width against sliding, which was 22.06 m. Conclusion: The equivalent cell width of the cofferdam at the basin side should be 22.06 m, which means that the diameter of the circular cells should be 22.06 / 0.875 = 25.21 m. Again it must be kept in mind that a berm on the inside of the cofferdam could significantly increase the resisting force.

5.3   Bed protection

To make sure that the bed will not be damaged, the maximum flow velocity for the bed protection calculation is determined by the highest possible head: the difference between HHW and LLW, which is 8.70 m. At this head the flow velocity at the turbine throat is 13.06 m/s (see formula 5.16). The design flow velocity for the bed protection can now be calculated from the ratio between the shaft's exit area and the throat area:

$$u_{throat} = \sqrt{2gH} \tag{5.16}$$

$$u_{exit} = \frac{A_{exit}}{A_{throat}}u_{throat} = \frac{1/4 \cdot \pi D^2}{1.5 \cdot 2.0 \cdot D^2}u_{throat} = \frac{\pi}{12}u_{throat} \tag{5.17}$$

So u_{exit} = 3.42 m/s, as the flow velocity is assumed to have equally spread over the shaft section. The required particle diameter $D_{part,req}$ is calculated using Izbash' formula (u_c is
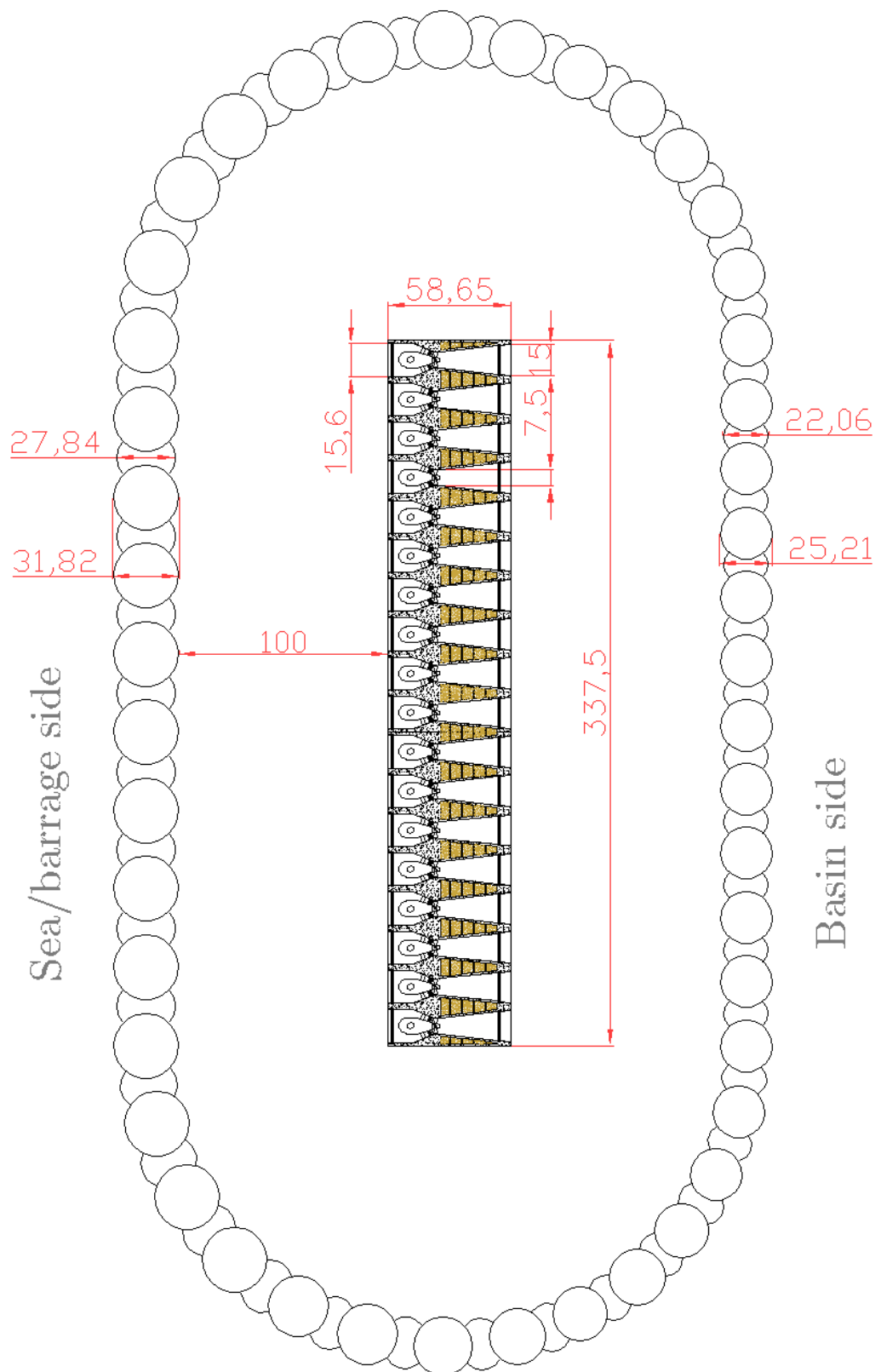
Figure 5.17: *Cofferdam and powerhouse*
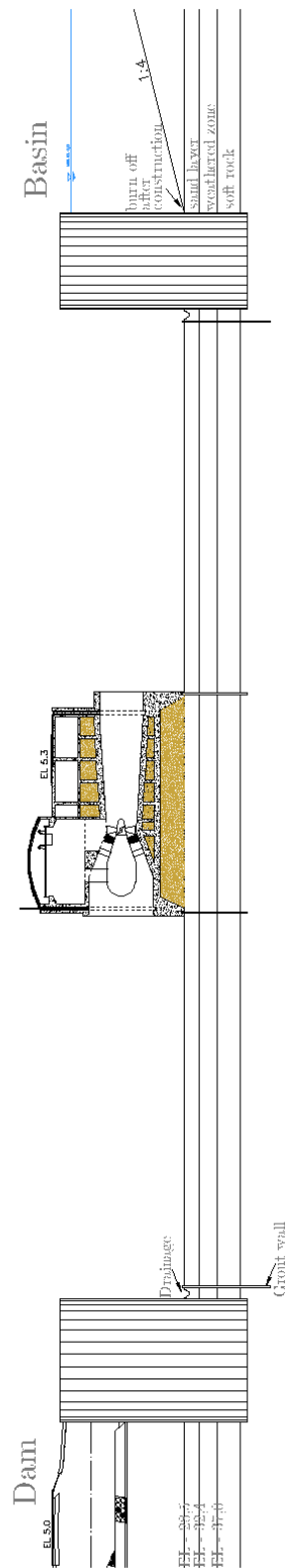
Figure 5.18: *Section over construction site including cofferdams*

the critical flow velocity and Δ is the relative density):

$$\Delta \cdot D_{part,req} = 0.7 \frac{u_c^2}{2g} \qquad with \qquad \Delta = \frac{\rho_s - \rho_w}{\rho_w} \qquad (5.18)$$
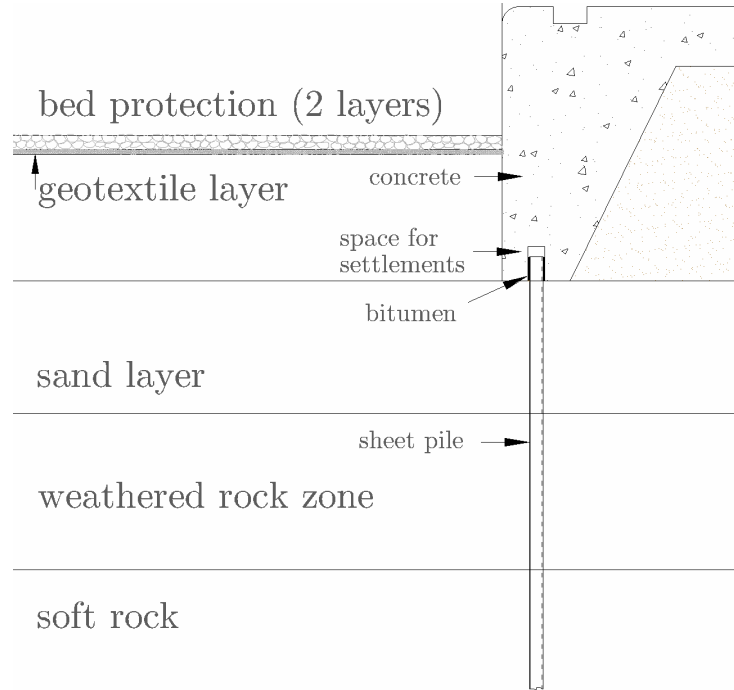
Figure 5.19: *Detail: Connection between sheet pile and concrete structure*

Assuming a rock weight of 25 kN/m^3, this means that a minimal particle diameter of 27.8 cm (or 0.28 m) should be used. From the standard classes of rock grading (EN 13383) it follows that stones of class LMA 40-200 should be used; These stones have a median grain diameter D_{50} of 37 - 42 cm and $D_{n50} = 34$ cm. According to EN 13383 the layer thickness should be at least $1.5 \cdot D_{n50} = 52$ cm. The bed protection can be constructed in the dry within the cofferdam area. To prevent the subsoil from flushing away, geotextile should be placed on the bottom first. Between the the geotextile and the large stones ($D_{n50} = 34$ cm), a thin layer of smaller stones should be placed. This layer should exist of stones with a diameter of about one fifth of 34 cm. The standard classes of rock grading show that $D_{n50} = 6.4$ cm would be the best suitable grain size. (Class name: CP45/125, range: 45/125 mm, $D_{50} = 6.3$ - 9.0 cm). The layer thickness should be at least $1.5 \cdot D_{n50} = 9.6$ cm.

Length of bed protection

Nomenclature:

To compute the required length of the bed protection, the maximum flow velocity at the end of the bed protection must be calculated. At this location a scour hole will develop.

α	Dust bin parameter (scour calculation)	-
Δ	Relative density	-
ν	Kinematic viscosity	-
Ψ	Shield's parameter	
C	Chézy's coefficient	$m^{1/2}/s$
D	Step height	m
d_{50}	Nominal grain diameter	m
d*	Dimensionless grain diameter	-
f_c	Coefficient by Hoffmans (1993)	-
h_0	Original water depth	m
h_{sc}	Maximum scour depth	m
k_r	(bottom) Roughness coefficient	-
L	Length of bed protection	m
R	Hydraulic radius	m
r_0	Coefficient by Hoffmans and Hinze	-
$\overline{u}$	Vertically averaged velocity at end of protection	m/s
$\overline{u}_c$	Critical velocity	m/s

The final depth of the scour hole determines the minimum length of the bed protection: The slope (to be determined) times the scour depth gives the minimum required length of the bed protection.

The maximum average flow velocity in the throat of the turbine opening is 13,06 m/s (u_{throat}). This is when the head over the turbines is at its theoretical maximum: 8.75 m. The area of the turbine throat is $F_{1t} = \frac{1}{4}\pi D^2$. The flow area behind one power house unit on basin side is $F_{p,u} = W_{p,u} \cdot h$, where h is the depth at the basin side of the power house and $W_{p,u}$ is the width of one power house unit. The depth-averaged flow velocity at the end of the bed protection follows from the following relationship:

$$\overline{u} = \frac{F_{1t}}{F_{p,u}} u_{throat} = 0.1108 \cdot 13.08 = 1.447 \ m/s$$

The d_{50} of the sand at Saemangeum is 90 μm. The Chézy coefficient for the flow above the bed protection can be computed with the following equation. The median grain diameter is 34 cm (as computed earlier in this section) and k_r is a bottom roughness coefficient, assumed to be twice the median grain diameter.

$$C = 18 \log\left(\frac{12R}{k_r}\right) \tag{5.19}$$

$$C = 18 \log\left(\frac{12 \cdot 21.27}{2 \cdot 0.34}\right) = 46.34 \ \sqrt{m}/s$$

Alpha is an amplification factor for the velocity, which expresses the disturbance in the flow, hence it is expected to be related to the turbulent fluctuations in the flow. It is to be expected that a longer bottom protection will lead to lower α values, due to dissipation of turbulence [Schiereck, 2001]. The roughness of the bottom protection is also of influence. With a smooth protection, the velocities near the bed are high and cause more scour. The

influence of the roughness on α is given by Hoffmans and Booij (1993):

$$\alpha = 1.5 + 5 \cdot r_0 f_c \tag{5.20}$$

The r_0 in Equation 5.20 is a parameter for the relative turbulence. It is defined by Hinze (1975):

$$r_0 = \sqrt{0.0225 \left(1 - \frac{D}{h}\right)^{-2} \left(\frac{L - 6D}{6.67h} + 1\right)^{-1.08} + \frac{1.45g}{C}} \tag{5.21}$$

Where D is the step height (difference between bed level and lowest part of shaft's intersection with the basin side of the power house), which is 6.60 m.

$$r_0 = \sqrt{0.0225 \left(1 - \frac{6.60}{21.27}\right)^{-2} \left(\frac{L - 6 \cdot 6.60}{6.67 \cdot 21.27} + 1\right)^{-1.08} + \frac{1.45 \cdot 9.81}{46.34}}$$

The f_c in Equation 5.20 is a friction coefficient defined by:

$$f_c = \frac{C}{40} \tag{5.22}$$

$$f_c = \frac{46.34}{40} = 1.159$$

In order to determine the Shield's parameter, which is needed to calculate the critical flow velocity (incipient motion), the dimensionless grain diameter d* must be calculated. In this equation ν is the kinematic viscosity of water ($1.33 \cdot 10^{-6}$ m^2/s). Here Δ is the relative density ($\Delta = \frac{\rho_s - \rho_w}{\rho_w} = 1.5$);

$$d* = d \left(\Delta \cdot g / \nu^2\right)^{1/3} \tag{5.23}$$

$$d* = 0.000090 \left(1.5 \cdot 9.81 / (1.33 \cdot 10^{-6})^2\right)^{1/3} = 1.8236$$

Now the Shield's parameter can be derived from the Shield's diagram, see Figure 5.20. In the right part of the figure it can be seen that for d* = 1.8236 the Shield's parameter $\Psi_c \approx 0.13$
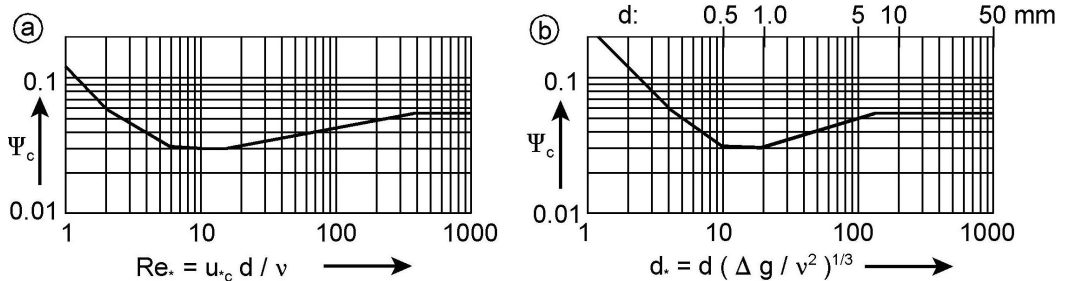
Figure 5.20: *Shield's diagram*

Knowing the critical value of the Shield's parameter Ψ_c, the critical flow velocity $\overline{u}_c$ can be calculated; In the following equation the Chézy coefficient does not have the same value as above, because now it indicates the bottom roughness of sand instead of the roughness of the bed protection; $C = 18 \log\left(\frac{12 \cdot 21.27}{2 \cdot 0.000090}\right) = 110.7 \sqrt{m}/\text{s}$

$$\overline{u}_c = C\sqrt{\Delta \cdot d_{50} \Psi_c} \tag{5.24}$$

$$\overline{u}_c = 110.7\sqrt{1.5 \cdot 0.000090 \cdot 0.13} = 0.464 \; m/s$$

The depth of the scour hole is calculated with the following equation:

$$\frac{h_{sc}}{h_0} = \frac{0.5 \cdot \alpha \cdot \overline{u} - \overline{u}_c}{\overline{u}_c} \tag{5.25}$$

The value of α results from Equation 5.20. But α is not known as long as r_0 is unknown. r_0 is dependent on the Length of the bed protection, so the value of L must be calculated by iteration. Where L = required length of bed protection. L can be calculated with the following equation [Jorissen & Konter, 1992] $(\cot(\gamma) = 8$ for sand, if not sensitive for settlement):

$$L = \frac{h_{max}}{2}\left(\cot(\gamma) - 4\right) \tag{5.26}$$

Equation 5.25 is just an approximation, not accurate enough. There exist no precise formulas. To be sure the length of the bed protection should be much longer. If this method is used, iteration gives L = 275.5 m. The depth of the scour hole would be 137.7 m. This is not possible at Saemangeum, because of the rock layer at EL - 37 m. Thus the maximum scour depth would in practice probably amount to 8.5 m (the difference between the level of the sand layer on which the power house is constructed and the level of the rock layer). According to Equation 5.26 this would mean that the length of the bed protection would then be 17 m. To be sure that the bed protection will be long enough, it is decided that a bed protection is placed in the whole area within the cofferdam structure and that the cofferdam will be burned off after watering the power house structure. This leaves a bed protection length of 125.2 m at the basin side of the power house and a bed protection length of 131.8 m at the estuary dam/ sea side of the power house. At that side the flow velocities will be much lower, due to the larger entrance gate area of the power house structure.

6 Economic Feasibility

The answer to the question whether a power plant should be built or not is mainly based on economic conditions. The benefits should be greater than the construction, operation and maintenance costs.

The economic value of tidal power is discussed in Section 6.1. This includes variations in energy price (both in time and in regions) and comparisons with other energy sources. Section 6.2 outlines the construction costs.

The economic feasibility depends on a number of economic parameters: the discount rate, the economic lifetime expectancy and the future price of energy. These are discussed in Section 6.3, where the Net Present Value is calculated.

In Section 6.4 the resulting main parameters for the plant are listed (Number of turbines, Annual energy output, Installed power, construction costs). In Section 6.5 the sensitivity for changes in the parameters is investigated.

6.1   The economic value of tidal energy

When celebrating the 30th anniversary of the La Rance TPP in 1996, EDF (Electricite de France) reported that the cost of energy produced by the La Rance plant was well below the average of the EDF system [Bosc, 1997]. This illustrates the fact that capital intensive projects can in time turn out to be the most economical option.

At the time of its early operation in 1966, it was realized that the energy produced by the La Rance plant was costly. In 1982, sixteen years after commissioning, the cost was 16.9 centime/kWh (1 centime = .01 French Franc), which is equal to US$ 0.0376 in 2007, of which the financial component was 11 centime/kWh (US$ 0.0245 in 2007). EDF's nuclear stations generated at 20 centime/kWh (US$ 0.0445 in 2007) while the best run-of-the-river plants produced energy at 10 centime/kWh (US$ 0.0233 in 2007).

The Saemangeum TPP should produce energy at a competitive price. Therefore it is important to get some insight in energy prices and the differences between the different types of generation methods. In Table 6.1 the generation price of different types of thermal power plants are listed, while in Table 6.2 the same is done for renewable energy sources. [1]

Table 6.1: *Fossil-Fuel Energy Costs*

Fossil-Fuel Technologies Costs	cents/kWh (US$)
Diesel engine-generators	6.3 - 8.5
Natural gas combined cycle plant	3.1 - 3.4
Pulverised coal steam-electric plant	3.2 - 3.9

---

[1] Source of these tables: HEA 2003

Table 6.2: *Renewable Energy Costs (worldwide price ranges)*

Renewable Technologies Costs	cents/kWh (US$)
Geothermal energy	2 - 10
Large Hydroelectricity	2 - 8
Small Hydroelectricity	4 - 10
Solar photo voltaic electricity	25 - 125
Wind electricity	5 - 13
Biomass energy	5 - 15

Table 6.3: *Prices of power worldwide; US$ cents/kWh at 5 % discount rate, 40 years economic lifetime, 85% load factor . Source: OECD/IEA NEA 2005.*

	nuclear	coal	gas
Finland	3.10	4.09	
France	2.85	3.74	4.40
Germany	3.21	3.95	5.50
Switzerland	3.23		4.89
Netherlands	4.02		6.78
Czech Rep	2.58	3.30	5.58
Slovakia	3.51	5.36	6.27
Romania	3.43	5.11	
Japan	5.39	5.56	5.85
Korea	2.63	2.42	5.22
USA	3.38	3.04	5.24
Canada	2.92	3.49	4.49

The construction costs for a Tidal Power Plant are relatively high, compared to conventional plants (gas, coal, nuclear), but on the other hand the operation costs are relatively low, see Figure 6.1. Thus the longer the lifetime expectancy, the more competitive a tidal power plant could be.

In France the La Rance TPP has already demonstrated that, if the natural, site specific conditions allow it, tidal power can be competitive. It has also showed that an economic lifetime of 40 years is likely to be obtained.
From this section can be concluded that the energy production price should be about US$ 0.03 to be competitive. In this study environmental allowances are not taken into account! If these allowances were to be granted, tidal power could be much more profitable!

6.2   Construction costs

The construction costs are defined to be those expenses which have to be made to build the TPP and the necessary other structures (like dams) in comparison to the situation without the plant. This means that, for example, the dikes protecting the polders are not included in the construction costs, unless they would have to be adjusted to the presence of the TPP, for instance if a higher dike crest is needed because of a higher basin level.
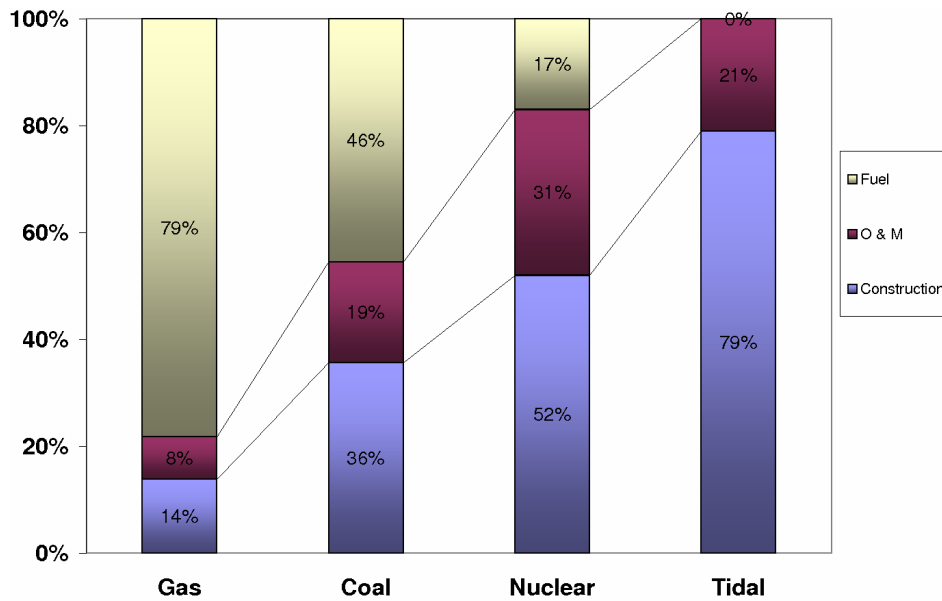
Figure 6.1: *Breakdown of total expenditures (Construction, Operation & Maintenance, Fuel) for gas, coal, nuclear and tidal energy; Data from NEA OECD 2005 (except for tidal energy; data come from this study), economic lifetime 40 years, discount rate 5 %*

To estimate the total civil construction costs, a method is used based on empirical formulas, developed by Fay and Smachlo [Fay & Smachlo, 1983a]. The costs of the electromechanical equipment (turbines, generators and transmission lines) are also described by an empirical formula, partly based on a graph provided by turbine manufacturer Alstom. This method is extensively described in appendix D.

The design of the TPP could be based on the ratio between the investment cost and installed power. But a large installed capacity does not guarantee that the investment is justified. So it would be better to optimise the ratio between the investment costs and the amount of energy generated per year (or cycle). This is an improvement, but still there are some shortcomings. The lifetime of the TPP and the future price of energy are not accounted for. So it is decided that the TPP should be designed such that the Net Present Value (NPV) of all the cash flows involved after 40 years of operation is the highest.

6.3   Net Present Value

As concluded in the previous section, the best way to come to the design parameters for the TPP is to optimise the Net Present Value (NPV). Before the NPV can be calculated, some assumptions have to be made.

To make the TPP in Saemangeum a competitive plant, the goal is to produce energy at a low price. From Table 6.3, it can be seen that the lowest price at which energy is produced today in Korea is about US\$ 0.03 per kWh, so this should be the price at t = 0 in the

NPV calculation. These numbers date back to 2005, but they are the most actual numbers available. Knowing that the energy prices in Europe have risen over 12.5 % annually over the last 5 years the assumption that the actual energy production price in Korea is about US$ 0.03 per kWh seems to be accurate.

The lifetime expectancy of the Saemangeum TPP is estimated to be 40 years. This is a conservative estimate, as the La Rance TPP is now already in its 41st year of operation and the end of service is not yet in sight. It is very likely that the lifetime expectancy of the civil works could be about 50 years. The lifetime of the mechanical parts is shorter (about 25 years). However, in the calculations this is replaced by intensive maintenance every five years, estimated to amount to 3 % of the construction costs every time, because it would not be fair to charge new mechanical equipment only once in 25 years, since it would then make no difference if the lifetime of the plant would be, for example, 30 or 40 years.

The construction costs are equally spread over the three years of construction. The running costs of the TPP per year are a fixed percentage of the construction costs. They are estimated to be 1 % of the construction costs.

The annual rise of the real energy price is expected to be 4 % and the discount rate is expected to be 4 %.

The NPV's have been calculated for $N_t = 1$ until $N_t = 100$. The NPV's as a function of the number of turbines are plotted in the graph in Figure 6.2. The maximum is reached at $N_t = 18$. The corresponding NPV is US$ 187,589,376.
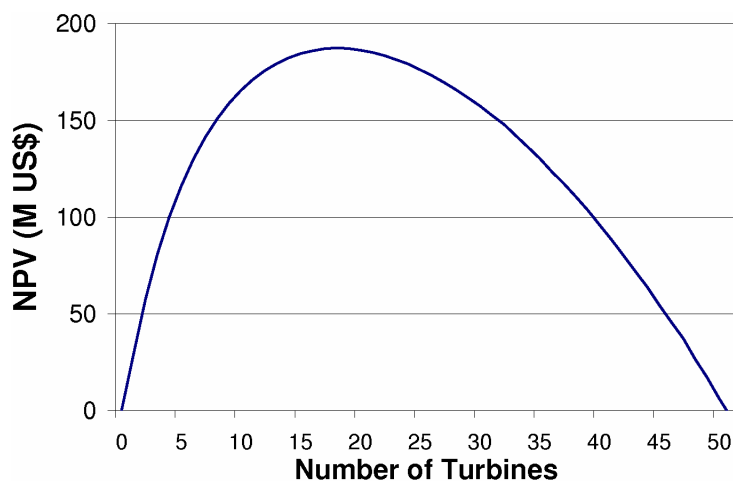
Figure 6.2: *Net Present Value for a lifetime of 40 years as a function of Number of turbines*

For $N_t = 18$ the calculation of the NPV is specified in Table 6.4. All expenses are accounted for at the beginning of the year, all income is accounted for at the end of the year. In each row the expenditures (construction, maintenance and running costs), benefits, discounted costs and benefits (at different discount rates) and the NPV for that particular year are listed (all amounts in Millions of US$). In Figure 6.3 the NPV is plotted as

Table 6.4: *Net Present Value with after a construction time of 3 years and a lifetime of 40 years in millions of US$ with an annual rise of the energy price of 4 %*

	Expenditure				Discounted costs			Discounted benefits			NPV		
Year	Construction	Maintenance	Running costs	Benefits	at 2%	at 4%	at 6%	at 2%	at 4%	at 6%	at 2%	at 4%	at 6%
0	95.34				95.34	95.34	95.34				-95.34	-95.34	-95.34
1	95.34				93.47	91.67	89.94				-188.80	-187.00	-185.27
2	95.34				91.63	88.14	84.85				-280.43	-275.15	-270.12
3			2.86		2.70	2.54	2.40				-283.13	-277.69	-272.52
4			2.86	15.93	2.64	2.44	2.27	14.71	13.61	12.62	-271.06	-266.52	-262.17
5			2.86	16.56	2.59	2.35	2.14	15.00	13.61	12.38	-258.64	-255.25	-251.93
6			2.86	17.23	2.54	2.26	2.02	15.30	13.61	12.14	-245.89	-243.90	-241.80
7		8.58	2.86	17.92	9.96	8.69	7.61	15.60	13.61	11.92	-240.25	-238.98	-237.50
8			2.86	18.63	2.44	2.09	1.79	15.90	13.61	11.69	-226.79	-227.45	-227.60
9			2.86	19.38	2.39	2.01	1.69	16.21	13.61	11.47	-212.97	-215.85	-217.82
10			2.86	20.15	2.35	1.93	1.60	16.53	13.61	11.25	-198.78	-204.17	-208.17
11			2.86	20.96	2.30	1.86	1.51	16.86	13.61	11.04	-184.22	-192.41	-198.63
12		8.58	2.86	21.80	9.02	7.15	5.69	17.19	13.61	10.83	-176.06	-185.94	-193.49
13			2.86	22.67	2.21	1.72	1.34	17.52	13.61	10.63	-160.74	-174.04	-184.20
14			2.86	23.58	2.17	1.65	1.27	17.87	13.61	10.43	-145.04	-162.08	-175.04
15			2.86	24.52	2.13	1.59	1.19	18.22	13.61	10.23	-128.95	-150.05	-166.00
16			2.86	25.50	2.08	1.53	1.13	18.58	13.61	10.04	-112.46	-137.97	-157.09
17		8.58	2.86	26.52	8.17	5.87	4.25	18.94	13.61	9.85	-101.69	-130.22	-151.49
18			2.86	27.58	2.00	1.41	1.00	19.31	13.61	9.66	-84.38	-118.02	-142.82
19			2.86	28.68	1.96	1.36	0.95	19.69	13.61	9.48	-66.65	-105.76	-134.29
20			2.86	29.83	1.92	1.31	0.89	20.08	13.61	9.30	-48.50	-93.45	-125.88
21			2.86	31.02	1.89	1.26	0.84	20.47	13.61	9.13	-29.92	-81.09	-117.59
22		8.58	2.86	32.27	7.40	4.83	3.17	20.87	13.61	8.95	-16.45	-72.31	-111.82
23			2.86	33.56	1.81	1.16	0.75	21.28	13.61	8.79	3.02	-59.85	-103.78
24			2.86	34.90	1.78	1.12	0.71	21.70	13.61	8.62	22.94	-47.35	-95.87
25			2.86	36.29	1.74	1.07	0.67	22.12	13.61	8.46	43.32	-34.81	-88.08
26			2.86	37.75	1.71	1.03	0.63	22.56	13.61	8.30	64.17	-22.23	-80.41
27		8.58	2.86	39.26	6.70	3.97	2.37	23.00	13.61	8.14	80.46	-12.58	-74.64
28			2.86	40.83	1.64	0.95	0.56	23.45	13.61	7.99	102.27	0.08	-67.21
29			2.86	42.46	1.61	0.92	0.53	23.91	13.61	7.84	124.57	12.78	-59.90
30			2.86	44.16	1.58	0.88	0.50	24.38	13.61	7.69	147.37	25.51	-52.71
31			2.86	45.92	1.55	0.85	0.47	24.86	13.61	7.54	170.68	38.28	-45.64
32		8.58	2.86	47.76	6.07	3.26	1.77	25.34	13.61	7.40	189.95	48.63	-40.01
33			2.86	49.67	1.49	0.78	0.42	25.84	13.61	7.26	214.30	61.46	-33.17
34			2.86	51.66	1.46	0.75	0.39	26.35	13.61	7.12	239.19	74.32	-26.44
35			2.86	53.73	1.43	0.72	0.37	26.86	13.61	6.99	264.62	87.21	-19.82
36			2.86	55.87	1.40	0.70	0.35	27.39	13.61	6.86	290.61	100.13	-13.31
37		8.58	2.86	58.11	5.50	2.68	1.32	27.93	13.61	6.73	313.04	111.07	-7.91
38			2.86	60.43	1.35	0.64	0.31	28.48	13.61	6.60	340.17	124.04	-1.62
39			2.86	62.85	1.32	0.62	0.29	29.03	13.61	6.48	367.88	137.03	4.56
40			2.86	65.36	1.30	0.60	0.28	29.60	13.61	6.35	396.19	150.05	10.64
41			2.86	67.98	1.27	0.57	0.26	30.18	13.61	6.24	425.11	163.09	16.61
42		8.58	2.86	70.70	4.98	2.20	0.99	30.78	13.61	6.12	450.90	174.50	21.74
43			2.86	73.53	1.22	0.53	0.23	31.38	13.61	6.00	**481.06**	**187.59**	**27.51**

a function of time. At the time the graph crosses the horizontal axis, the cumulative discounted benefits equal the cumulative discounted expenditures. This is called the break even point. From this moment on profit is generated. From the graph it can be seen that the break even point is reached 28 years after the beginning of construction (which is after 25 years of operation).

The Internal Rate of Return (IRR) is a capital budgeting method used to decide whether long-term investments should be made or not. Mathematically the IRR is defined as any discount rate that results in an NPV of zero. The NPV for the selected number of turbines (18) as a function of discount rate is plotted in Figure 6.4, which is nothing less than a graph of the penultimate column of Table 6.4; the IRR turns out to be 6.50 %.
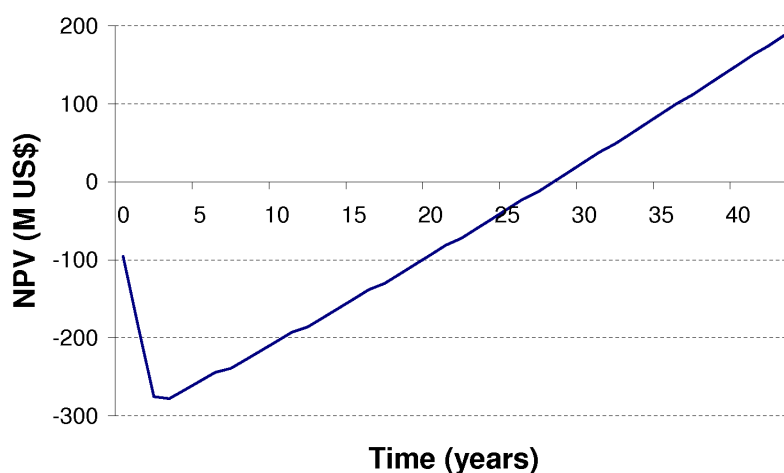
Figure 6.3: *Net Present Value as a function of time*
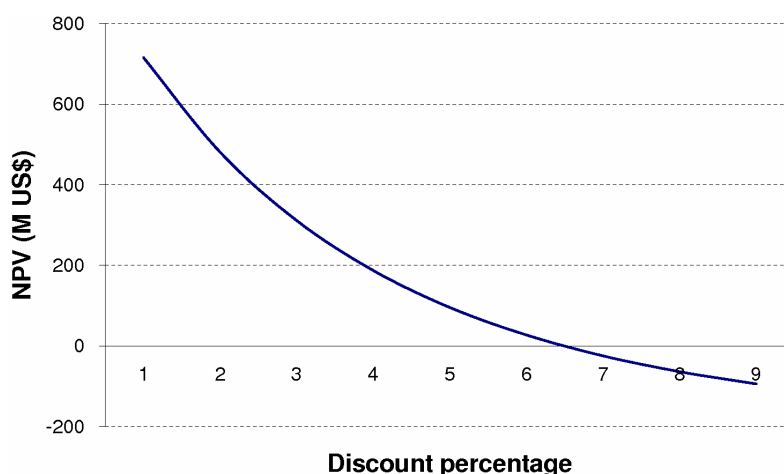
Figure 6.4: *Internal Rate of Return: NPV as a function of discount rate*

6.4   Resulting plant parameters

The result is that the NPV has its optimum of US\$ 187.6 Million for $N_t = 18$ turbines.

Table 6.5: *Specifications of TPP Saemangeum*

Parameter	Symbol	amount	unit
Powerhouse Length	L_p	337.5	m
Number of turbines	N_t	18	
Total power installed	P_i	142	MW
Annual energy output	E_y	453.8	GWh
Total construction costs	C_t	286.0	Million US\$
Annual rise of real energy price		4	%
Discount rate		4	%
Economic lifetime		40	years

Table 6.6: *Breakdown of the construction costs of Saemangeum TPP*

Part	Costs
Turbines and generators	\$ 151,716,104
Power house	\$ 104,147,591
Cofferdam	\$ 28,721,455
Bed protection	\$ 1,420,345
Total	\$ 286,005,495

6.5   Sensitivity analysis for changes in parameters

The NPV calculations are sensitive to changing economic parameters. What will happen if the discount rate differs from the assumed 4 %? What will happen if the plant's lifetime turns out to be shorter than expected? What will happen if the assumed annual rise in energy price turns out not to be as high as expected (i.e. 4 %)? Answers to these questions can be found in Figures 6.5 to 6.7; These are all graphs of the NPV as a function of the number of turbines, but with changing economic parameters.
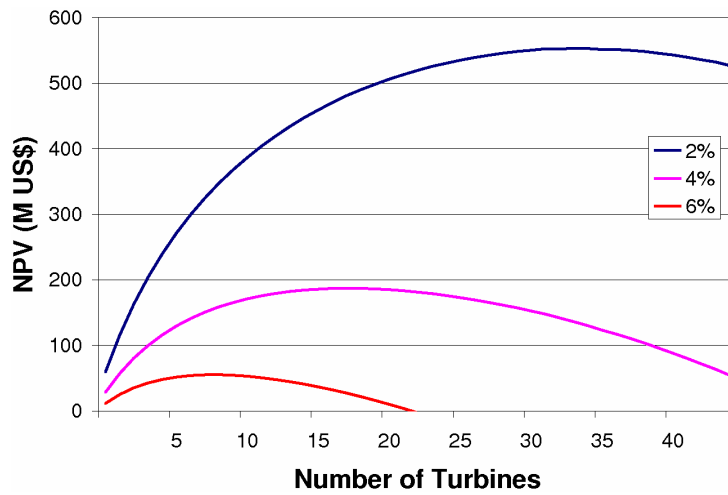
Figure 6.5: *Influence of different discount rates (lifetime expectancy of 40 years and expected annual rise of energy price 4%)*
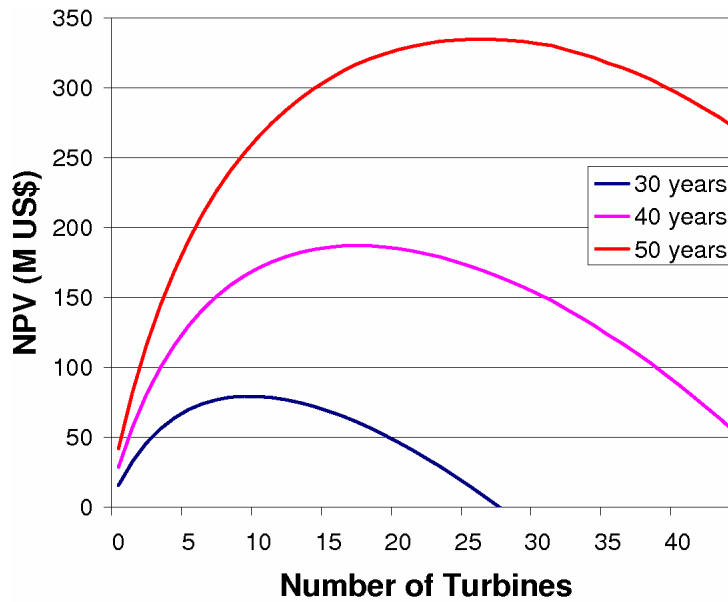
Figure 6.6: *Influence of different lifetime expectancies; discount rate = 4% and expected rise of real energy price = 4%*
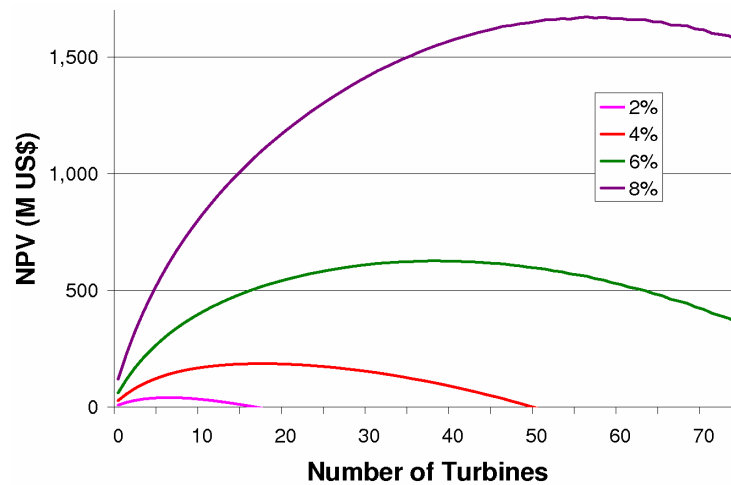
Figure 6.7: *Influence of expected rise of real energy price (for lifetime of 40 years and discount rate of 4%) in Millions of US$; The graph for a 0 % rise is not shown here, because it is negative for all numbers of turbines*

From the figures it can be concluded that it is most important to accurately predict the economic parameters!

If there will be no rise in real energy price, the NPV is negative for all numbers of turbines (with a minimum loss of US$ - 383,425 for $N_t = 2$), see Figure 6.7. This means that the TPP will not be economically feasible for the given parameters! It will always be possible to change the energy price. The assumed price was US$ 0.03 per kWh. What should the price be to obtain an NPV of zero after the economic lifetime? The answer is given in Figure 6.8. For example: If the discount rate is 4 %, the real rise in energy price is zero and the economic lifetime is 40 years, the production price turns out to be 4.47 cents per kWh.
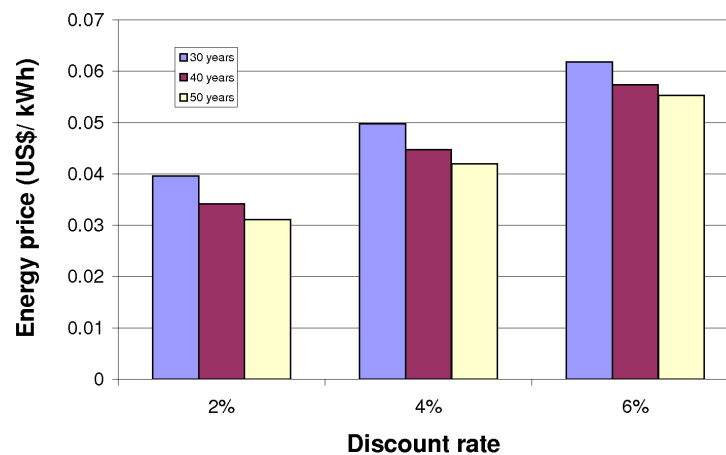
Figure 6.8: *Required price of energy in case the real rise in energy price is zero; Lifetime = 40 years, 18 turbines*

7 Conclusions and recommendations

7.1 Conclusions

Taking into account the multiple future destinations of the Saemangeum area, the optimal layout of the area would comprise a tidal power basin of 114 km^2 (at MSL), 90 km^2 of fresh water basin and about 194 km^2 of polders for farmland and industrial purposes. Choosing a low basin scheme would allows the presence of an inter tidal zone and also turns out to be the economically most feasible option.
If the TPP is designed for a maximum Net Present Value after 40 years, the optimal dimensions would be as given in Table 7.1.
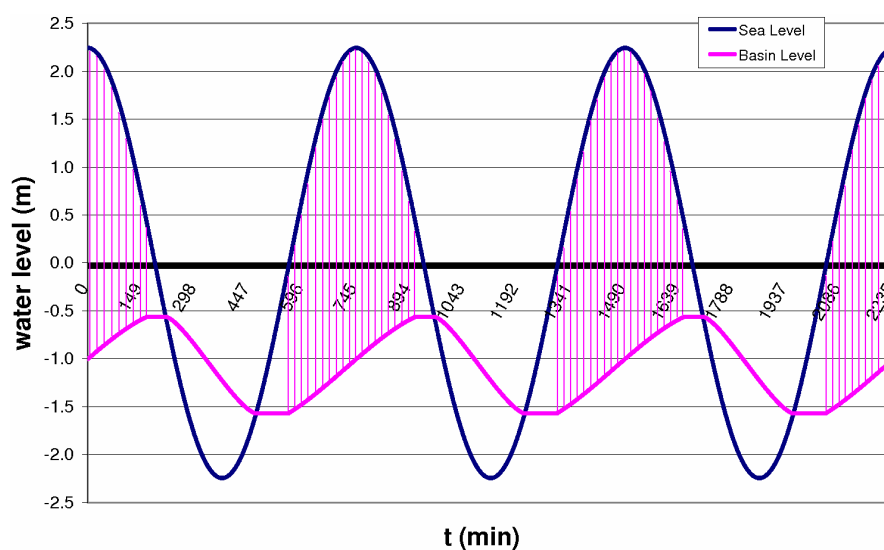
Figure 7.1: *Saemangeum TPP's generation scheme; The hatched area shows when energy is generated (output of Storage Area Approach Model)*

The plant should be built in the dry behind a cofferdam. Construction takes about 3 years, after which the plant becomes operational, generating about 454 GWh per year with an installed capacity of 142 MW. No extra sluicing capacity is needed, as the 300 m sluice length of the Sinsi sluices is sufficient and economically optimal.

Tidal power in Saemangeum seems to be economically attractive. An important design parameter is the expected lifetime. In this study the lifetime is assumed to be 40 years.

Table 7.1: *Main specifications of TPP Saemangeum*

Parameter	Symbol	amount	unit
Powerhouse Length	L_p	337.5	m
Sluice Length	L_{sl}	300	m
Basin area at MSL	A_b	114	km^2
Turbine Diameter	D	7.50	m
Number of turbines	N_t	18	
Total power installed	P_i	142	MW
Annual energy output	E_y	453.8	GWh
Total construction costs	C_t	286	Million US$
High High Water level inside basin		- 0.41	m
Mean High Water level inside basin		- 0.56	m
Mean Low Water level inside basin		- 1.57	m
Low Low Water level inside basin		- 2.25	m
Plant load factor (turbines generating)		47.5	%
Turbines in orifice mode		33.5	%
Turbines closed		19,0	%
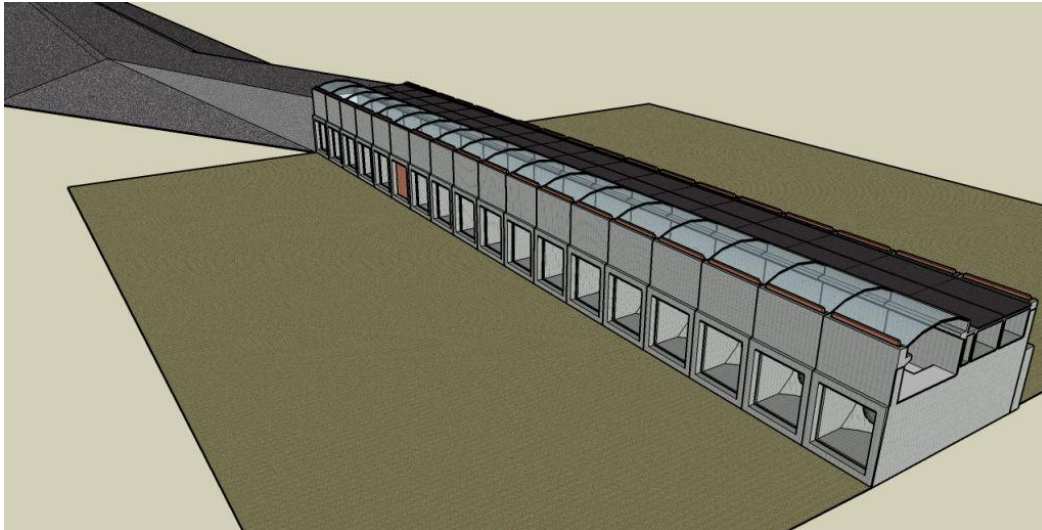
Figure 7.2: *Aerial view of the power house of the Saemangeum TPP*

This is quite a pessimistic estimation, because the La Rance plant in France has already been in operation for 41 years, but the financial risks are minimised this way. Other assumptions are a discount rate of 4 %, an expected rise of the energy price by an additional 4 % per year, and an energy production price of US$ 0,03 per kWh, which is necessary to be able to compete with other sources of energy (like coal and nuclear power).

The Net Present Value after 40 years of operation is US$ 187.6 Million.

The break even point will be reached after 25 years of operation.

7.2   Recommendations

1. The morphological situation must be studied as it may change when the TPP is built.

2. Improve the accuracy of the design criteria: A more accurate prediction of the future energy price is necessary if the plant will be built for real. The same counts for the discount rate.

3. Study possibilities to connect to the power grid, as the periodical input of energy into the power system might cause problems.

4. Study the possibility to create a paired basins scheme to obtain a constant power output (this means connecting both a low basin plant and a high basin plant, situated elsewhere, to the electricity grid). A paired basins-plant with Sihwa is unfortunately not possible in this case, as they both generate at the same time (incoming tide).

5. Study longer lifetime expectancy ranges. A lifetime of 10 years more would have resulted in a much larger plant. Optimisation for an NPV after 50 years shows a much larger plant (27 turbines), provided that the other assumptions made remain constant (annual rise of energy price, discount rate and selling price stay the same).

6. Study the consequences of a sea level rise due to climate changes. Will this shorten the economic lifetime of the plant and should extra expenses be taken into account in case the crest level of the dikes and dams turn out to be not sufficiently high anymore?

Appendices

A Tide Table

군산 (외항)　　GUNSAN (OUTER PORT)

조석 2006　　위도 35-58 N.　　경도 126-37 E.

추석표의 저작권 및 소유권은 국립해양조사원에 있으며, 사전 승인없이 판매 및 복제, 유사간행물 제작 등을 할 수 없습니다

1 월 (January)

Day	Time (h m)	Ht. (cm)
1	03 45 / 10 24 / 16 26 / 23 17	573 / 15 / 698 / 93
2	04 31 / 11 12 / 17 10	585 / 7 / 702
3	00 01 / 05 18 / 11 57 / 17 56	86 / 593 / 12 / 693
4	00 44 / 06 06 / 12 43 / 18 40	85 / 593 / 33 / 671
5	01 27 / 06 56 / 13 29 / 19 26	91 / 586 / 69 / 637
6	02 11 / 07 50 / 14 20 / 20 14	103 / 571 / 117 / 592
7 ◐	02 59 / 08 50 / 15 18 / 21 08	119 / 553 / 170 / 544
8	03 55 / 09 59 / 16 33 / 22 13	135 / 539 / 211 / 503
9	05 02 / 11 19 / 18 02 / 23 29	143 / 539 / 225 / 480
10	06 12 / 12 35 / 19 21	138 / 558 / 212
11	00 41 / 07 20 / 13 37 / 20 22	480 / 121 / 584 / 188
12	01 41 / 08 14 / 14 28 / 21 11	495 / 102 / 607 / 165
13	02 30 / 09 00 / 15 11 / 21 54	515 / 86 / 624 / 149
14 ○	03 11 / 09 42 / 15 47 / 22 29	533 / 74 / 634 / 138
15	03 48 / 10 18 / 16 21 / 23 00	547 / 67 / 639 / 131
16	04 22 / 10 49 / 16 51 / 23 30	557 / 64 / 640 / 127
17	04 54 / 11 20 / 17 20 / 23 58	563 / 66 / 636 / 123
18	05 26 / 11 50 / 17 50	564 / 75 / 627
19	00 25 / 05 58 / 12 21 / 18 19	123 / 561 / 92 / 610
20	00 54 / 06 32 / 12 54 / 18 50	126 / 552 / 120 / 586
21	01 25 / 07 12 / 13 32 / 19 25	135 / 538 / 156 / 554
22	02 00 / 07 56 / 14 14 / 20 05	148 / 521 / 198 / 517
23 ◑	02 44 / 08 54 / 15 16 / 21 01	164 / 504 / 239 / 479
24	03 44 / 10 09 / 16 46 / 22 15	177 / 498 / 262 / 454
25	05 02 / 11 36 / 18 26 / 23 43	176 / 501 / 251 / 454
26	06 22 / 12 53 / 19 42	152 / 557 / 214
27	00 58 / 07 33 / 13 54 / 20 44	481 / 113 / 607 / 169
28	01 59 / 08 36 / 14 46 / 21 36	521 / 68 / 655 / 125
29 ●	02 50 / 09 31 / 15 33 / 22 22	563 / 26 / 693 / 86
30	03 39 / 10 21 / 16 17 / 23 04	600 / -5 / 717 / 55
31	04 24 / 11 07 / 16 59 / 23 45	629 / -23 / 724 / 36

2 월 (February)

Day	Time (h m)	Ht. (cm)
1	05 09 / 11 50 / 17 40	647 / -18 / 714
2	00 23 / 05 52 / 12 31 / 18 16	30 / 652 / 8 / 686
3	01 00 / 06 36 / 13 10 / 18 54	38 / 641 / 54 / 643
4	01 36 / 07 22 / 13 52 / 19 34	60 / 616 / 115 / 588
5 ◐	02 15 / 08 12 / 14 40 / 20 19	93 / 579 / 183 / 527
6	03 00 / 09 17 / 15 47 / 21 20	132 / 538 / 243 / 468
7	04 03 / 10 42 / 17 32 / 22 50	169 / 511 / 272 / 432
8	05 34 / 12 21 / 19 16	184 / 518 / 252
9	00 27 / 07 02 / 13 33 / 20 20	437 / 168 / 549 / 213
10	01 36 / 08 06 / 14 24 / 21 05	469 / 137 / 582 / 177
11	02 24 / 08 56 / 15 02 / 21 41	507 / 106 / 608 / 147
12	03 02 / 09 34 / 15 34 / 22 14	540 / 82 / 628 / 125
13 ○	03 37 / 10 06 / 16 03 / 22 41	566 / 64 / 640 / 108
14	04 07 / 10 38 / 16 30 / 23 07	585 / 54 / 647 / 94
15	04 36 / 11 07 / 16 56 / 23 33	597 / 52 / 647 / 84
16	05 05 / 11 35 / 17 21 / 23 58	604 / 59 / 639 / 80
17	05 35 / 12 05 / 17 47	605 / 76 / 623
18	00 25 / 06 05 / 12 33 / 18 12	82 / 600 / 104 / 599
19	00 50 / 06 36 / 13 06 / 18 42	93 / 587 / 143 / 567
20 ◑	01 17 / 07 14 / 13 42 / 19 18	112 / 566 / 188 / 527
21	01 51 / 08 05 / 14 29 / 20 04	137 / 537 / 238 / 482
22	02 41 / 09 17 / 15 54 / 21 24	167 / 510 / 278 / 440
23	04 06 / 11 00 / 18 00 / 23 13	189 / 508 / 276 / 433
24	05 53 / 12 34 / 19 33	176 / 548 / 227
25	00 44 / 07 21 / 13 42 / 20 34	473 / 129 / 606 / 164
26	01 48 / 08 29 / 14 33 / 21 21	532 / 70 / 661 / 104
27	02 41 / 09 26 / 15 18 / 22 04	592 / 17 / 702 / 54
28 ●	03 31 / 10 10 / 15 58 / 22 43	642 / -18 / 723 / 18

3 월 (March)

Day	Time (h m)	Ht. (cm)
1	04 10 / 10 53 / 16 36 / 23 20	677 / -31 / 724 / -2
2	04 51 / 11 33 / 17 12 / 23 56	694 / -20 / 705 / -3
3	05 32 / 12 11 / 17 47	693 / 15 / 671
4	00 30 / 06 13 / 12 50 / 18 21	12 / 674 / 67 / 624
5	01 01 / 06 54 / 13 26 / 18 58	44 / 638 / 132 / 567
6	01 33 / 07 41 / 14 08 / 19 40	88 / 589 / 201 / 505
7 ◐	02 12 / 08 39 / 15 06 / 20 36	140 / 533 / 265 / 444
8	03 08 / 09 53 / 17 09 / 22 16	193 / 491 / 297 / 404
9	04 57 / 12 02 / 19 05	223 / 493 / 267
10	00 15 / 06 51 / 13 19 / 20 05	419 / 203 / 527 / 220
11	01 26 / 07 41 / 14 07 / 20 45	464 / 162 / 564 / 177
12	02 11 / 08 41 / 14 39 / 21 14	512 / 122 / 595 / 140
13	02 50 / 09 13 / 15 08 / 21 45	554 / 91 / 618 / 110
14 ●	03 16 / 09 46 / 15 35 / 22 11	586 / 69 / 633 / 86
15 ○	03 45 / 10 17 / 16 01 / 22 37	610 / 57 / 639 / 68
16	04 13 / 10 46 / 16 26 / 23 02	626 / 54 / 638 / 57
17	04 41 / 11 16 / 16 50 / 23 29	635 / 62 / 628 / 54
18	05 09 / 11 46 / 17 14 / 23 53	637 / 80 / 612 / 60
19	05 38 / 12 16 / 17 39	632 / 110 / 589
20	00 19 / 06 09 / 12 47 / 18 12	74 / 619 / 148 / 559
21	00 46 / 06 47 / 13 22 / 18 46	95 / 594 / 193 / 520
22 ◑	01 18 / 07 37 / 14 10 / 19 38	126 / 560 / 242 / 475
23	02 10 / 08 52 / 15 36 / 21 03	163 / 524 / 280 / 435
24	03 34 / 10 38 / 17 46 / 23 00	194 / 516 / 269 / 438
25	05 36 / 12 14 / 19 13	185 / 554 / 211
26	00 30 / 07 10 / 13 19 / 20 09	491 / 133 / 609 / 143
27	01 33 / 08 15 / 14 09 / 20 55	561 / 73 / 657 / 80
28	02 26 / 09 07 / 14 51 / 21 36	625 / 25 / 688 / 32
29 ●	03 08 / 10 23 / 15 30 / 22 15	676 / -4 / 699 / 1
30	03 49 / 10 34 / 16 07 / 22 51	706 / -5 / 690 / -11
31	04 30 / 11 13 / 16 42 / 23 25	716 / 14 / 666 / -5

4 월 (April)

Day	Time (h m)	Ht. (cm)
1	05 08 / 11 50 / 17 17 / 23 56	707 / 51 / 631 / 17
2	05 47 / 12 26 / 17 52	681 / 100 / 588
3	00 27 / 06 29 / 13 01 / 18 28	53 / 640 / 157 / 539
4	00 57 / 07 13 / 13 42 / 19 11	99 / 588 / 216 / 486
5 ◐	01 33 / 08 08 / 14 38 / 20 05	152 / 533 / 269 / 436
6	02 26 / 09 30 / 16 29 / 21 44	206 / 489 / 296 / 404
7	04 09 / 11 20 / 18 28 / 23 43	242 / 482 / 271 / 419
8	06 15 / 12 39 / 19 25	228 / 507 / 226
9	00 54 / 07 22 / 13 27 / 20 03	466 / 189 / 540 / 181
10	01 40 / 08 08 / 14 01 / 20 35	516 / 149 / 570 / 141
11	02 15 / 08 48 / 14 32 / 21 04	561 / 117 / 593 / 107
12	02 47 / 09 18 / 15 00 / 21 32	598 / 93 / 607 / 79
13	03 16 / 09 50 / 15 26 / 22 01	625 / 79 / 612 / 60
14 ○	03 46 / 10 23 / 15 53 / 22 29	643 / 75 / 609 / 51
15	04 14 / 10 55 / 16 19 / 22 58	653 / 83 / 600 / 50
16	04 44 / 11 29 / 16 47 / 23 26	655 / 100 / 584 / 58
17	05 18 / 12 01 / 17 16 / 23 54	650 / 127 / 565 / 73
18	05 52 / 12 36 / 17 51	635 / 162 / 540
19	00 25 / 06 34 / 13 16 / 18 36	95 / 610 / 200 / 508
20 ◑	01 05 / 07 27 / 14 13 / 19 37	126 / 578 / 237 / 474
21	02 02 / 08 44 / 15 38 / 21 05	163 / 547 / 257 / 453
22	03 32 / 10 17 / 17 20 / 22 45	190 / 542 / 235 / 471
23	05 20 / 11 41 / 18 36	181 / 586 / 183
24	00 07 / 06 48 / 12 44 / 19 33	525 / 140 / 602 / 123
25	01 08 / 07 51 / 13 35 / 20 20	590 / 95 / 632 / 71
26	02 00 / 08 43 / 14 19 / 21 03	648 / 62 / 648 / 33
27	02 44 / 09 31 / 14 59 / 21 43	689 / 46 / 649 / 12
28 ●	03 27 / 10 13 / 15 37 / 22 19	709 / 50 / 636 / 9
29	04 07 / 10 53 / 16 14 / 22 54	710 / 69 / 614 / 21
30	04 47 / 11 31 / 16 52 / 23 27	696 / 99 / 586 / 45

시 각 : 9hE

조고의 기준면 : 평균해면하 362 cm

Datum : 362 cm below mean sea level

Figure A.1: *Tide table Gunsan Outer Port from January till April 2006*

산（외항）　　GUNSAN（OUTER PORT）

조석　위도 35-58 N.　　경도 126-37 E.

2006

5 월

Day	Time	Ht.	Day	Time	Ht.
1	05 27 / 12 09 / 17 29 / 23 59	669 / 137 / 555 / 77	16	05 04 / 11 53 / 17 06 / 23 41	662 / 144 / 551 / 76
2	06 08 / 12 44 / 18 09	632 / 178 / 520	17	05 45 / 12 35 / 17 50	651 / 166 / 536
3	00 30 / 06 51 / 13 24 / 18 53	116 / 590 / 218 / 485	18	00 22 / 06 33 / 13 22 / 18 42	95 / 633 / 188 / 519
4	01 08 / 07 41 / 14 15 / 19 49	159 / 547 / 253 / 451	19	01 08 / 07 29 / 14 19 / 19 44	121 / 609 / 205 / 504
5	01 57 / 08 47 / 15 31 / 21 06	203 / 509 / 273 / 429	20	02 10 / 08 35 / 15 27 / 21 00	152 / 587 / 208 / 501
6	03 14 / 10 07 / 17 07 / 22 40	239 / 490 / 265 / 435	21	03 27 / 09 47 / 16 40 / 22 21	175 / 574 / 190 / 521
7	05 02 / 11 25 / 18 16 / 23 59	245 / 495 / 233 / 469	22	04 54 / 10 58 / 17 49 / 23 36	179 / 574 / 157 / 561
8	06 25 / 12 25 / 19 02	222 / 514 / 193	23	06 16 / 12 01 / 18 49	164 / 582 / 118
9	00 54 / 07 20 / 13 08 / 19 41	515 / 190 / 537 / 153	24	00 39 / 07 23 / 12 57 / 19 41	608 / 141 / 591 / 83
10	01 35 / 08 04 / 13 45 / 20 16	560 / 159 / 557 / 118	25	01 34 / 08 20 / 13 46 / 20 30	650 / 122 / 595 / 58
11	02 11 / 08 44 / 14 18 / 20 50	599 / 134 / 570 / 90	26	02 23 / 09 10 / 14 30 / 21 11	679 / 112 / 593 / 47
12	02 46 / 09 22 / 14 50 / 21 23	629 / 118 / 576 / 72	27	03 08 / 09 56 / 15 13 / 21 52	691 / 114 / 585 / 49
13	03 17 / 09 58 / 15 22 / 21 58	649 / 111 / 576 / 62	28	03 50 / 10 38 / 15 54 / 22 30	689 / 125 / 573 / 59
14	03 51 / 10 36 / 15 54 / 22 31	661 / 115 / 571 / 60	29	04 32 / 11 18 / 16 35 / 23 06	677 / 142 / 559 / 77
15	04 25 / 11 14 / 16 29 / 23 06	665 / 126 / 562 / 65	30	05 12 / 11 56 / 17 15 / 23 40	658 / 162 / 544 / 99
			31	05 52 / 12 34 / 17 55	634 / 183 / 528

6 월

Day	Time	Ht.	Day	Time	Ht.
1	00 14 / 06 32 / 13 09 / 18 38	124 / 608 / 204 / 510	16	00 25 / 06 30 / 13 21 / 18 43	79 / 673 / 148 / 568
2	00 51 / 07 15 / 13 49 / 19 26	154 / 579 / 221 / 491	17	01 15 / 07 19 / 14 09 / 19 40	101 / 655 / 152 / 565
3	01 34 / 08 01 / 14 37 / 20 24	187 / 549 / 233 / 476	18	02 08 / 08 13 / 15 00 / 20 42	131 / 628 / 154 / 564
4	02 29 / 08 57 / 15 36 / 21 31	220 / 523 / 236 / 471	19	03 09 / 09 10 / 15 58 / 21 51	165 / 599 / 153 / 568
5	03 41 / 09 59 / 16 42 / 22 46	244 / 506 / 226 / 485	20	04 21 / 10 12 / 16 59 / 23 02	194 / 571 / 146 / 583
6	05 05 / 11 04 / 17 44 / 23 53	250 / 501 / 203 / 515	21	05 41 / 11 18 / 18 04	207 / 553 / 132
7	06 20 / 12 01 / 18 37	235 / 509 / 173	22	00 13 / 06 57 / 12 22 / 19 04	608 / 202 / 545 / 115
8	00 47 / 07 19 / 12 51 / 19 24	554 / 211 / 522 / 142	23	01 15 / 08 00 / 13 21 / 20 00	634 / 187 / 546 / 101
9	01 32 / 08 08 / 13 35 / 20 07	592 / 186 / 535 / 115	24	02 09 / 08 57 / 14 13 / 20 50	656 / 173 / 551 / 91
10	02 13 / 08 54 / 14 17 / 20 49	625 / 165 / 547 / 94	25	02 58 / 09 46 / 15 00 / 21 36	668 / 164 / 557 / 88
11	02 53 / 09 38 / 14 55 / 21 31	650 / 152 / 556 / 79	26	03 42 / 10 30 / 15 44 / 22 17	672 / 161 / 561 / 90
12	03 33 / 10 22 / 15 38 / 22 13	669 / 144 / 562 / 70	27	04 21 / 11 09 / 16 25 / 22 55	670 / 162 / 564 / 96
13	04 15 / 11 06 / 16 21 / 22 56	680 / 141 / 566 / 66	28	04 59 / 11 45 / 17 03 / 23 29	663 / 165 / 564 / 106
14	04 58 / 11 49 / 17 04 / 23 41	686 / 141 / 569 / 68	29	05 34 / 12 17 / 17 40	653 / 170 / 561
15	05 43 / 12 35 / 17 52	684 / 144 / 569	30	00 03 / 06 08 / 12 47 / 18 18	119 / 639 / 175 / 555

7 월

Day	Time	Ht.	Day	Time	Ht.
1	00 36 / 06 43 / 13 18 / 18 58	139 / 619 / 181 / 545	16	01 07 / 06 58 / 13 44 / 19 23	78 / 690 / 102 / 630
2	01 10 / 07 19 / 13 52 / 19 41	165 / 594 / 188 / 533	17	01 53 / 07 42 / 14 26 / 20 17	120 / 651 / 115 / 616
3	01 53 / 07 59 / 14 34 / 20 34	198 / 564 / 197 / 520	18	02 44 / 08 31 / 15 14 / 21 19	172 / 603 / 135 / 598
4	02 44 / 08 46 / 15 24 / 21 34	234 / 533 / 204 / 514	19	03 47 / 09 27 / 16 13 / 22 31	224 / 554 / 155 / 585
5	03 50 / 09 43 / 16 23 / 22 46	263 / 506 / 205 / 522	20	05 10 / 10 39 / 17 26 / 23 53	257 / 516 / 165 / 589
6	05 14 / 10 51 / 17 29 / 23 56	274 / 491 / 195 / 546	21	06 40 / 11 59 / 18 39	258 / 503 / 160
7	06 33 / 11 57 / 18 32	262 / 494 / 173	22	01 06 / 07 55 / 13 11 / 19 46	610 / 235 / 513 / 144
8	00 58 / 07 38 / 13 00 / 19 30	582 / 236 / 510 / 145	23	02 06 / 08 53 / 14 09 / 20 41	635 / 207 / 536 / 124
9	01 49 / 08 33 / 13 52 / 20 23	620 / 206 / 523 / 116	24	02 54 / 09 40 / 14 57 / 21 30	656 / 183 / 560 / 109
10	02 37 / 09 24 / 14 41 / 21 16	657 / 178 / 557 / 88	25	03 34 / 10 21 / 15 37 / 22 09	670 / 165 / 579 / 99
11	03 23 / 10 13 / 15 27 / 22 45	687 / 152 / 581 / 65	26	04 09 / 10 54 / 16 13 / 22 45	677 / 154 / 594 / 96
12	04 07 / 10 59 / 16 14 / 22 53	711 / 129 / 603 / 48	27	04 41 / 11 24 / 16 47 / 23 16	678 / 147 / 603 / 98
13	04 51 / 11 42 / 16 59 / 23 39	724 / 111 / 620 / 42	28	05 11 / 11 52 / 17 19 / 23 46	675 / 142 / 607 / 106
14	05 34 / 12 23 / 17 46	727 / 100 / 632	29	05 40 / 12 18 / 17 52	666 / 139 / 606
15	00 25 / 06 16 / 13 04 / 18 34	51 / 715 / 96 / 636	30	00 15 / 06 08 / 12 44 / 18 26	123 / 649 / 141 / 599
			31	00 47 / 06 38 / 13 13 / 19 02	149 / 624 / 149 / 585

8 월

Day	Time	Ht.	Day	Time	Ht.
1	01 21 / 07 09 / 13 45 / 19 43	184 / 591 / 164 / 567	16	02 17 / 07 53 / 14 34 / 20 46	192 / 583 / 137 / 603
2	02 02 / 07 46 / 14 23 / 20 34	226 / 553 / 184 / 546	17	03 17 / 08 48 / 15 30 / 22 05	256 / 523 / 180 / 568
3	02 56 / 08 38 / 15 14 / 21 42	269 / 513 / 204 / 532	18	04 49 / 10 10 / 16 54 / 23 41	296 / 477 / 207 / 563
4	04 13 / 09 44 / 16 27 / 23 09	301 / 480 / 215 / 538	19	06 39 / 11 53 / 18 29	287 / 472 / 200
5	05 54 / 11 14 / 17 50	300 / 472 / 203	20	01 05 / 07 52 / 13 14 / 19 44	589 / 247 / 504 / 170
6	00 30 / 07 18 / 12 35 / 19 04	572 / 268 / 495 / 169	21	02 00 / 08 45 / 14 06 / 20 37	623 / 206 / 545 / 137
7	01 34 / 08 22 / 13 36 / 20 10	621 / 222 / 537 / 125	22	02 44 / 09 25 / 14 48 / 21 20	651 / 172 / 582 / 111
8	02 26 / 09 13 / 14 29 / 21 06	671 / 174 / 582 / 81	23	03 19 / 09 58 / 15 23 / 21 55	670 / 147 / 610 / 95
9	03 11 / 09 59 / 15 17 / 21 58	713 / 129 / 626 / 43	24	03 48 / 10 28 / 15 55 / 22 26	681 / 129 / 630 / 87
10	03 53 / 10 43 / 16 02 / 22 45	743 / 92 / 661 / 20	25	04 16 / 10 54 / 16 25 / 22 56	685 / 116 / 643 / 87
11	04 34 / 11 23 / 16 46 / 23 28	757 / 65 / 686 / 16	26	04 41 / 11 19 / 16 54 / 23 24	681 / 107 / 649 / 95
12	05 13 / 12 00 / 17 29	753 / 51 / 698	27	05 07 / 11 44 / 17 23 / 23 54	671 / 104 / 648 / 113
13	00 09 / 05 51 / 12 37 / 18 13	33 / 731 / 52 / 696	28	05 33 / 12 07 / 17 53	652 / 107 / 640
14	00 50 / 06 29 / 13 12 / 18 58	71 / 694 / 68 / 677	29	00 23 / 05 58 / 12 34 / 18 25	141 / 625 / 120 / 624
15	01 31 / 07 09 / 13 49 / 19 48	127 / 643 / 97 / 644	30	00 54 / 06 26 / 13 01 / 19 01	178 / 592 / 140 / 600
			31	01 29 / 06 59 / 13 35 / 19 46	223 / 552 / 169 / 570

C시 각 : 9hE

조고의 기준면 : 평균해면하 362 cm

Datum : 362 cm below mean sea level

Figure A.2: Tide table Gunsan Outer Port from May till August 2006
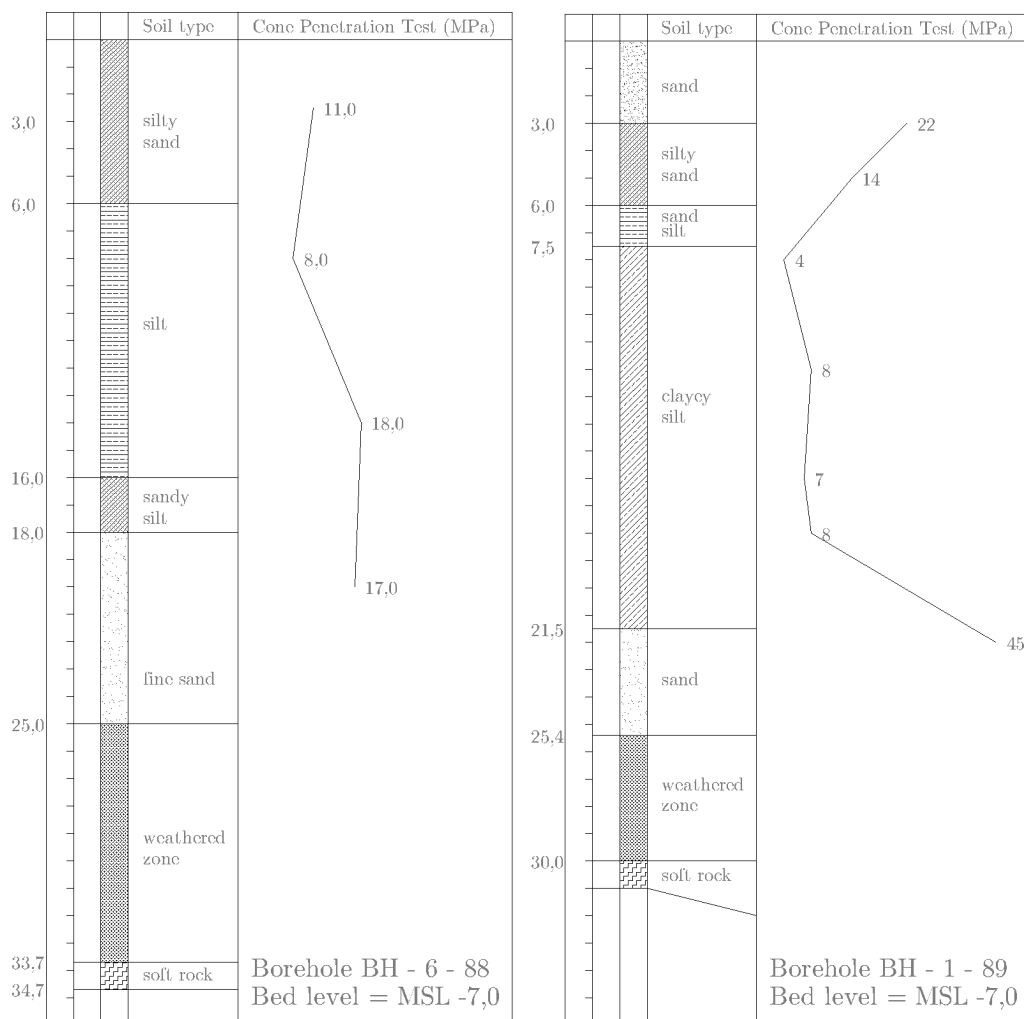
B Geotechnical information

Boreholes

Figure B.1: *Borehole BH-1-89 and Borehole BH-6-88; All levels refer to ground level, located at EL - 7.0 MSL*

C Rules of thumb for preliminary design

Song and Van Walsum have made up a method to evaluate the tidal energy potential of a site [Song & Van Walsum, 2006] :

Step 1: Determine the type of TPP.
- For a single-basin site with $R_{mean} < 9$ m, consider a single, high-basin plant. Such a plant would produce two blocks of energy per moon-day.
- If absorption of the tidal energy into the surrounding utility system is going to be a problem, consider a single basin, double-effect TPP, which would, at these tidal ranges, produce less energy but in the form of four rather than two blocks per day.
- For a single-basin site with $R_{mean} > 9$ m, consider a single, double-effect TPP.
- For a site where a linked-basins scheme might be feasible, consider a two stage development. In the first stage of construction, build a single, high-basin TPP with large sluicing capacity. The second stage then consists of the creation of the low basin by constructing a barrage equipped with large-capacity dewatering sluices. This completes the linked-basins TPP.
- For a location where a paired-basins scheme seems feasible and where $R_{mean} < 9$ m, consider a paired-basins scheme with one high- and one low-basin TPP. In this way, one plant would produce energy on the incoming tide, the other on the outgoing tide, resulting in four blocks of energy per moon-day.
- In the event $R_{mean} < 9$ m, consider a paired-basins scheme in which both basins operate in double effect, producing four blocks of energy per day. This arrangement could become particularly attractive if the two basins are so far apart that there is an appreciable difference in the tidal phases between the two sites. A phase difference of two hours would result in a continuous power supply while operating each plant individually for maximum energy production.

Step 2: Establishing the lower limit of a TPP's installed capacity.
If the criterion is to achieve tidal energy at the lowest possible cost per kWh, then the following guidelines will be helpful in starting up a trial-and-error approach to achieving the objective:
- For a single, high-basin plant, choose a net installed capacity in [MW] of approximately 0,09 times the site's annual natural energy expressed in [GWh] as a first trial. Choose a rated head of $H_{rated} \approx 0,66 \cdot R_{mean}$ (for conventional Bulb or Straflo machines). The same rule applies for phase I of a linked-basins plant.

- For a single, double-effect TPP, choose an installed capacity in [MW] of approximately 0,1 times the site's annual natural energy expressed in [GWh] as a first trial. Choose a rated head of $H_{rated} = 0.5 \cdot R_{mean}$ (for conventional bulb or Straflo machines).
- A systematic, trial-and-error search for the installed capacity with the lowest unit cost of energy can be carried out. The optimization curves are typically quite flat which means that a higher installed capacity will yield more energy at a slightly higher unit cost. In future years, such additional energy might well be desirable. This means that, if at all possible, a TPP should be so designed that additional capacity can be readily added at some future date.

Step 3: Pumping.
The net output of a single basin TPP, which includes paired single basins, can be increased through pumping. Only the plant's turbines should be considered to perform the pumping function. Do not consider building a separate pumping plant. To increase the output of a linked basins plant through pumping would require the construction of separate pumping plants, the economics of which would be doubtful.

Step 4: Sluices.
Single high-basin schemes, single low-basin schemes and linked-basins schemes all require sluices. These sluices will all work in one direction only, i.e. either to fill a high-basin or to empty a low basin so that only simple flap gates would be required.

D Construction Costs

Fay and Smachlo (Massachussettes Institute of Technology) developed a method to quickly estimate the total construction costs of a tidal power plant. Costs not examined in this analysis are the additional construction costs associated with locks or service facilities, relocations, transmission lines, real estate, and service equipment. These costs are generally not significant in comparison to the costs of the system components examined in this analysis.

Nomenclature:

A_b	Cross-sectional area of barrage	m^2
B_b	Unit cost of barrage material	US\$/m^3
B_{bed}	Unit cost of bed material	US\$/m^3
B_c	Unit cost of cofferdam material	US\$/m^3
B_p	Unit cost of power house material	US\$/m^3
B_{sl}	Unit cost of sluice material	US\$/m^3
C_b	Cost of barrage	US\$
C_{bed}	Cost of bed protection	US\$
C_c	Cost of cofferdam	US\$
C_p	Cost of power house	US\$
C_{sl}	Cost of sluices	US\$
C_{t+g}	Cost of turbines and generators	US\$
C_{tot}	Total construction cost	US\$
D_b	Depth of barrage structure	m
$D_{part,req}$	Required diameter of particles for bed protection	m
L_b	Length of barrage	m
L_c	Length of closure	m
L_p	Length of power house (parallel to flow direction)	m
L_{sl}	Length of sluices (parallel to flow direction)	m
m	slope of barrage walls	
V_b	Volume of barrage material	US\$/m^3
V_{bed}	Volume of bed material	US\$/m^3
V_c	Volume of cofferdam material	US\$/m^3
V_p	Volume of power house material	US\$/m^3
V_{sl}	Volume of sluice material	US\$/m^3
W_p	Width of power house (perpendicular to flow direction)	m
W_{sl}	Width of sluices (perpendicular to flow direction)	m
Y_{basin}	length of bed on basin side, perpendicular to dam	m
Y_{sea}	length of bed on sea side, perpendicular to dam	m

Except for the turbine and generator costs, all calculation methods, formulas and unit costs are taken from Fay and Smachlo [Fay & Smachlo, 1983a]. All original prices in their formulas are 1983 prices in US\$. To obtain the prices for 2007 the original prices have been divided by 0.484[1]. The total construction costs are:

[1]Inflation conversion factors from file downloaded from www.oregonstate.edu, by Robert C. Sahr

$$C_{tot} = C_{t+g} + C_b + C_p + C_{sl} + C_{bed} + C_c \tag{D.1}$$

D.1 Turbines and generators

The costs of the electrical equipment (turbines and generators) form the largest part of the total construction costs. Unfortunately, turbine manufacturers are not very willing to share information about turbine and generator costs. In Figure D.1 nine graphs are plotted for the estimated prices for bulb units (turbines only), in thousands of euros.
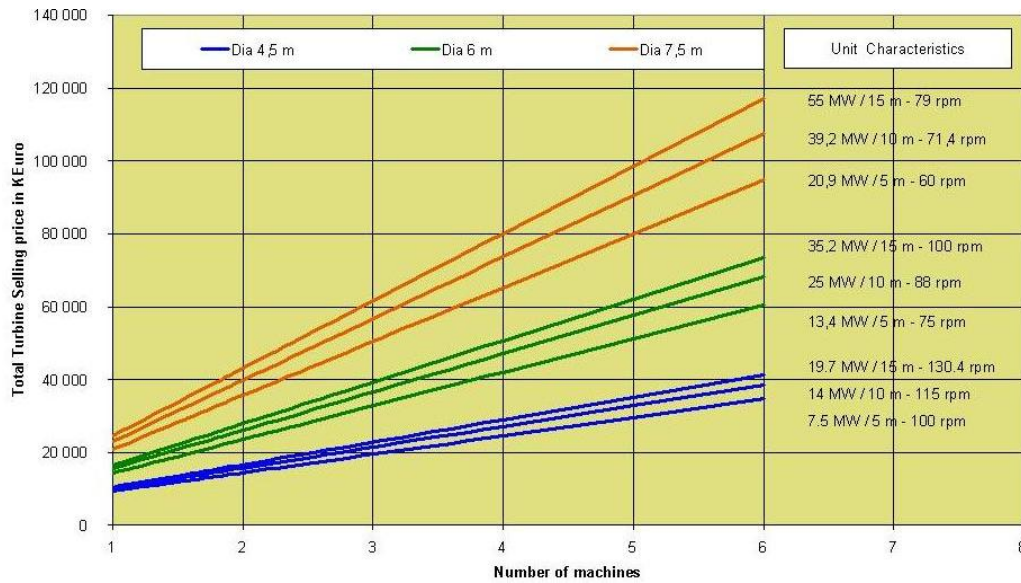

Figure D.1: *Estimative prices (in k€) for double regulated bulb units (by Alstom); Dia = runner diameter; the numbers on the right are rated power/ rated head/ rated rotational speed*

As one can see, the costs depend on the head, the diameter and the number of turbines. Only the graphs are shown for diameters of 4.5 , 6 and 7.5 m and heads of 5, 10 and 15 m. So in case other heads or diameters are preferred, it is not possible to directly read the total costs from these graphs. Knowing that the total price for the 10 bulb turbines ordered by Daewoo for the Sihwa TPP (manufactured by VA Tech) was 94 million US\$ including all electromechanical main components (like generators and transmission lines)[2], this chart cannot be regarded as accurate enough, because for the parameters of Sihwa (H_r = 5.82 m and D_t = 7.5 m), the chart predicts a total selling price of about € 160 Million, which is US\$ 215 Million for the turbines only (if a line is drawn between the second and the third line in the figure provided by Alstom and extrapolated to 10 turbines). Nevertheless, the chart can be used to deduct a formula that predicts the selling costs of all electromechanical components, assuming that the additional costs of the electromechanical

---

[2]Source: www.waterpowermagazine.com, may 2005: VA Tech wins Sihwa contract

equipment (generators, transmission lines) are usually about 50 % of the turbine price. From Figure D.1 it can be seen that the graphs are built up as follows:

- Fixed starting costs, independent of number of turbines (= US$ 5.5 Million)

- A linear relationship with the number of turbines (proportional to N_t)

- An exponential relationship with the turbine diameter (proportional to D_t^2)

- An exponential relationship with the rated head (proportional to $H_r^{0.18}$)

The proportionality factors are deducted from the total selling price of the Sihwa turbines. Conversion to US$ and a correction for inflation then in the end leads to the following formula:

$$C_{t+g} = 5.500.000 + 118500 \cdot H_r^{0.18} N_t D_t^2 \qquad \text{(D.2)}$$

To check the reliability of this formula, it is tested on some contracts in the past, all projects include all electromechanical equipment (turbines, generators, transmission lines). It can be seen that the formula is quite accurate, as the calculated price difference varies between 0.9 % and -7.8 %. Also can be seen that the accuracy increases for a higher number of turbines and a higher project sum[3].

Table D.1: *Check of turbine costs formula on contracts in the past*

Location Plant and Year of Contract	Da Pu China, 2002	Guangxi Fangyuan China, 2005	Sihwa South Korea, 2005
Manufacturer	VA Tech	Alstom	VA Tech
H_r (m)	10.8	10	5.82
N_t	3	4	10
D_t (m)	6	7.4	7.5
P_{1t} (MW)	30.7	57	25.4
Total Power installed (MW)	92.1	228	254
Costs then (US$)	$25.200.000	$43.000.000	$94.000.000
Costs now (inflation US$)	$27.096.774	$44.375.645	$97.007.224
Formula prediction (US$)	$25.140.764	$44.786.359	$97.022.319
Difference (%)	-7.8%	0.9%	0.0%

D.2   Power house

It is assumed that both the power house and the sluices occupy a rectangular volume. The length of the power house L_p (in the flow direction) and the height are expected to be proportional to the tidal range R. The product of the width (perpendicular to flow direction) and the height of the power house will be proportional to the turbine flow area (or D_t^2) and the number of turbines N_t. Next it was assumed that the in-place volume of power house material V_p is a fixed fraction of the gross volume. In this manner, using the corresponding values of these quantities based on representative values taken from two different Cobscook

---

[3]Sources: www.waterpowermagazine.com, www.alstom.com, www.andritz.com

feasibility studies[4], two Bay of Fundy feasibility studies[5], La Rance (existing plant) and Half Moon Cove study[6], Fay and Smachlo evaluated the proportionality constant arriving at the following formulas:

$$V_p = 42 \cdot N_t R D_t^2 \tag{D.3}$$

The cost of the power house is then obtained by multiplying V_p by the unit cost B_p of composite material put in place. $B_p \approx$ US\$ 545 /m^3 (price in 1983: US\$ 264 /m^3, taken from [Fay & Smachlo, 1983a]).

$$C_p = B_p V_p \tag{D.4}$$

D.3   Sluices

The cost estimates for the sluices are performed in the same way as described above. The unit cost of sluice material is $B_{sl} \approx$ US\$ 599 /m^3 (price in 1983: US\$ 290 /m^3). This is more than the unit cost of the powerhouse, which can be explained by the fact that here not only the concrete construction, but also the gates and mechanical equipment are taken into account, while for the powerhouse the electromechanical equipment is not taken into account, as all electromechanical equipment is included in the turbine and generator costs. This leads to the following formulas for the sluices:

$$V_{sl} = 18 \cdot R F_{sl} \tag{D.5}$$

$$C_{sl} = 18 \cdot B_{sl} R F_{sl} \tag{D.6}$$

D.4   Cofferdam

The cofferdam is to enclose only the sluice and power house structures, in a circular fashion. The perimeter of the cofferdam structure would be proportional to the combined widths of the power house and the sluices. The height and thickness of the cofferdam structure are assumed to be to a dimension D_b, which is the sum of the depth of the soil layer with sufficient bearing capacity at the site of the powerhouse in relation to the maximum water level plus 3 m of free board. The area surrounded by the cofferdam is proportional to the size of the sluices and power house structures. This is taken into account in the equations below. The average space between the future construction and the cofferdam is about 100 m.

---

[4]U.S.Army Corps of Engineers: Investigation of tidal power Cobscook Bay, Maine, 1980
[5]Stone & Webster Engineering Corp.: Tidal Power Study for the U.S.E.R., Boston, 1980
[6]Charles T. Main Inc: Half Moon Cove Tidal Project, Boston, 1980

$$C_c = B_c V_c \tag{D.7}$$

Where $B_c \approx$ US\$ 99 /m^3 (price in 1983: US\$ 48 /m^3)

$$V_c = 0.94(W_{sl} + W_p)D_b^2 \tag{D.8}$$

D.5 Barrage

As the tidal barrage already exists, the costs will be 0 \$. But if a new dam is built to separate the sea water and the fresh water, the costs of this new dam should be taken into account. Also the difference in costs for a high dike (in case a high-basin plant is built) or a low dike (in case a low-basin scheme is chosen) for protecting the polders should be taken into account.

The crest height of the dam separating the sea from the fresh water is determined by the acceptable amount of water which may run over the dam into the basin because of waves and the same counts for the dikes protecting the polders against inundation. Figures D.2 and D.3 show which part of the dam and dike cross sections are due to a higher water level if the plant is to be a high basin plant instead of a low basin plant. This is taken into account in Section 4.7, for deciding whether a high or a low basin plant should be built.
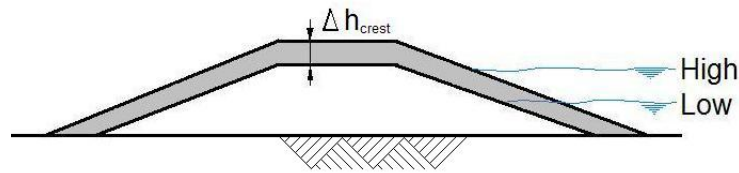

Figure D.2: *Influence of crest height difference between low and high basin on dam section*
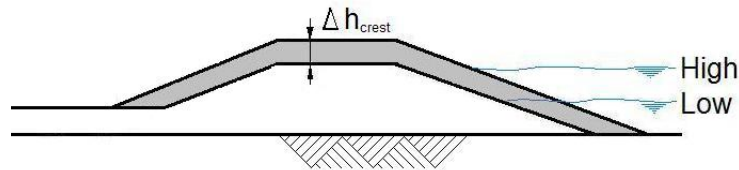

Figure D.3: *Influence of crest height difference between low and high basin on dike section*

$$V_b = mD_b^2 L_b/2 \tag{D.9}$$

$$L_b = L_{closure} - W_s - W_p \tag{D.10}$$

Where $B_b \approx$ US\$ 25 /m^3

D.6   Bed protection

$$C_{bed} = B_{bed}V_{bed} \tag{D.11}$$

The cost of bed material B_{bed} is estimated to be about the same as the cost of barrage material B_b, so $B_{bed} \approx$ US\$ 25 /m³ (price in 1983: US\$ 12.3 /m³). The length of the bed protection Y perpendicular to the powerhouse or sluices is estimated to be 100 m on both the basin side and the sea side, which is the same as the distance between the structure and the cofferdam within the construction pit. This 100 m must be enough, because then the flow velocities are assumed to have spread over the total depth and width and thus the flow velocities will have significantly decreased. The bed protection is put in place at ground zero of the construction site when the construction is finished and the area enclosed by the cofferdam is still dewatered.

$$V_{bed} = 2 \cdot D_{part,req}(W_p + W_{sl})(Y_{basin} + Y_{sea}) \tag{D.12}$$

D.7   Check on Sihwa TPP

To check the accuracy of this method, the values of the design parameters of the Sihwa TPP are put into the model. Since Fay and Smachlo developed their method in 1983, the costs for the Sihwa project have not had influence on the proportionality constants in the different formulas in this method (except for the the turbine and generator costs).
The project sum of Sihwa TPP was US\$ 250 Million in 2005. A correction due to inflation makes this US\$ 263.4 Million in 2007. Some design parameters for Sihwa are listed in Table D.2.

Table D.2: *Parameters for Sihwa TPP*

Parameter	Value	Unit
R_{mean}	5.57	m
D_t	7.5	m
N_t	10	-
P_{1t}	25.4	MW
H_r	5.82	m
W_{sl}	120	m

The output of the model is quite accurate: US\$ 270,619,589 which is 2.73 % higher than the project sum. For the composition of the total construction costs, see Table D.3. From the result for Sihwa can be concluded that the model is sufficiently accurate and can perfectly serve to predict the total construction costs for the Saemangeum TPP.

Table D.3: *Breakdown of the construction costs of Sihwa TPP, according to Fay & Smachlo*

Part	Costs
Turbines and generators	$ 97,022,319
Power house	$ 71,777,045
Sluices	$ 72,087,769
Cofferdam	$ 27,056,443
Bed protection	$ 2,676,012
Total	$ 270,619,589
Project sum (corrected for inflation)	263,415,765
Difference	2.73 %

References

Nova scotia power... a tidal power pioneer. *Electrical line*, march/april 2002.

AVELLAN, F. Introduction to cavitation in hydraulic machinery. In *The 6th International Conference on Hydraulic Machinery and Hydrodynamics*, Timisoara, Romania, October 21-22 2004.

BANAL, M. Génèse technique de l'usine marémotrice. *La Houille Blanche, Revue Internationale de l'eau*, 3, 1997a.

BANAL, M. Histoire de l'énergie marémotrice en france. *La Houille Blanche, Revue Internationale de l'eau*, 3, 1997b.

BATTJES, J.A. *Vloeistofmechanica CT2100*. Delft University of Technology Reader, Delft, 2002.

BERNSHTEIN, L.B. *Tidal energy for electric power plants*. Israel program for scientific tanslations Ltd. Gosudarstvennoe Energeticheskoe Izdate'stvo, 1965.

BOSC, J. Les groupes bulbes de la rance après trente ans d'exploitation retour d'expérience. *La Houille Blanche, Revue Internationale de l'eau*, 3, 1997.

BRAITSCH, W. & HAAS, H. *Renewable energy*, volume 3C, chapter 2.7: Turbines for hydroelectric power, pages 197–222. Springer Berlin Heidelberg, 2006.

CAZENAVE, P. L'utilisation des groupes bulbes dans les aménagements de basse chute. *La Houille Blanche, Revue Internationale de l'eau*, 3(3), 1997. 30èmeanniversaire de la Rance: l'énergie marémotrice.

D'ANGREMOND, BEZUYEN, VAN DER MEULEN ET AL. *Inleiding waterbouw CT3020*. Delft University of Technology Reader, Delft, January 2001.

D'ANGREMOND K.& VAN ROODE, F.C. *Breakwaters and closure dams*. VSSD, 2001.

DELFGAAUW, S. Aspects of a tidal power scheme in the wyre estuary. Master's thesis, TU Delft, november 1991. Binnie & Partners.

DELORY, R.P. & ENG, P. The annapolis tidal generating station. In Jane Stanbury, editor, *Water for Energy*. BHRA, May 1986.

DUIVENDIJK, J. VAN. *Waterpower Engineering Principles and Characterisitics, CT5304*. Delft University of Technology, Delft, 2004.

EDF. L'usine marémotrice de la rance: brochure published by edf, 1996.

ESHA. *Guide on How to Develop a Small Hydropower Plant.* ESHA, 2004.

FAY, J.A. & SMACHLO, M.A. Capital cost of small-scale tidal power plant. *Journal of energy*, 7(6):536–541, 1983a.

FAY, J.A. & SMACHLO, M.A. Performance of small-scale tidal power plant. *Journal of energy*, 7(6):529–535, 1983b.

GIBRAT, R. *l'Énergie Des Marées.* Paris:Presses Universitaires de France, 1966.

GORDON, J.L. Hydraulic turbine efficiency. *Canadian Journal of Civil Engineering*, 28: 238–253, 2001.

HARN, J. VAN. Feasibility study on tidal power barrages. Master's thesis, TU Delft, february 2007.

HEUNG-NYUN KIM, DOO-HYUN PAIK, DEUK-KYU PARK. Commercializing method of sihwa tidal power. In *19th World Energy Congress, Sydney, Australia September 5-9, 2004.* Korea Water Resources Corporation, Daejeon, South Korea, 2004.

HR WALLINGFORD LIMITED 2002. Computational and physical modelling on saemangeum closure works. Technical report, 2002.

HSAI-YANG FANG. *Foundation Engineering Handbook.* Kluwer Academic Publishers, 2 edition, 1991.

JORISSEN,R.E., KONTER, J.L.M. *Afsluitdammen, regels voor het ontwerp.* Bouwdienst Rijkswaterstaat, Utrecht, march 1992.

KJØLLE, A. *Hydropower in Norway - Mechanical equipment.* Norwegian University of Science and Technology Trondheim, 2001.

KOWACO & DAEWOO. Sihwa-lake tidal power plant, 2006.

KOWALIK, Z. Tide distribution and tapping into tidal energy. *OCEANOLOGIA*, 3:315–321, 2004.

KPORDZE, C.S.K. AND WARNICK, C. C. Selection of turbine diameter and speed for francis, kaplan, and pelton hydraulic turbines. In *Water Power '87*, pages 1893–1902. American Society of Civil Engineers, 1988.

KRC. Technical Report 3, 2006. Ministry of Agriculture and forestry of South Korea.

KRUEGER, R.E. *Selecting hydraulic Reaction Turbines.* United States Department of the Interior, Bureau of Reclamation, Denver, Colorado 80225, 20 edition, 1976.

LAMBERT, M. Bilan de la protection cathodique des ouvrages du barrage de la rance, de la conception au résultat final. *La Houille Blanche, Revue Internationale de l'eau*, 1997.

Lee, Kwang-soo. Tidal and tidal current power study in korea, May 2006. KORDI (Korea Ocean Research & Development Institute).

Miller, H. Choice of hydro-electric equipment for tidal energy. In *Proceedings Korea Tidal Power Symposium*. Sulzer Escher Wyss, okt/nov 1978.

Minister of Natural Resources Canada. *Small hydro project analysis*. RETScreen International, Clean Energy Decision Support Centre, 2004. www.retscreen.net.

Mosonyi, E. *Low-head power plants*. Akademia Kiado, Budapest, 1987.

NEDECO. Severn tidal barrage scheme. Technical report, NEDECO, March 1977.

NEDECO and Delft Hydraulics. Saemankum nabeschouwing. Technical report, 1992.

Raabe, J. *Hydro power : the design, use, and function of hydromechanical, hydraulic, and electrical equipment*. VDI-Verlag, Duesseldorf, 1985.

Remery, F.R. Hydroturbines. *Energiewaterbouw*, 1982. faculteitsbibliotheek CiTG: CT-EW8.

Schiereck, G.J. *Introduction to bed, bank and shore protection*. Number ISBN 90-407-1683-8. Delft University Press, 2001.

Schneeberger, M. Tidal turbine development. *International water power & dam construction*, pages 28–30, February 2007.

Schweiger, F., Gregori, I. Comparison of turbine parameters for small and large axial units. *Water Power & Dam Construction*, 44(11):46–48, 1992.

Song Won Oh & Walsum, W. van. *Renewable energy*, volume 3C, chapter 2.5: Tidal power plants, pages 129–164. Springer Berlin Heidelberg, 2006.

Tester, J.W. *Sustainable Energy: Choosing Among Options*. MIT press, Cambridge, MA, 2005.

Tol, A.F. van , Everts, H.J. *Damwandconstructies, CUR 166, CT5331*. Delft University of Technology, Delft, 2002.

Torre, S. de la. Influence of tidal power generation in the self-scheduling of a price-maker producer. *Universidad de Malaga, Malaga*, 2005.

Walsum, E. van. Barriers against tidal power. *Waterpower magazine*, 3/9/2003(?), 9 2003a. URL www.waterpowermagazine.com.

Walsum, E. van. Barriers to tidal power: environmental effects. *Waterpower magazine*, 30/9/2003, 2003b. URL www.waterpowermagazine.com.

Walsum, E. van. Barriers to tidal power: multi basin plants. *Waterpower magazine*, 21/4/2004, 2003c. URL www.waterpowermagazine.com.

WEICHENG WU. The prospects of the tidal energy development in the pacific countries. In *International Digital Earth Conference, Beijing*, November 1999. URL `www.Digitalearth.net.cn`.

WILSON, E.M. *Tidal-energy development.*

Design of Sheet Pile Cellular Structures, Cofferdams and Retaining Walls. US Army Corps of Engineers, Washington, DC 20314-1000, September 1989.